POLITECNICO DI TORINO

Corso di Laurea Magistrale

in Ingegneria Energetica e Nucleare

Tesi di Laurea Magistrale

Modelling of stand-alone H_2-based energy storage systems for electricity production and H_2 mobility

Relatori: Prof. Andrea Lanzini

Prof. Massimo Santarelli

Co-Relatore: Ing. Paolo Marocco

Candidato: Andrea Calvo

Anno Accademico 2019/2020

Abstract

The application of renewable energy sources (RES) during the last decades increase, to reduce the carbon dioxide emission and to developed sustainable and efficient energy solutions. To obtain a perfect interaction between energy supply and demand, considering the non-continuous production of the main renewable solutions, an energy storage system (ESS) is required, mainly for isolated microgrid and off-grid remote application because of the invasive grid connections or the environmental impact of diesel generators. Also a Fuel Cell Vehicle (FCV) can be selected to substitute the utilization of conventional engine buses for public transport application, considering the high range of heavy-duty vehicles based on hydrogen technologies. Intermittent RES integrated with H_2-based storage systems can become an interesting option because of the high energy density, long-term storage capability and modularity of H_2. The present study is part of the European REMOTE project, to analyze, from a technical and economical point of view, a hybrid P2P and P2H system for demo 3 (Ambornetti). The aim of this work is to find the optimal system configuration, with the minimum Net Present Value (NPV) at the end of system lifetime; also the Levelized Cost Of Energy (LCOE) and the Levelized Cost Of Hydrogen (LCOH) are computed, to understand the economic viability for, respectively, electricity and mobility loads. These values derived using cost inputs only from literature, and a comparative analysis is done for the different system configurations. Results from the energy simulations revealed that the need for an external source is significantly reduced thanks to RES together with the hybrid storage system, but the energy curtailment, that for a standalone system with a ESS must be lower to reduce energy waste, is still too high mainly for the only PV energy source configuration. Instead, also considering a biomass-based CHP system as energy source, the energy curtailment is reduced until a reasonable value. For the electricity load, a more profitable energy solution is found than the current one only in the case of PV-CHP coupled system, either in the short term or in the longer term; instead in a completely CO_2-free solution with only PV, the LCOE value is too high, due to the component oversizing. For the mobility load, in all the scenarios a too high LCOH value is obtained; this is due to the less development status of hydrogen technologies for automotive application than energy production one, with still high investment cost for the Hydrogen Refueling Station (HRS).

Keywords: Hydrogen, Standalone systems, Off-grid applications, Energy management, Energy storage, Fuel cell, Electrolyzer, Hydrogen refueling station, Fuel Cell Vehicles

Contents

List of abbreviations

Abbreviations	*Meaning*
RES	Renewable Energy Sources
IEA	International Energy Agency
P2P	Power-2-Power
P2H	Power-2-Hydrogen
DER	Distributed Energy Resources
DG	Distributed Generation
EMS	Energy Management System
AC	Alternating Current
DC	Direct Current
ESS	Energy Storage System
CHP	Combined Heat and Power
PSA	Pressure Swing Adsorption / Particle Swarm Algorithm
ICE	Internal Combustion Engine
PEMFC	Proton Exchange Membrane / Polymeric Electrolyte Membrane Fuel Cell
SOFC	Solid Oxide Fuel Cell
ALKEL	Alkaline Electrolyzer
PEMEL	Proton Exchange Membrane / Polymeric Electrolyte Membrane Electrolyzer
OCV	Open Circuit Voltage
SOC	State Of Charge
LOH	Level Of Hydrogen
PR	Performance Ratio
NOCT	Normal Operating Cell Temperature
EOT	Equation Of Time
DST	Daylight Savings Time
LPSP	Loss Of Power Supply
LHSP	Loss Of Hydrogen Supply
HRS	Hydrogen Refueling Station
SAE	Society of Automotive Engineers
FCV	Fuel Cell Vehicle
FCEV	Fuel Cell Electric Vehicle
EV	Electric Vehicle
BEV	Battery Electric Vehicle
FCHEV	Fuel Cell Hybrid Electric Vehicle
CEPCI	Chemical Engineering Plant Cost Index
O&M	Operational & Maintenance
NPC	Net Present Cost
LCOE	Levelized Cost Of Electricity
LCOH	Levelized Cost Of Hydrogen
WACC	Weight Average Cost of Capital
IRS	Interest Rate Swap
EMRP	Equity Market Risk Premium

List of figures

List of tables

List of equations

1 Introduction

With the issue of climate change and fossil fuels availability during the last decades, the role of RES (Renewable Energy Sources) increase in importance in the energy sector and market. As explained by the following figure, the world energy consumption increase during the years and mainly in the last century, and the main energy sources operated are fossil fuels; but fossil fuels are not able to satisfy all the actual and future energy because of the limited availability on the earth and are not CO_2-free as RES. So, one of the main problems in the energy but also transport sectors is the production of greenhouse gases that causes climate change. The transition from a fossil fuel-based power generation to a sustainable power production is mandatory, with a progressive depletion and mitigation of greenhouse gas emissions. For the transport sector, the utilization of fossil fuels have the same problem as in the energy production sector; for example, one of the higher environmental impact in the automotive emission is the nitrogen dioxide (NO_2), that can causes different health problems for humans, as respiratory tract inflammation.

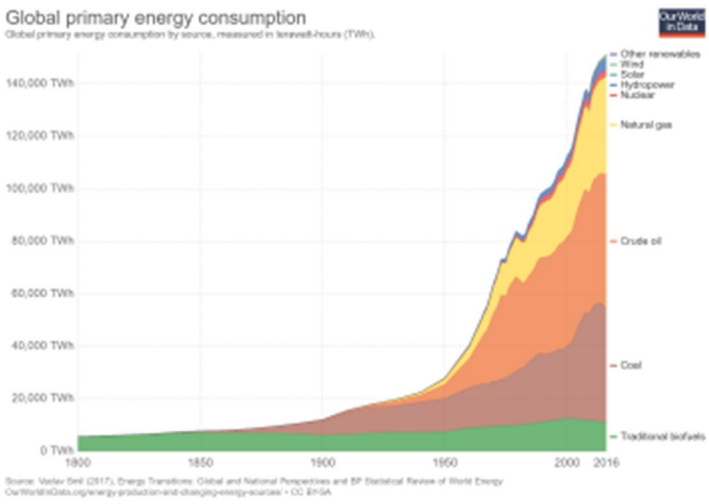

Figure 1 Global primary energy consumption and related source diversification [1]

To help the governments of the world to get a clear scientific vision of the state of climate change and the potential consequences environmental and socio-economic, an international association was founded: this is the IPCC, Intergovernmental Panel on Climate Change, that produce annual report of the global situation [2]. An important action made by

the global governments was the Paris agreement during the COP 21 in France, with the aim of “keep the global average temperature rise well below 2° C compared to pre-industrial levels and continue the action taken to limit the temperature rise to 1.5° C compared to pre-industrial levels, recognizing that this could reduce in significantly the risks and effects of climate change” [3]. After this agreement, different projects have been started in the world, and the Europe is one of the main promoters of renewable sources. The first European reply is the 20-20-20, a set of targets for the end of 2020: 20 % of reduction in primary energy consumption (with an increase in energy efficiency), 20 % of reduction in GHG emission and 20 % of the total energy production from the RES, with also at least 10 % for the transport sector. Obviously, RES have different advantages considering environmental impact and availability of the source, but they have also some disadvantages respect to conventional fuels; the main are the low energy density, the discontinuity in the production, the difficult energy storage, the higher costs and also the higher problems in management with the network. But the energy storage from RES is an important research sector in order to avoid the problem of intermittency of electricity production. Hydrogen, in particular, represents an interesting storage solution because of its high energy density per mass and long-term storage capability [4].

The presented work is performed in the framework of REMOTE (Remote area Energy supply Multiple Options for integrated hydrogen-based Technologies), a 4-year project (2018–2021) of the EU’s Horizon 2020 program [5]. The self-sustainability in energy terms for a remote village is very important, because of the difficulty in the transport and management of the electricity through the national grid. REMOTE objective is to demonstrate the technoeconomic feasibility of hydrogen-based energy storage solutions in isolated micro-grids and off-grid remote areas, with the analysis of four Demos energy consumption and management. The variety of the involved demo cases and locations, as better explained in following chapters, will thus allow gaining significant learning from integration with existing infrastructure in real sites, paving the way for the deployment of Power-to-Power (P2P) storage systems at large scale. Initially, only the electricity load is considered, but in this Master Thesis also a hydrogen mobility load is selected in order to demonstrate the feasibility of hydrogen-based automotive technologies for public transport application; the utilization of RES solution in the transport sector is now a very well-known research field, but respect to energy sector is newer. The two main solutions for automotive sector are electric-based and hydrogen-based vehicles, with the first more developed than the second options also from a refueling station point of view.

2 Standalone systems

One of the main problems in the energy production and utilization in the world is the access at the electricity that in remote areas is very difficult to provide. As affirm by the IEA in the 2012 World Energy Outlook, more than one billion people can't get access to electricity [6]. To compensate this issue, a possible decentralized and distributed generation system can be applied in these areas; moreover, this type of solution can avoid part of the electricity losses along the grid, that in case of the European Union grid correspond to around 8 % of the total electric energy production [7]. A distributed generation system can be defined in different way; for example, the IEEE defines distributed generation as the generation of electricity by facilities that are sufficiently smaller than central generating plants so as to allow interconnection at nearly any point in a power system [8]. But this small-scale generation definition can be loose respect to the new concept in the electricity market. These concepts of distributed generation and also self-generation of energy are more and more important during these years, promoting the use of microgrid and the intelligent management and control of the energy production and utilization.

A distributed generation system can have different advantages and disadvantages as explained below [9].

Advantages:

- Alternative to expansion of the distribution network, reducing the costs for new transmission lines
- Transmission energy losses reduction and energy production diversification
- Plant location flexibility and opportunity to work connected to the grid or off-grid
- Efficient use of cheap fuel opportunities
- Incentive in the use of combined heat and electricity production system, to reduce the environmental impact (more if are used RES)
- Improvement in the system continuity and reliability

Disadvantages:

- High investment cost, due to the lower system size
- Less choice between more costly primary fuels

- Less energy efficiency, so higher environmental impact (only when fossil fuels are used)

There are different types of distributed generation systems and are shown in the following figure.

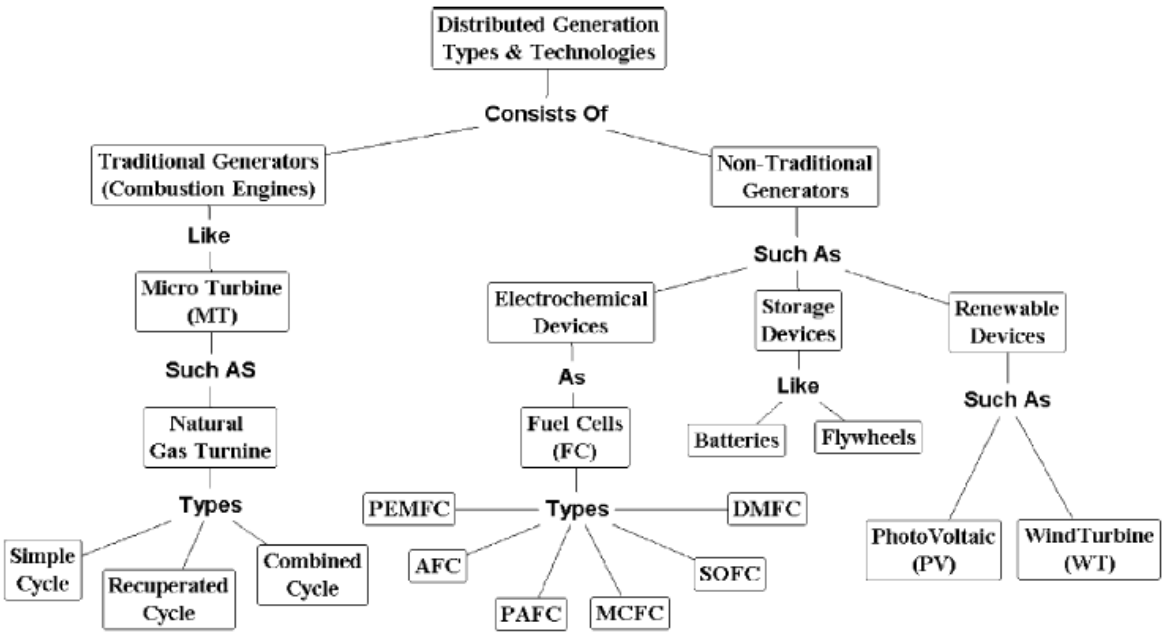

Figure 2 Distributed generation types and technologies [10]

Obviously, according to the environmental impact reduction policy, it's better considered non-traditional generators as RES and electrochemical devices; in this study, a hybrid system is selected, considering both electrolyzer/fuel cell technologies, energy storage devices and renewable energy system. The grid network will change in the future with the increase in number of distributed generation systems, that can provide the energy to supply the local loads. A distributed energy resource (DER) is closely related to the definition of microgrid and smartgrid. A microgrid is a small network that provide the energy (electricity and heat) only for a small community in the local area of the system considered. It can be also a set of different DGs and DERs of the same community that provide the enough energy to meet the local load. Usually, a microgrid take advantage of the local RES to provide this energy, in order to avoid also the environmental impact of energy production. Instead a smartgrid is the whole of the information and electricity distribution network managed in such a way as to allow a more efficient and rational management of energy to minimize losses and possible overloads in the network.

A microgrid can operate both in grid-connected and off-grid/isolated modes; the second choice require a very high reliability of the system because in case of failures there will not be an external energy source as in the case of the national grid. In the case of a remote world area, to increase the access population to the electricity a high number of isolated distributed generation systems are required, so is needed a decentralization of the energy production. This is also because a possible grid-extension is this areas is probably very expensive and not suitable, and also the utilization of fossil fuel can be a problem, because of the high costs for the transportation of it, pollution and greenhouse gas emission. So, the best solution as an off-grid microgrid application is the utilization of local renewable energy source. In this way, also partial of the network losses can be avoided but there will be other technical challenges as the selection of well-defined frequency and voltage reference. All the microgrids that operate in islanded mode required another source of energy respect to the RES that can substitute the grid; an energy storage system is needed to provide energy because of the discontinuity in energy production of the RES, due to the daily meteorological variation. For example, a photovoltaic system requires a constant irradiance during the day, but it is impossible in the night; instead, a wind turbine always requires a wind speed higher than its cut-in velocity to start produce.

In literature, different study standalone system based on hydrogen technology and RES supply can be found; in the following rows, a technical review is done to better understand the development of standalone systems operating in off-grid applications. In the work of Agbossou et al. is studied a typical hydrogen-based standalone system, with an energy supply provided a photovoltaic system and a wind turbine, a PEM electrolyzer, a hydrogen storage tank and a PEM fuel cell system. A communication station is considered and this system will give stabilized electrical power for it; through the different storage technologies on the market, the hydrogen technique is retained [11]. In the reference [12], different renewable energy sources are considered to satisfy residential load of a remote mountain village in Italy (as in our case) during a complete year: solar irradiance (transformed by an array of photovoltaic modules), hydraulic energy (transformed by a micro-hydro turbine in open-flume configuration) and wind speed (transformed by a small-size wind generator). Between these possibilities, it has been found that wind-solution it is absolutely the least convenient, instead the micro-hydro solution has a lower constant availability respect to solar one, so need a higher seasonal storage, but due to the higher efficiency of the turbine is the best plant option. In the Gokcek report instead, a small-scale wind turbine electrolysis system is studied, in different configuration mode; respect to the off-grid application, the

grid-integrated system can be considered more profitable, because of the opportunity to sell the excess energy produced instead of transforms it in hydrogen through an electrolyzer system [13]. Different load type is considered in the Stojkovic techno-economic analysis; in this case, three stand-alone hybrid power systems based on renewable energy sources and hydrogen technologies which supply a specific group of low-power consumers are considered. As other references overhauled in this Master Thesis, the HOMER (Hybrid Optimization Model for Electric Renewable) software tool for the numerical simulation method and optimization algorithm is used [14]. This analysis suggests that the use of hydrogen power systems for supplying low power-consumers is entirely justifiable, because of the reduction of the batteries number needed, and the cost increase is acceptable [15]. Also in reference [16] HOMER software is used; in this study, a hybrid renewable energy system using hydrogen energy as energy storage option is conceptually modeled for the Bozcaada Island in Turkey. As result, they have found that increasing potential of the renewable energy sources, such as annual average wind speed or solar radiation, decreases both LCOE and NPC. Instead in the Gracia et al. assessment, different standalone system configurations are considered; producing green hydrogen through an electrolyzer system can represent a feasible solution to compensate the drawback of using RES in remote locations. Obviously, the less environmental impact solution is the totally RES supply system, but diesel-based system still represents the best solution in economic term [17]. A more detailed study is done by Rullo et al., where to find the optimal sizing configuration apply a genetic optimization algorithm, that must be also integrated with an Energy Management Strategy (EMS) [18]. In the work of Torreglosa et al. the use of lifetime degradation models based on the well-known statement that the lifetime depends on the hours of operation and the power profiles that the components are subjected to from which there positions are made to check how they affect to the cost calculation and, consequently, to the EMS performance is proposed. Different techno-economic criteria are considered to minimize the operation cost and the lifespan of the hydrogen-based standalone system [19]. Also in the work of Zoulias et al. an optimized techno-economic analysis is done for an off-grid hydrogen application; the results shown that the replacement of fossil fuels with hydrogen technologies is feasible from a technical point of view, but less in economic term [20].

Also several examples of standalone systems with a hydrogen refueling system can be found in literature, but it’s more difficult to find studies that consider a hydrogen-based standalone system with both electrical load and hydrogen mobility requirement. In the

Ulleberg et al. report, a hydroelectric-based electrolyzer system is considered to provide a hydrogen refueling station for heavy-duty vehicles (trucks). The study shows that there is a relatively good business case for local water electrolysis and supply of hydrogen to captive fleets of trucks in Norway, particularly if the size of the fleet is sufficiently large to justify the installation of a relatively large water electrolyzer system, due to economies of scale [21]. Instead, in the Izmir-Cesme case study in Turkey, a hydrogen refueling system is designed to provide the daily mobility load for 25 fuel cell electric vehicles; as power source, a wind-PV hybrid power system is installed. The results obtained show that the HRS installation is economically appropriate for the considered site, so it can be an encouragement for other possible investments in Turkey [22]. In the Nistor et al. study, different hydrogen refueling station configurations are considered; the results show that hydrogen fuel can be competitive with petrol if the return on investment period is over 10 years for PEM electrolyzers and 5 for Alkaline electrolyzers, but a grid connected system is preferable because of the higher customers number [23]. Also in Sweden an economic analysis is done in three different locations, producing green hydrogen from local wind energy production, in order to increase the possibility of a fuel transition in the transport sector. As results, they have found that is possible to provide enough hydrogen for 200 FCEV per day; but an implementation on a bigger scale can be very difficult, despite it can provide some economic and environmental benefits in Sweden [24]. A supporting green urban mobility report is done in Denmark to investigates the potential of small-scale autonomous hydrogen refueling stations with onsite production via an alkaline electrolysis system powered by a small wind turbine. In this case, fuel cell electric bicycles are considered with a daily load of 6 kg per bicycle; to achieve a positive internal rate of return, a relative high hydrogen price must be considered, but nowadays these initiatives are fundamental for urban environments where problems of low air quality and high traffic are intense [25].

2.1 Microgrid configuration

In a standalone system, there are different components required to satisfy all the loads in an isolated community. In addition to production and storage systems, it is required also inverters, energy flow control units or energy management systems (EMS), voltage converters and, obviously, electric load. Other components are required depending on the technology under study; for example, in a hydrogen isolated system, also an electrolyzer for

the H_2 production and a fuel cell for the re-production of electricity through the water formation reaction is needed, and the ESS will be a hydrogen storage system.

There are two possible configurations to connect all the system equipment, production system and end users: AC coupled and DC coupled. In the first configuration, all the energy producer system that generate electricity in AC are connected to an AC bus line, instead all the other systems that generate DC electricity require the presence of a DC/AC converter before the connection to the main bus line. Example of systems that produce AC energy are wind turbines and biogas engines. Instead in the second configuration, all the energy producer system that generate electricity in DC, as a photovoltaic system, are connected to a DC bus line and all the other systems that generate AC electricity require the presence of a AC/DC converter before the connection to the main bus line [26].

In the following figure, an example of a DC microgrid configuration is shown, with all the components needed.

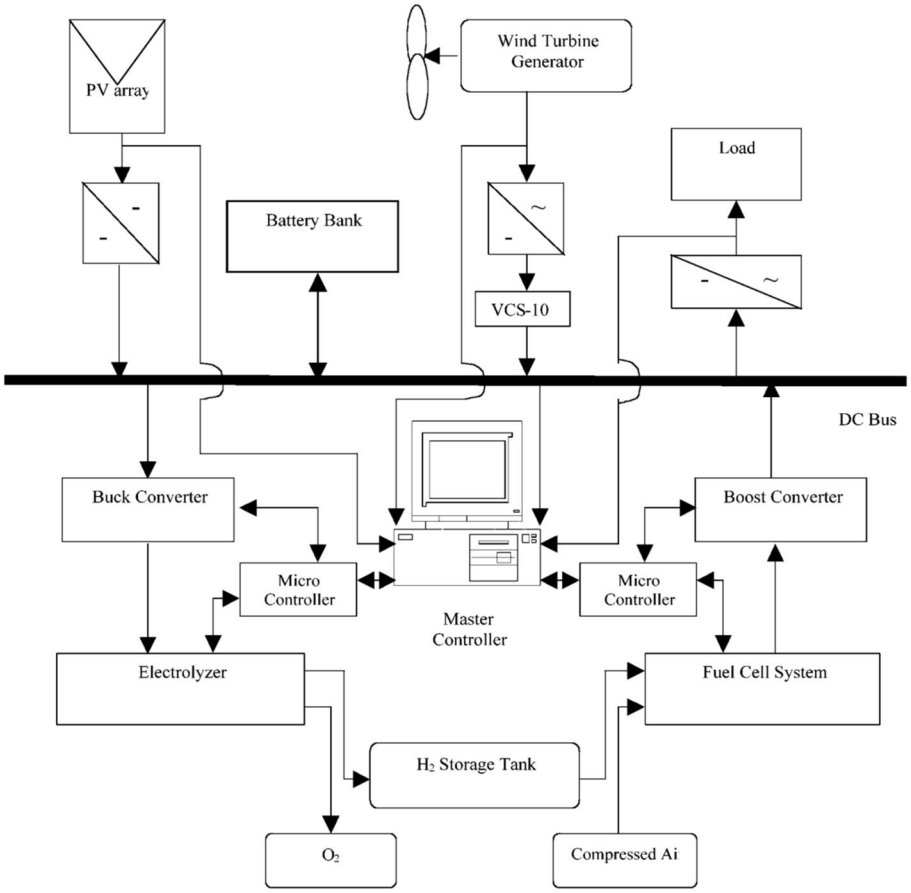

Figure 3 DC microgrid configuration: stand-alone PV and WTG system with energy storage as hydrogen [27]

Instead in the next figure, a less detailed configuration is presented, but it is the initial configuration used in our case study of the REMOTE project, that is explained in a next subchapter.

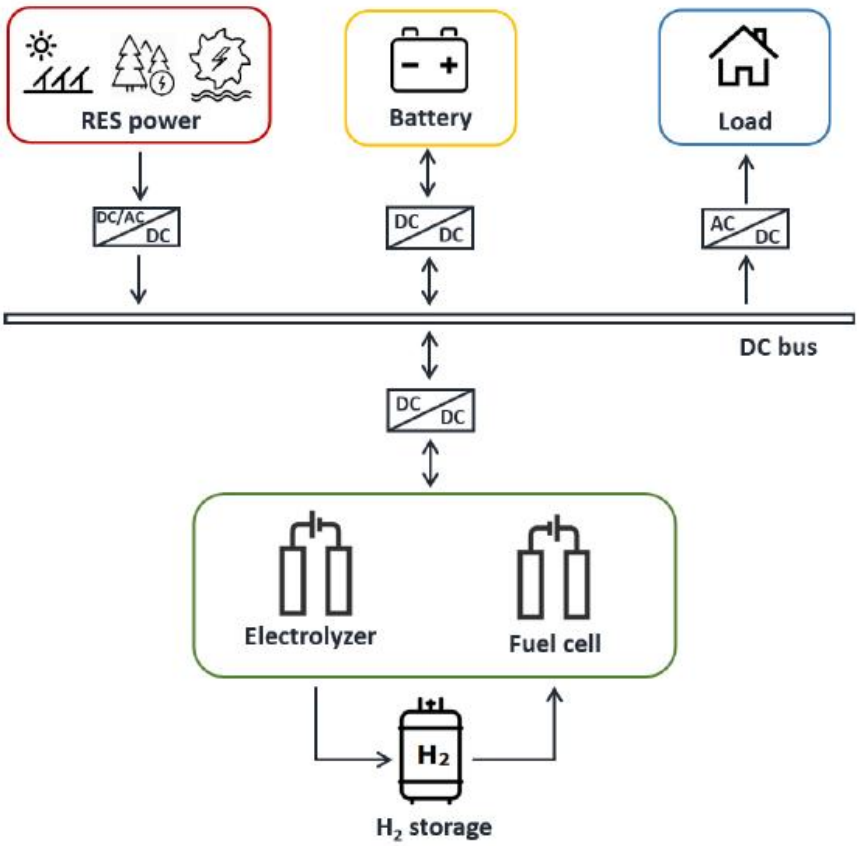

Figure 4 General configuration of a hybrid stand-alone RES H2 system for DEMOs 1, 2 and 3 (integrated P2P) [28]

2.2 Energy storage systems

As seen in the previous chapter, for a standalone energy system the adoption of an energy storage system is required to obtain different benefits, as reduce energy losses, increase the energy supply reliability and improve the operation of the power system (avoiding the equipment oversizing). Coupling a RES system with an ESS, a very innovative and efficient energy production plant can be obtained, with a relatively neglectable environmental impact.

Depending on the microgrid network typology (AC or DC), an ESS could require an inverter; the main energy storage technologies produce a DC energy, so a AC transformation is needed to satisfy the AC loads during the deficit RES supply period. Instead, when there is

an energy surplus, electricity generates by RES must be converted in DC (for example with a wind turbine) to store it in the storage system. But energy cannot be stored in electricity form, so an energy conversion is required; the main energy forms used for stored energy are chemical, thermal, mechanical and electromagnetic.

The operation of an energy storage system depends on the variation of the load curve but also on the variation of the energy production system. So, we can see that is needed a daily storage, but also monthly and yearly in order to meet perfectly the energy required by loads. For example, in the case of a photovoltaic system, we obtain the highest production around noon, but in most of the cases the load peak is during evening, when people return to home from work. A daily storage system is required in this case, to store the energy produced during the day and exploit it in the evening when needed. Both load and RES production have an annual variation, due to the different climate; according to the load need, in winter more energy is used due to heating, but the same during summer because of air conditioning. The same for RES production; for example, with a PV system, in summer the energy produced will be very higher respect to winter, because of the more irradiance from the sun and the longer days. To compensate and balance this variation, an optimal energy storage system size will be found; in the market, a temporal classification can be done.

A storage can be long-term, medium-term and short-term [29]. A long term storage means that the energy is stored for a seasonal storage, to balance the energy surplus and deficit during the different annual seasons; this type of storage must carry a large amount of energy, so require a large capacity with great autonomy and negligible self-discharging. An example of long-term storage can be the hydropower system provided of reservoir, that produce electricity when need accumulating water during the most rainy or snowy season. The second option is a medium term storage, that means an energy accumulation for daily or weekly load variations; typical problem for this type of system is the maximum number of on/off cycle, the expression of the durability intended as number of times the storage unit can release the energy level is designed for, because of the continuous charging and discharging cycle which they are subjected. There are different technologies of medium-term storage as CAES (Compressed Air Energy Storage), hydrogen storage system or also some typologies of batteries. The last storage system is the short-term, in order to compensate the very fast load transient; this means an accumulation for minutes or even seconds, due, most of the cases, to a voltage instability of the grid because of a high reactive operation of the system. To reduce the problem of short-term instability, a rapid response

characteristic is needed as a storage system, and for example, flywheel, battery system and supercapacitor can be used.

In the following table, a more summarized classification is done to understand the typical fields of use for each technology.

Table 1 Storage technology and application fields [29]

Full Power Duration of Storage	Applications of Storage and Possible Replacement of Conventional Electricity System Controls.	Biomass.	Hydrogen. Electrolysis +Fuel Cell	Large Hydro	Compressed Air Energy Storage (CAES)	Heat Or Cold Store + Heat Pump.	Pumped Hydro	Redox Flow Cells.	New And Old Battery Technologies	Flywheel	Superconducting Magnetic Energy Storage (SMES)	Supercapacitor	Conventional Capacitor or Inductor
4 Months	Annual smoothing of loads, PV, wind and small hydro.	✓	✓	✓									
3 Weeks	Smoothing weather effects: load, PV, wind, small hydro.	✓	✓	✓									
3 Days	Weekly smoothing of loads and most weather variations.	✓	✓	✓	✓	✓	✓	✓					
8 Hours	Daily load cycle, PV, wind, Transmission line repair.	✓	✓	✓	✓	✓	✓	✓	✓				
2 Hours	Peak load lopping, standing reserve, wind power smoothing. Minimisation of NETA or similar trading penalties.	✓	✓	✓	✓	✓	✓	✓	✓				
20 Minutes	Spinning reserve, wind power smoothing, clouds on PV		✓	✓	✓	✓	✓	✓	✓	✓			
3 Minutes	Spinning reserve, wind power smoothing of gusts.		✓				✓	✓	✓	✓			
20 Seconds	Line or local faults. Voltage and frequency control. Governor controlled generation.							✓	✓	✓	✓	✓	✓

With the increase of distributed generation and standalone system in the future, an increase of fabrication and utilization of energy storage system is expected, and all different storage technology will probably involve. In this study, in accordance to the technology used, hydrogen storage systems are considered; this type of ESS is better explained in a following dedicated chapter.

2.3 REMOTE project

REMOTE, acronym of “Remote area Energy supply with Multiple Options for integrated hydrogen-based Technologies”, is an European project of the Eu’s Horizon 2020 program,

also supported by the Fuel Cell and Hydrogen Joint Undertaking (FCH JU), with the aim to demonstrate the technical and economic feasibility, but also energy and environmental advantages, of two fuel cells-based H2 energy storage solutions (one integrated P2P system, one nonintegrated P2G+G2P system) [5]. Four DEMOs, with supply by RES, will be installed in isolated micro-grids and off-grid remote areas to guarantee the complete self-sustainability of the site without any need for fossil fuels. The selection of the 4 DEMOs was carried out in order to obtain a variety of situations to be studied; in this way, all the cases can help suppliers, end users and general stakeholders to gain experience.

In the locations selected, different typology of users is considered, with different load profiles, as residential or small industrial (SME) loads [30]. This variation changes also the design of the fuel cells-based energy storage solutions and, in particular, protocols to manage the micro-grids. The electricity used to meet the load variation will be operated directly, both with intermitted energy supply, as photovoltaic system or wind turbine, and more predictable and stable sources, as mini-hydro application. In this way, different models and energy management of microgrids will be apply in the DEMOs, in order to

- design hydrogen-based energy storage solutions (size of the electrolyzer, size of the H2 storage);
- identify methodologies to optimize the design of these typologies of systems;
- design protocols to manage the electric flows inside the micro-grids.

In the following subchapters a description of the different DEMOs will be done and a more detailed explanation is carried out for DEMO 3, that is the microgrid considered in this study.

2.3.1 The 4 Demos

The four different DEMOs and the relative starting energy system solutions under study are explained in the list below [5]:

- DEMO 1 – Ginostra is an island of the south Italy not connected to the national grid (off-grid application); to substitute completely the diesel generator and obtain an almost complete substitution of fossil fuels, a PV system is designed in order to satisfy residential loads available on-site.
- DEMO 2 – Agkistro is a remote village of the north-east Greece that can be considered an isolated micro-grid application; to satisfy industrial loads available on

site, a RES based on hydro-generator is designed, in order to a complete substitution of fossil fuels and avoid the costs for a new transmission line to connect at national grid.

- DEMO 3 – Ambornetti is a remote village of the north-west Italian Alps that operates in off-grid application, so there is not a national grid connection; to substitute the utilization of fossil fuels in a diesel generator, a hybrid system with PV-biomass CHP system is studied in order to satisfy the residential local load available on site.
- DEMO 4 – Froan is a remote island in the north of Norway, that can be considered as an isolated microgrid application, because the existing network connection to the national grid must be substituted; to satisfy the residential and fish industry local loads available on site a hybrid system based on PV and wind turbine is selected; in this way, the utilization of fossil fuels to produce the energy and also the costs for a new sub-marine power line are avoided.

In the following figures, the REMOTE concept and locations are explained for the different DEMOs.

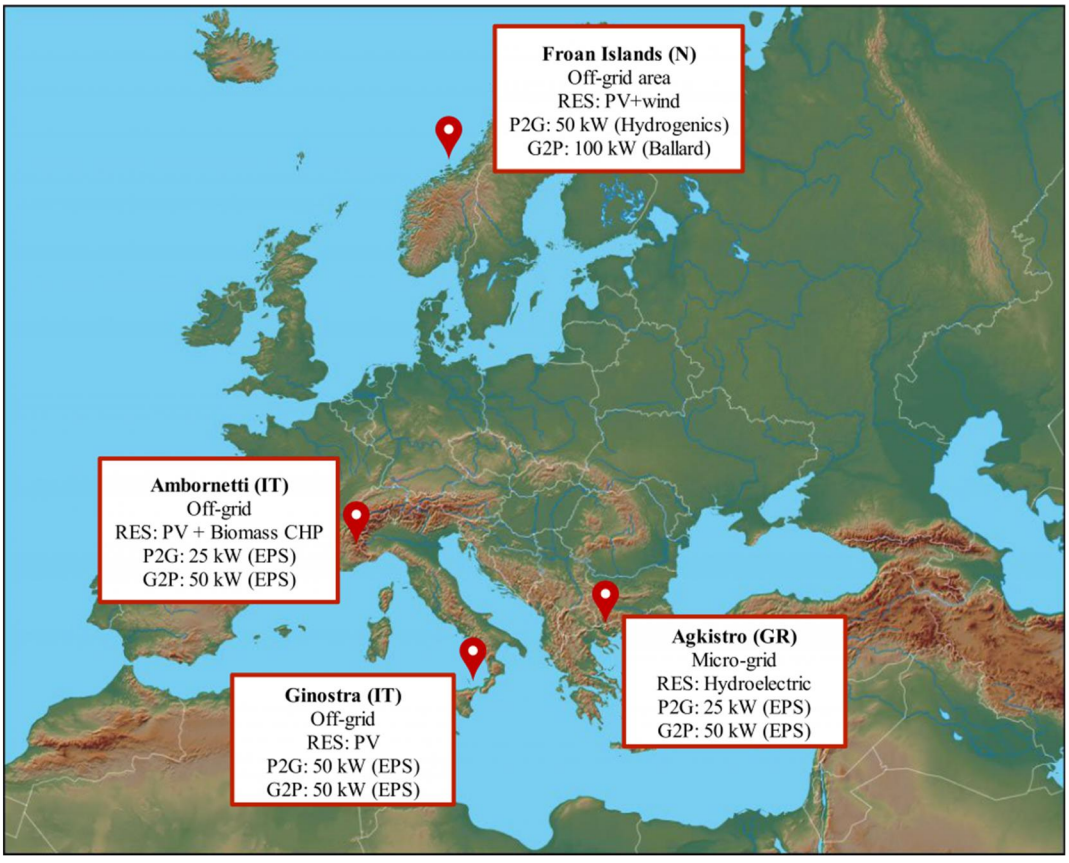

Figure 5 Geographical locations and solutions of the 4 DEMOs (REMOTE project) [30]

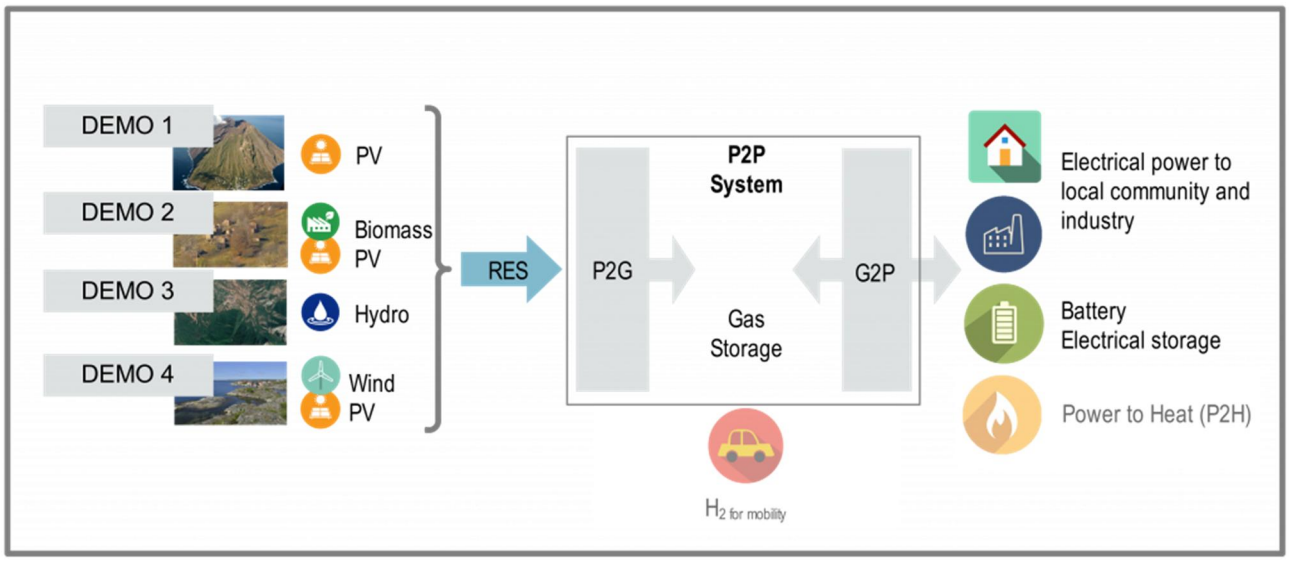

Figure 6 REMOTE concept and innovation potential [5]

To obtain a more detailed overview of the different solutions, in the following table all the most important characteristics are summarized.

Table 2 Components of the RES + H2-based storage solution for the REMOTE demo sites [31]

		1. Ginostra	2. Agkistro	3. Ambornetti	4. Rye/Froan[1]
RES	*Typology*	PV	Hydro	PV + Biomass	PV + Wind
	Size	170 kW	0.9 MW	75 kW PV 49 kW Biomass	250 kW PV 675 kW Wind
P2P	*Typology*	Integrated	Integrated	Non-integrated	Non-integrated
	Supplier	ENGIE-EPS	ENGIE-EPS	BPSE, ENGIE-EPS	HYG, BPSE, POW
	P2G				
	Technology	Alkaline	Alkaline	Alkaline	PEM
	Rated Power	50 kW (2 stacks)	25 kW	18 kW	50 kW
	G2P				
	Technology	PEM (O_2 fed)	PEM (O_2 fed)	PEM	PEM
	Rated Power	50 kW (2 stacks)	50 kW (2 stacks)	85 kW (6 stacks)	100 kW (6 stacks)
	H_2 storage				
	Gross energy (LHV)	1793 kWh	996 kWh	498 kWh	3333 kWh
	Battery				
	Technology	Li-ion	Li-ion	Li-ion	Li-ion
	Rated energy	600 kWh	92 kWh	92 kWh	550 kWh

2.3.2 Demo 3: Ambornetti

As explained before, Ambonetti is a remote mountain hamlet of the north west Italian Alps, in the Piedmont region. In the last years, private local investors including IRIS company want to convert Ambornetti in a completely energy autonomous community; this neutral environmental impact configuration is in accordance to the object with their renovation project [32]. This is also because it is never connected to the national grid, so this type of

renovation will be completely off-grid with the aim of restart technology and economic activities in that rural area. Ambornetti is contained in the “Parco del Monviso” area, a protected mountain nature reserve; this is another motivation to exclude the connection to national grid, because of too invasive connection works that will be not approved by local authorities. The energy production system is initially composed by a 75 kW PV power plant and a 49 kW biomass-based CHP generator, in order to provide electricity to the off-grid community. The critical lifecycle impact of the energy storage system will be minimized by the hydrogen-based technology and this demo represents a first of its kind example of integrating energy storage with power generation from biomass and from PV.

In the plot below, a more detailed geographical location of Ambornetti is shown.

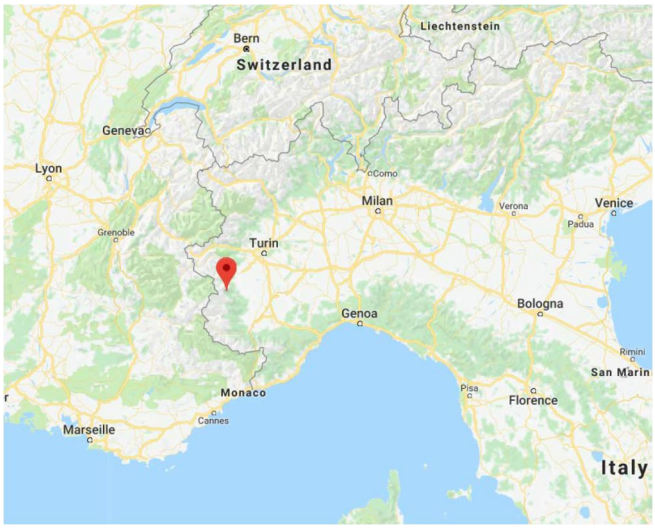

Figure 7 Ambornetti's geographical location

The energy management system governs the power flows from each component and the related control function to obtain an optimized configuration based on the site's requirements. There are different advantages of a P2P+RES solution for this location, as

- minimizing the overall lifecycle impact based on the renovation project aim;
- avoiding expensive and invasive works and infrastructures for connection to the grid;
- avoiding the employment of traditional fossil fuel generators;
- gaining experience in the P2P storage solution for potential replication in other Alpine areas.

In the following figure, the two alternatives (traditional and RES-based) are illustrated.

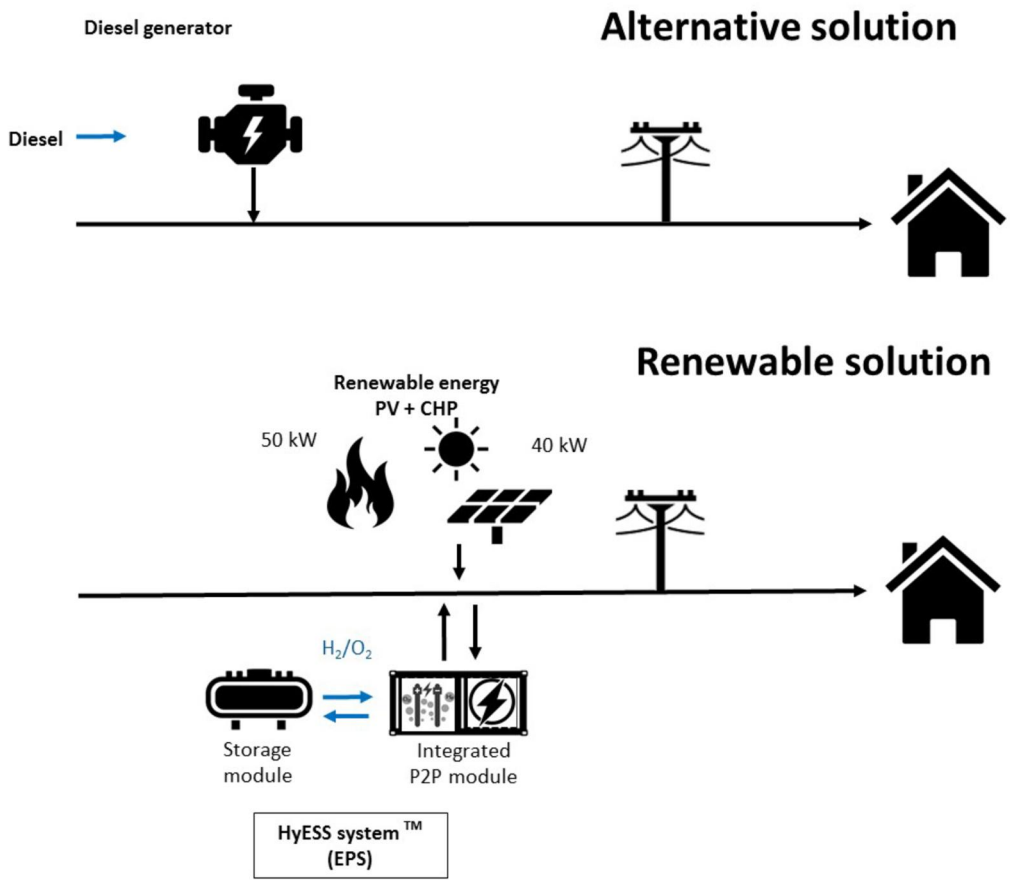

Figure 8 Traditional and RES-based solutions for Ambornetti DEMO site [30]

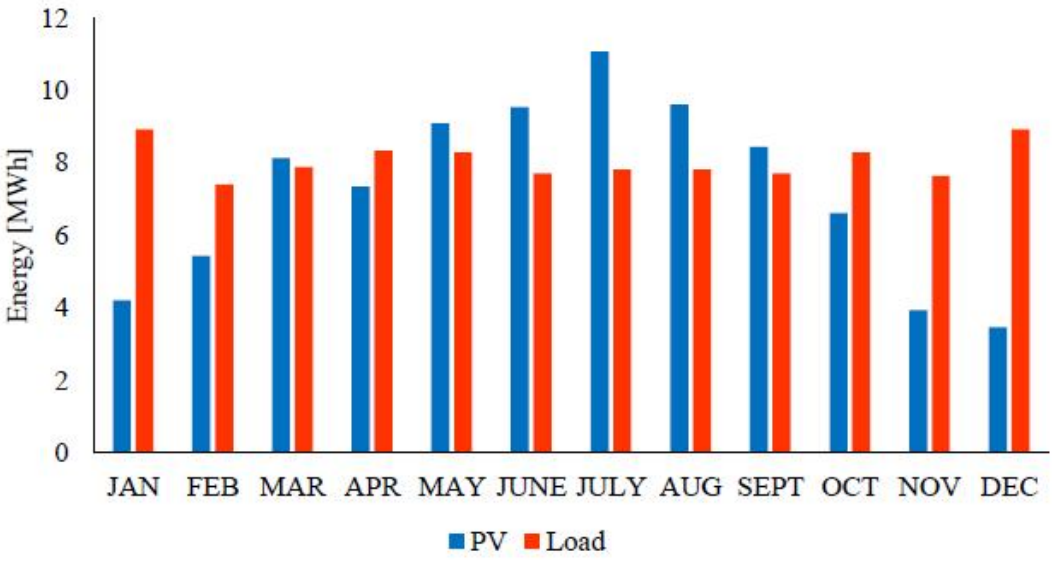

Figure 9 Monthly distribution of PV production and load [28]

An initial energy management overview can be done, to understand the variation of the photovoltaic production and the electricity load of the community, with an annual electric energy required of around 348 MWh; during the year, electric load has not a relevant variation, as shown in the graph before. Also the surplus and deficit graph is plotted below, in order to understand the real need of a storage system, to meet the community energy demand without oversized the energy production components and avoid the energy waste.

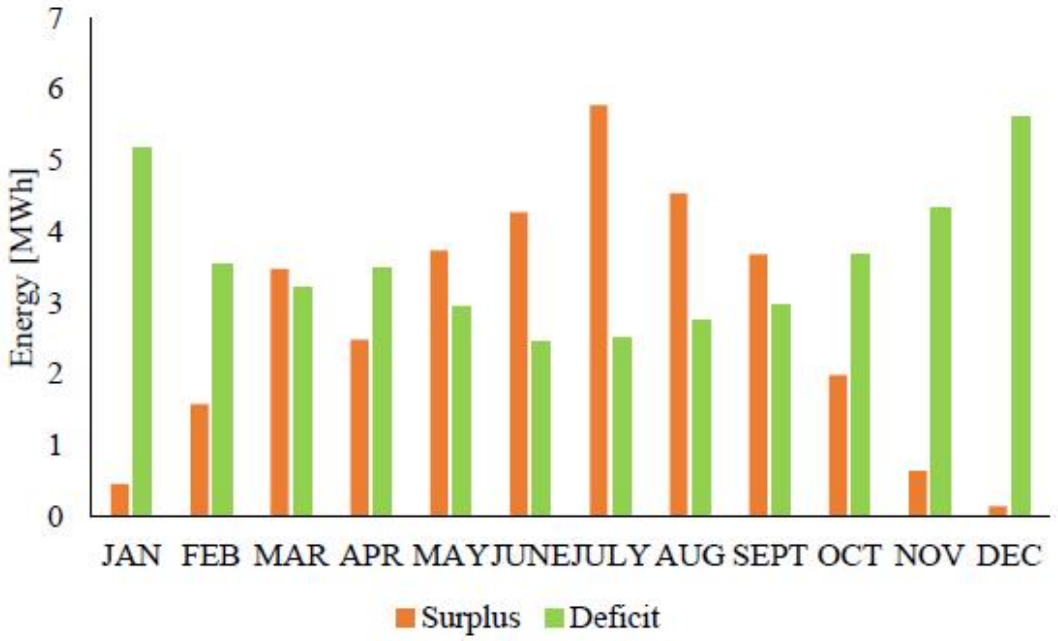

Figure 10 Energy surplus and deficit along the year [28]

3 Hydrogen technologies

In this study is considered a hydrogen-based technology that can be used in a direct way but also in the reverse way and is an electrochemical cell. Respect to a closed battery with a certain autonomy, the reaction materials required for this technology are not contained inside the cell but are taken from the environment. The direct-way component is the fuel cell that through the spontaneous reaction of hydrogen and oxygen produced a coherent flow of electrons and water; instead the reverse-way one is the electrolyzer that required water and electric power to split the water molecules in oxygen and hydrogen. Hydrogen is considered one of the elements for future decarbonization of energy sector and industrial processes (for example steel industry) and can be also used as fuel for mobility.

3.1 Hydrogen properties

Hydrogen is the most abundant element of the universe, as shown by the spectral analysis of the light emitted by the stars, which reveals that most of them are composed just of hydrogen. In nature, hydrogen is a mixture of three isotopes, ordinary hydrogen, deuterium and tritium, but the last is very rare because is radioactive with a halved time not so important. Instead, the firsts two isotopes are composed in proportion of 3200:1.

Hydrogen is present in two different form that coexist and depend on the protons spin inside the atom:

- Orto-H_2 (or normal-H_2), with a parallel protons spin
- Para-H_2, with an anti-parallel protons spin

The two hydrogen types have a very small differences in the thermodynamic properties.

The molar fraction of them depends on the temperature; at normal temperature condition (20 °C), there are about 75 % of orto-hydrogen and the rest 25 % of para-hydrogen in equilibrium. Instead when we reduce the temperature, the amount of para-hydrogen increase (so the equilibrium shifts to the para-H_2) because of the exothermic transformation from orto to para-H_2, and at 21 K the fraction of orto-hydrogen is only 0.2 %.

The hydrogen properties can be an advantage but also a disadvantage. For examples, considering the value of the specific heat at constant pressure of about 14 kJ/(kg·K), to compress the hydrogen we require a very high cost in terms of energy; but when we heat it, the temperature difference is lower respect to other material so is better in terms of thermal safety because is less probable to reach a risky temperature. Another property that can show both an advantage and a disadvantage for the hydrogen is the diffusion coefficient of 0.61 cm^2/s, respect to the same coefficient of the air of 0.16 cm^2/s. This means a good tendency to escape, so it's more difficult to generate condition near the autoignition limit but also a problem for the hydrogen storage.

In the following table, the main properties of hydrogen are shown; the low-temperature properties all refer to hydrogen which has the parahydrogen concentration corresponding to its low-temperature equilibrium value.

Table 3 Hydrogen properties [33]

Property	Value
Atomic weight	1.00797
Molecular weight	2.01594
Melting point	-259.34 °C
Boiling point at 1 atm	-252.87 °C
Density of gas at 0 °C and 1 atm	0.08987 kg/m^3
Density of liquid at -252.87 °C	70.8 kg/m^3
Density of solid at -259.34 °C	85.8 kg/m^3
Critical temperature	-240.17 °C
Critical pressure	12.8 atm
Critical density	0.0312 g/cm^3
Specific heat at constant pressure and 25 °C	14345 J/kg/K
Thermal conductivity at 25 °C	0.182 W/m/K
Viscosity at 25 °C	0.00892 centipoise
Specific gravity	0.0695 compared to air
Lower Heating Value	119.96 kJ/kg

3.2 Hydrogen production

There are different ways to produce hydrogen, but the most important are:

- Steam reforming of natural gas
- Coal gasification
- Biomass pyrolysis and gasification
- Water electrolysis

The methane reforming usually required before a desulphurization of the natural gas (that contain a little amount of S-compounds) to avoid the formation of sulfur acids. Then, the reforming reaction can be done and a syngas is obtained.

$$CH_4 + H_2O \rightarrow 3H_2 + CO \qquad (1)$$

this reaction is endothermic so require a high temperature to shifts the equilibrium to the product; some of the initial natural gas can be burned to heat the reaction. Then, a water gas shift reaction of the carbon monoxide can be applied to reduce the amount of CO and H_2O in the mixture (this reaction is used for all the processes that produced a syngas).

$$CO + H_2O \rightarrow H_2 + CO_2 \qquad (2)$$

after that, a condenser removes all the water remained in the mixture and is recirculated at the beginning for the steam reformer (but is not enough, it's required a water make-up). The last component of the plant is the PSA, pressure swing adsorption, that through the syngas compression the only chemical not adsorbed is the hydrogen and the rest residual chemicals can be recirculated to the combustor that heat the steam reformer. The purity of the produced hydrogen is high (amount of 99.99 %), so can be used for the low temperature fuel cell.

The coal gasification instead exploits coal to produce hydrogen with an autothermal gasification that partially burn coal at high temperature and pressure. Obviously, this type of process required a high number of pre-treatment system to obtain a high-quality hydrogen, for example scrubbers, cyclones, filters, PSA and others that increase the plant cost. There are different types of gasifier and change the amount of ash and slag inside the syngas produced.

The biomass pyrolysis and gasification use local biomass to produce syngas and then, if we want, hydrogen. The typical problem for this type of plant is the TARS production during the gasification. There isn't a single definition of the TARS, but operationally are defined as the organics from the gasification process that are condensed on transfer lines, at inlet of ICEs; instead the IEA in the 1998 defined them as all organics boiling at temperatures above that of benzene. So, these organic compositions can be deposited inside the pipe and cause a block of the plant, but also a deactivation of the catalyst if we use the syngas in a SOFC. The TARS are classified in four different families and the formation depends on the gasification temperature. The formation can be reduced using a downdraft gasifier and avoided with subsequent scrubbers. This process is a thermo-chemical solution with biomass, but an interesting new solution under research is the biological one, considering the reaction with some microorganism to produce hydrogen inside a digestor.

The last process is the water electrolysis, that respect the others is completely renewable and without any contaminant production. It's not the only hydrogen production process that used RES energy but it's the state-of-the-art technology now, because it requires only a flow of electrons and a water supply. This is a very interesting process because of the possibility to store the hydrogen produced by the renewable energy in excess respect to the electrical load and re-used it when is required more energy than the RES supply through a fuel cell. The electrolysis can produce a very high-quality hydrogen, so all the pre-treatment equipment, both for electrolyzer and fuel cell, are not taken into account. The water electrolysis is explained in more detailed in an antecedent chapter.

These hydrogen production processes have different efficiency, evaluated by the ratio between the energy inside the hydrogen produced and the electric/thermal energy or chemical energy at the beginning of the reaction. In the following table average values of the efficiency production are shown.

Table 4 Average efficiency of different hydrogen production processes [34]–[36]

	Efficiency (LHV)
Methane reforming	72 %
Coal gasification	56 %
Biomass gasification	46 %
Water electrolysis	61 %

Other possible solutions using RES energy are thermochemical process and photocatalytic process. The first is a chemical looping, using a metal oxide and water in two steps, one at high temperature and the last at lower temperature. In the first step, a thermal reduction is applied to the metal oxide to generate some oxygen vacancies and oxygen molecular, instead in the second step the metal oxide at lower oxidation degree reacts with water (or other oxygen containing species) to produce the metal oxide at higher oxidation state (to reuse in the first step) and the species with lower oxygen amount. Using water as oxygen containing species, hydrogen can be produced in the second step; all the loop is based on the capability of the metal oxide considered to exchange oxygen. This is a two steps simplification, but usually more than two steps are required to a complete chemical cycle. The photocatalytic process instead, take advantage of the process in a photoelectrode that directly uses the photons instead of transforming them in electrons through a photovoltaic system. But only the photons with a sufficient energy to split the water molecules can be use, so the efficiency is reduced.

3.3 Hydrogen storage

Hydrogen storage is one of the possibility to store the renewable energy when the energy load is less than the energy production and reuse it when is needed; for example with a photovoltaic system is possible to produce hydrogen during the day and produce electricity through a fuel cell during the night.

There are different possibilities to store hydrogen, that are the following:

- Compressed gas
- Liquefaction
- Chemisorption on metal hydrides
- Physisorption

The first method is to store the hydrogen gas in a compressed vessel; the main problem is the very low density of the hydrogen, so a very high pressure is required. At ambient temperature and pression the hydrogen density is only 0.832 kg/m^3 and increase at 28.73

kg/m^3 when the pressure is around 350 bar, the storage pressure in a heavy FCEV as the minibus under study. The hydrogen compression is difficult and expensive, because of the high electric energy needed, due to the high value of specific heat at constant pressure. A possible improvement on the hydrogen compression is the application of membrane compressor in order to avoid contamination of oil; but this type of compressors is more expensive and still under research. The compressed vessel to store hydrogen must have three layers, and can be both spherical and cylindrical. The internal layer must avoid the embrittlement phenomena, that is a mechanical properties degradation due to the H_2 absorption inside the material; this will happen if a metal is selected as internal layer, so a polymer or glass fiber is considered. Between internal and external layer, a wrapping layer must be contained; this layer gives the mechanical structure to the cylinder, so stainless steel or aluminum can be used, but attention must be paid for the mass fraction inside it (to avoid the embrittlement phenomena as explained before). The external layer instead must be metal to resist to mechanical stress, so increase the mechanical properties. This type of hydrogen storage is the market standard now but is not the best solution.

The store of liquid hydrogen instead can be done at very low temperature (hydrogen boiling point at 20.39 K), and a density of 71 kg/m^3 is reached. To cool down the hydrogen at this temperature, a modified Claude cycle can be applied with a cryogenic turbine, and so using a regenerative exchange. The exothermic heat from the transformation orto-para hydrogen at very low temperature must be taken into account; this effect can cause the evaporation of half of the liquid hydrogen in ten days. This transformation must be forced during the liquefaction process through the utilization of a catalyst (for example chromium oxide CrO_2). Another important solution is the application of cryogenic insulated vessels to avoid the problem of heat generated from conduction, convection and irradiation; so, a double cylinder with ultra-low heat transfer material is required. Between the two cylinder walls, the vacuum must be maintained to avoid the conductive and convective heat exchange, instead for the irradiative one a low emissivity coating material is applied on the internal cylinder walls.

The best solutions for the future are chemi and physi-sorption in solid matrixes, where the hydrogen is absorbed in the solid powders. This method can increase the storage density; for example, in metal hydrides the density can reach a value of 180 kg/m^3 but with the problem that only the 2 % of the total storage weight is represent of the hydrogen. This means that this type of storage has a very high weight. From a thermodynamic point of view, an absorption-desorption cycle is applied. We can see that the absorption part is effective

at low temperature, instead the desorption part the opposite (at around 350 °C), so a hysteresis in the real operation is formed reducing the transformation efficiency. From a thermal management point of view, a desorption heat must be supply to the vessel, but there will be a delay in time to move the heat from the external to the center despite the utilization of high thermal conductivity metal powders. So, to speed up the kinetics of reaction a possible solution is to installed some tubes inside the vessel to transport a heating fluid; in this way the time delay is avoided but with the disadvantage of lower vessel volume, that means a lower storage capacity. At present, the best option for metal hydrides is the application of magnesium hydrides (MgH_2).

3.4 P2X and P2G concepts

As we have seen in the chapters before, Power-to-Power (P2P) systems are based on the concept of producing hydrogen via electrolysis when surplus electricity is available, thus storing energy as compressed hydrogen gas [37]. A P2P system includes the following routes, as also explained by the figure below [4]:

- Power-to-hydrogen (P2H), a segment common to all the other routes;
- Power-to-gas (P2G);
- Power-to-liquid (P2L) fuels;
- Power-to-chemicals (P2C).

The liquid and gaseous fuel energy vectors leaving the described process of conversion and storage of electricity can be finally converted back to power, performing the function of time-shifting to cover the power load as required for a P2P system. A P2L system means the production of liquid fuels as CH_3OH (methanol) or CH_3OCH_3 (dimethilether) to substitute diesel fuel in industrial engines or also for mobility. Instead, a P2C system exploits the RES production to convert it into chemical precursors for the production or other chemical in various technical fields; possible solutions can be synthetic diesel, ammonia, plastics, oil etc. At the end, a P2G system means the production of gas fuels; the main solution used now is hydrogen through a water electrolysis system, and different application options can be considered: electricity production through a fuel cell, injection in the natural gas grid and H_2-mobility. In this study the first and the last options are both taken into account.

A P2H and P2P system is considered in this study, and all the possible typologies of hydrogen production and storage have already been explained in previous subchapters. A natural gas grid injection of the hydrogen produced is not feasible for our locations, due to the impossibility of infrastructure work of big dimension in a protected natural area.

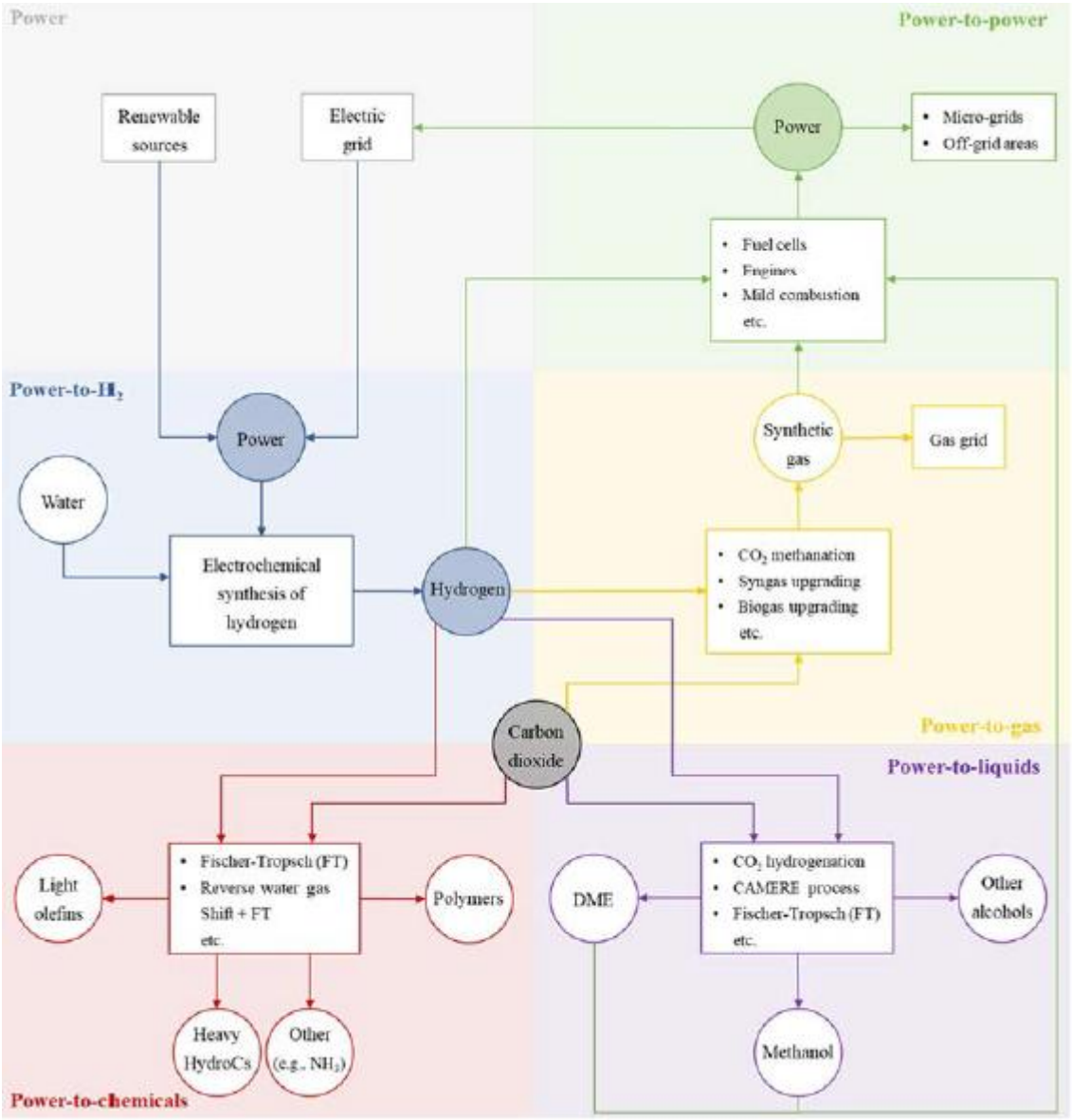

Figure 11 Scheme of the possible routes of the power-to-X concept [4]

As explained by reference [36], there are also some limitations for hydrogen injection, which for other operational options are not there:

- The influence on the gas characteristics, as Wobbe Index and heating value (a maximum of 15 % in tolerable now, but in the future this value will increase)

- The impacts on the gas infrastructure, because of a probably increase in leakage rates, due to a high value of diffusion coefficient for hydrogen
- The decrease in transport capacity, due to the three times lower volumetric heating value of the hydrogen respect to the gas
- The impacts on end user infrastructure, as domestic users, that required the adaption of the burner nozzles is necessary due to the higher flame velocities
- The impacts on underground gas storage facilities, because of the different behavior of hydrogen than other gases with porous materials.

In the following chapter, a detailed study for electricity production from hydrogen and automotive mobility with hydrogen is done.

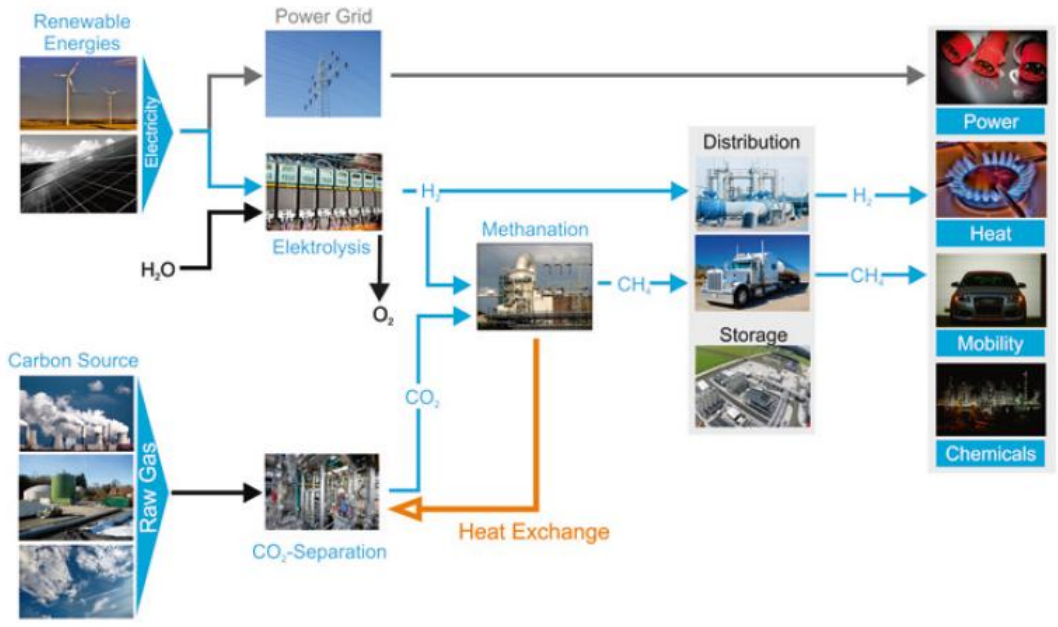

Figure 12 Summarize of different P2G options [36]

3.5 Fuel cell

A fuel cell is an electrochemical cell that through a spontaneous reaction, with the reaction Gibbs free energy lower than zero as the water molecules formation, produce electricity. This type of component is composed by three different layers: anode, cathode and electrolyte. Changing the electrolyte material, the ions transported by it can change and so also the semi-reactions at the electrodes. The electrons and ions flow generate a separation

of charge between the anode and the cathode, and when the external electric circuit between the electrodes is open, we obtain the open circuit voltage from the Nernst equation.

$$OCV = E = -\frac{\Delta g_{reaction}}{z_F \cdot F} = -\frac{\Delta g(T,p_0)}{z_F \cdot F} + \frac{RT}{z_F \cdot F} \cdot ln\left(\frac{\prod\left({}^{p_i}/_{p_0}\right)^{\nu_{reac}}}{\prod\left({}^{p_i}/_{p_0}\right)^{\nu_{prod}}}\right) \quad (3)$$

As we can see from the equation, the reactants and products partial pressure and the reaction temperature will affect the fuel cell Nernst voltage. In detailed, to obtain an improvement in the fuel cell operation, a high reactants pressure, a low products pressure and a high temperature are required; this means that we have to remove as much as possible the products, although when the reaction reach the equilibrium, they can return to the reactants. The voltage value evaluated with the equation before is in ideal condition, and so in open circuit; when the circuit is closed, three different voltage drop effect start to affect the cell, due to the domination of transport phenomena, in order of current increase:

- Charge transfer, considering the ions movement in the electrolyte due to the electrochemical reaction activation; it's represented by activation overvoltage η_{act}.
- Charge transport, for the electron conduction and ions migration due to the ohmic behavior of the cell; it's represented by ohmic overvoltage η_{ohm}.
- Mass transport, when the current increase and new electrons are required, but the reactants diffusion into the electrodes becomes the limiting effect; it's represented by diffusion (or concentration) overvoltage η_{diff}.

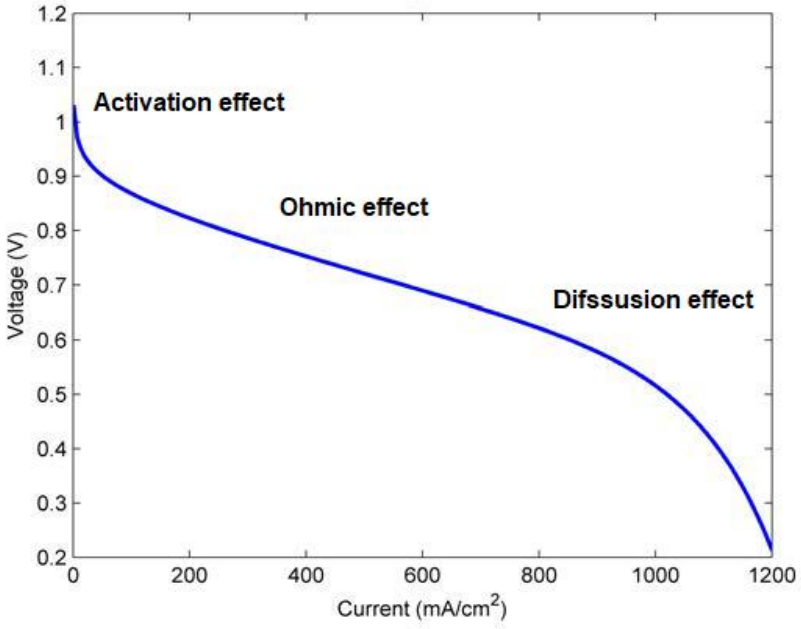

Figure 13 Typical voltage/current fuel cell characteristic [38]

In the previous figure and following relation, typical voltage/current characteristic and cell voltage equation are shown.

$$V_{cell} = E - \eta_{act}(I) - \eta_{ohm}(I) - \eta_{diff}(I) \quad (4)$$

where E is the Nernst voltage evaluated with the equation above in the previous page; as expressed by the relation, the three overvoltages are function of the current.

Fuel cell technologies have different advantages but also disadvantages; in the following list, a summarize of the main ones is done.

Advantages [39]:

- fuel cells are generally more efficient than combustion engines; small systems can be just as efficient as large ones (this is very important in the case of small local power-generating systems needed for combined heat and power systems)
- fuel cells are very simple, with few if any moving parts; this can lead to highly reliable and long-lasting systems
- the byproduct of the main reaction is pure water, when the fuel is only hydrogen, meaning “zero emission”; however, it should be noted that in the production of the hydrogen needed as fuel, the emission of CO_2 is always involved
- fuel cells are very quiet; this is very important in portable power applications and local power generation combined heat and power (CHP) generation schemes.

Instead, fuel cells have two main disadvantages [40]:

- The component durability, that is lower than other energy supply technologies; but the FC lifetime is expected to be improved by continuous research (in a following subchapter, a more detailed deepening on the lifetime is done)
- The component costs, the other major challenge to FC commercialization, but the gap between the ICE cost and the FC system cost has been decreasing during the recent years.

At the moment, two main fuel cell typologies are present in the market:

- Low temperature fuel cell, represented by Proton Exchange Membrane or Polymeric Electrolyte Membrane Fuel Cell (PEMFC);
- High Temperature fuel cell, characterized by Solid Oxide Fuel Cell (SOFC).

The main difference between the two typologies is the electrolyte material; for the PEMFC a polymeric membrane is used, as nafion, instead for the SOFC a solid oxide electrolyte is used, as yttira-stabilized-zirconia (YSZ, ZrO_2 doped with Y_2O_3).

Table 5 PEMFC and SOFC main characteristics

PEMFC	SOFC
• Necessity to maintain the membrane humidified to transfer hydrogen ions → necessity to operate at temperature lower than water evaporation point • No help from temperature in transport phenomena, so a high-quality catalyst is required • Risk of catalyst-poisoning from carbon-containing molecules → ultrapure hydrogen as fuel	• Operates at high temperature, so all the transport phenomena are improved, but a better quality materials for auxiliaries are required • No need of precious catalyst → very good fuel flexibility, it's not required an ultrapure H_2 • Availability of high T heat as by-product • No dynamic machine, it has a slow strat-up and slowest dynamic respect to a PEMFC

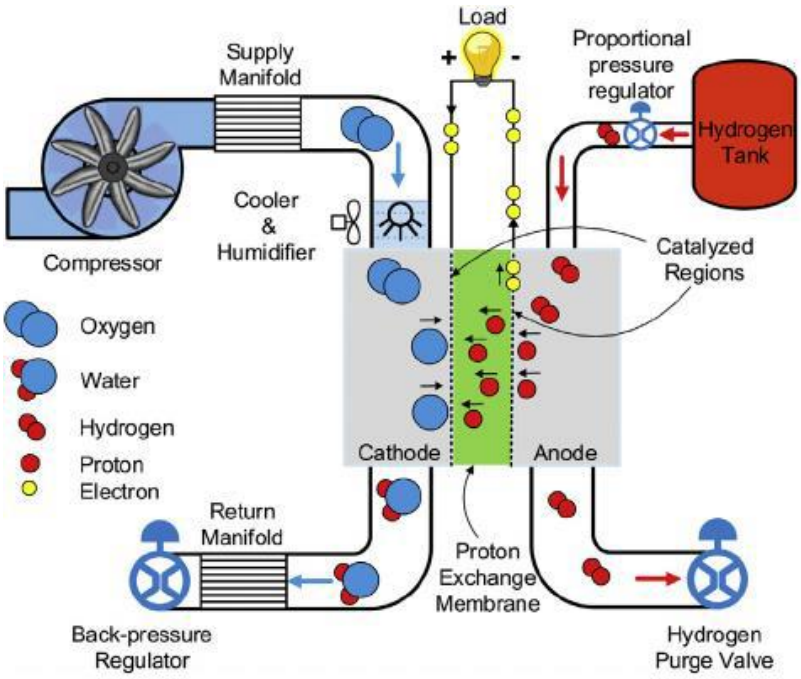

Figure 14 Representation of a PEMFC system including the FC and some of the auxiliary components [41]

In this Master Thesis, only a PEM fuel cell is considered in the standalone system simulation.

3.6 Electrolyzer

An electrolyzer is an electrochemical cell with the opposite operation of the fuel cell; through a non-spontaneous reaction, this is why the requirement of electric power, it splits water molecules in order to obtain hydrogen as product. The main characteristics are the same of a fuel cell, but the equations are a little different, as we can see below from the Nernst equation for a reaction with ∆g higher than zero and from the cell voltage equation.

$$E = +\frac{\Delta g_{reaction}}{z_F \cdot F} = +\frac{\Delta g(T,p_0)}{z_F \cdot F} + \frac{RT}{z_F \cdot F} \cdot ln\left(\frac{\prod\left({}^{p_i}/_{p_0}\right)^{\nu_{prod}}}{\prod\left({}^{p_i}/_{p_0}\right)^{\nu_{reac}}}\right) \quad (5)$$

$$V_{cell} = E + \eta_{act}(I) + \eta_{ohm}(I) + \eta_{diff}(I) \quad (6)$$

In the following figure, a typical electrolyzer voltage/current characteristic is shown, to better understand the difference in operation between a fuel cell and an electrolyzer.

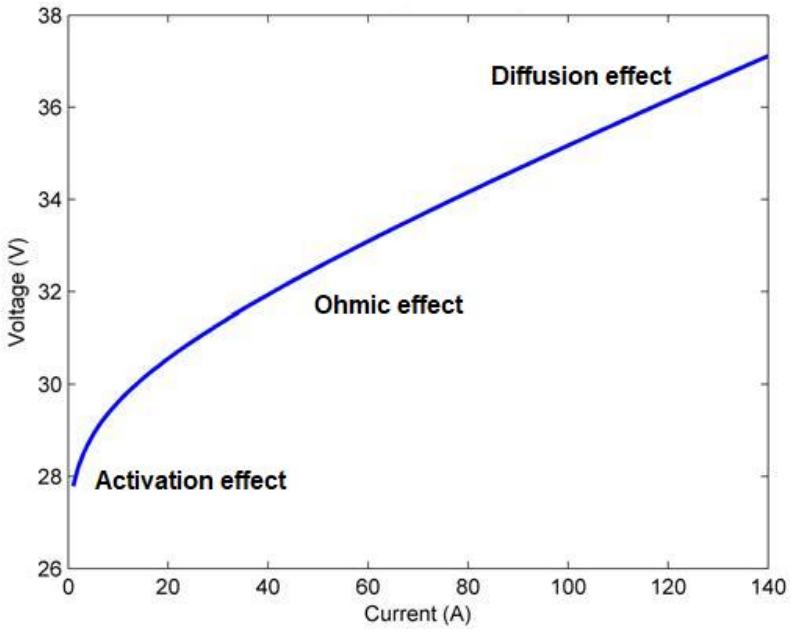

Figure 15 Typical voltage/current electrolyzer characteristic [38]

As seen also for the fuel cell, the electrolyzers are divided in low temperature and high temperature operation; solid oxide electrolyzer cell are the main studied high-temperature electrolyzer, instead for the low-temperature one, as well as the proton exchange membrane electrolyzer cell, also the alkaline electrolyzer cells (ALKEL) are in a great development status. Instead of using a polymer as electrolyte, they use a bland of H_20+KOH (potassium hydroxide) as liquid electrolyte, but with the problem of carbonate production from the reaction with carbon dioxide; a carbonate layer on the electrolyte surface causes the conductivity reduction with a performance worsening. In this Master Thesis, both alkaline and PEM electrolyzer are considered, in order to find the best system configuration; in the following subchapters, also some degradation differences are explained.

Now, a detailed study on the hydrogen production with an under-pressure electrolyzer can be done; a pressurized configuration of electrolyzer is not a free choice, because from the Open Circuit Voltage (OCV) equation below we can observe that working under pressure generates a Nernstian effect.

$$OCV = \frac{\Delta g(T,p)}{2F} + \frac{RT}{2F} ln\left(\frac{p_{H2} \cdot {p_{O2}}^{0.5}}{p_{H2O}}\right) \quad (7)$$

where the OCV is the open circuit voltage of the electrolyzer, $\Delta g(T,p)$ is the Gibbs free energy difference of the water split reaction, F is the Faraday constant (assume equal to 96485 C/mol), R is the ideal gas constant, T is the electrolyzer working temperature and inside the logarithm there is the ratio between the pressure of the products, considering the mole number, and the reactants. A high-pressure electrolysis means high pressure products and so an increase OCV; working at higher voltage requires more electric energy for the water split reaction in the electrolyzer. For these two reasons, we need a trade-off between the electric energy required from the electrolyzer and the electric energy required from the compressor. In the case of a light duty vehicles HRS, the ideal optimal pressure of the electrolyzer is around 50 bar, that means, considering a refueling pressure of 750 bar, an optimal compression ratio of 15 [42].

3.7 FC and EL lifetime

A detailed study is carried out for the lifetime of fuel cell and electrolyzer (both PEM and alkaline) considering the stack lifetime when operates at full charge. From literature we can find the maximum operating hour of the components.

Starting from the proton exchange membrane fuel cell (PEMFC), different studies are taken into account. A maximum operation hours of 30000 h is considered in this master thesis, due to the information find in the works of Marocco et al. [31], of Rullo et al. [18] and also of Kalinci et al. [16]. Different data instead are found in other studies; for example, in the Torreglosa et al. report a maximum lifetime of 23500 hours is considered for a PEM fuel cell [19]. Also, a lower maximum operating hour is counted by Zoulias et al., equal to only 15000 h [20]. Instead, in the work of Gracia et al. a higher lifetime is found, equal to 43800 hours (that corresponds at 5 years in total) [17]. So, an average lifetime value of 30000 hours is a precautionary decision.

A more interesting research for the FC lifespan is done by Torreglosa mentioned before, because they consider as lifetime the sum of two contributions, as we can see from the equation below. The fuel cell degradation is due to an output voltage reduction, that means a lower energy production during the FC life.

$$H_{FC}^{life} = H_{warr} + \frac{V_{fc}^{loss}}{R_{fc}} \qquad (8)$$

where H_{warr} is the initial warranty of the fuel cell in working hours, in which it assured that it does not suffer any voltage degradation at the output, V_{fc}^{loss} is the maximum voltage degradation allowed and R_{fc} is the fuel cell degradation rate [19]. But in addition to a deterioration due to continuous operating hours, the fuel cell also suffers start/stop cycles; starting to work from 0 to the nominal power represent for a degradation the fuel cell equal to 3 hours of continuous operation at the nominal power. Knowing it, Torreglosa found an equation for the evaluation of the real FC working hour that taken into account these two facts.

$$H_{fc} = \frac{P_{fc}}{P_{fc,nom}} + 3 \cdot K_{on} \cdot \frac{Cycle_{fc}}{Cycle_{fc,nom}} \qquad (9)$$

where K_{on} is a parameter that take as value 0 when the FC has a continuous operation respect the hour before and 1 when it starts to work, $Cycle_{fc}$ represents a start/stop cycle from zero to the current fuel cell power P_{fc} and $Cycle_{fc,nom}$ represents a start/stop cycle from zero to the nominal fuel cell power $P_{fc,nom}$ [19]. Considering this solution to find the yearly working hour of the fuel cell in the Ambornetti plant, a more detailed value of lifetime can be estimated dividing the maximum operating hour with this data. But, to avoid a possible

overestimation of the lifespan, the difference between the operation at a power lower than the nominal one is not considered.

A similar research to the fuel cell is done for both the electrolyzers types, PEM and alkaline. But, differently than the first equipment, the electrolyzer has, in addition to a maximum operating hour, also a maximum number of on/off cycles (this is an important consideration due to the fluctuating nature of the RES supply and to the intermittent operation apply in Ambornetti plant). The same study considered before, affirm that in the electrolyzer case the working hours affect its efficiency; this means that its degradation leads to a lower hydrogen production for the same quantity of input electric energy [19]. In the following relation, this fact is reflected.

$$H_{el}^{life} = \frac{R_{el}^{\eta} - 1}{R_{lz}} \qquad (10)$$

where R_{el}^{η} is the ratio between the maximum electrolyzer efficiency without degradation and the minimum efficiency considered and R_{lz} is the electrolyzer degradation rate.

Possible values for both the electrolyzers degradation rate can be found in literature from the Tractebel and Hinicio report and the Raggovidda energy analysis; the first sets as alkaline degradation rate the value of 0.13 % every 1000 hours and for PEM a value of 0.25 % every 1000 hours, and also the second study select a value of 0.25% per 1000 hours for the PEMEL. Also, the same works take as maximum efficiency degradation drop before replacement a value of 10 % [43][44]. Knowing these two data, the maximum operating hour can be evaluated by the ratio between the maximum efficiency drop before replacement and the degradation rate of each electrolyzer, obtaining a value of 76923 hours for alkaline type (Marocco et al. consider a value of 80000 hours [31]) and a value of 40000 hours for PEM type. From other references, different data could be found; for example, for alkaline electrolyzer is usually consider a higher lifespan, as in the work of Stojković et al. that select a lifetime of 10 years (equal to 87600 hours) or in the Siyal et al. study that use 15 years (equivalent to 131400 hours) [15][24]. Instead, for the PEM electrolyzer the data are for the most part the same, as we can see from the first work considered in this report [31]. This value of efficiency degradation drop before replacement (10 %) can be also used for the PEM fuel cell ([45][46]), but in our case we have not any information about a fuel cell degradation rate, so a maximum operating hour is taken from literature. In addition, a more detailed study on the real operating hour is done, so the maximum allowed efficiency drop can be neglected for the PEMFC.

Now, the maximum on/off cycles must be selected. For the PEM electrolyzer the Raggovidda energy analysis mentioned before fixed a value of 5000 [44]. Instead for the alkaline electrolyzer, the range of on/off cycle can be 2500÷10000 for the Ursua et al. study that improve to 5000÷10000 for the Brauns et al. review [47][48]. But a more detailed and updated work of Ursua et al. fixed the maximum on/off cycle for an alkaline electrolyzer equal to 5000, as for the PEM one [49]. Considering a value of 7500 in our study, a more conservative calculation has been made.

A new important study is done by Kuroda et al. for the alkaline electrolyzer, to avoid the electrode degradation due to the fluctuating electricity supply form RES. They demonstrate that the use of a new hybrid cobalt nanosheet suitably modified can form a highly stable self-repairing catalyst layer on a nickel anode under cycled potential [50]. In this way, a longer lifetime can be reached for alkaline electrolyzer, but this new solution is still under research.

To take into account the two contributions to electrolyzer degradation, the following equation is considered.

$$N_{el}^{life} = \left(\frac{H_{el}^{year}}{H_{el}^{life}} + \frac{Cycle_{el}^{year}}{Cycle_{el}^{life}}\right)^{-1} \qquad (11)$$

where H_{el}^{year} is the yearly operating hour, H_{el}^{life} is the maximum operating hour, $Cycle_{el}^{year}$ is the yearly number of on/off cycles and $Cycle_{el}^{life}$ is the maximum on/off cycle allowed by the electrolyzer under study. Considering the two degradation effects, a lower lifetime is obtained for both the electrolyzer types.

In the table below, all the fuel cell and electrolyzer lifetime assumption are summarized.

Table 6 Fuel cell and electrolyzer lifetime assumptions

	H^{life}	$Cycle^{life}$	$H\ per\ Cycle$	References
PEM Fuel Cell	30000	-	3	[16], [18], [19], [31]
Alkaline Electrolyzer	76923	7500	-	[43], [49]
PEM Electrolyzer	40000	5000	-	[43], [44]

3.8 Operational load range

Another important fuel cell and electrolyzer characteristic is the operating load range, because they can work at partial load but not until a very low fraction of the nominal power but also with a higher power than the nominal one.

Starting from the PEM fuel cell, the final report of study on early business cases for h2 in energy storage and more broadly power to h2 applications consider a range of 0÷100 % of the nominal stack power [43]. But a more detailed review is done by Raggovidda energy analysis that study a power range of 10÷110 %, so we can use less the fuel cell at very low power but it can be worked at higher power respect to the nominal one [44]. This last operation range is considered in this study.

Instead for electrolyzer, from the book of Stolten et al. we can see that both the types work in overload, but usually the alkaline not because of the more limited operating range and therefore the nominal load is very high relative to its performance; so, the maximum load considered for an alkaline electrolyzer is equal to the nominal load. However, the minimum operation load selected by Stolten for an alkaline electrolyzer is in the range 20÷40 % [51]. In the Brauns et al. review, a lower range is considered, between 10÷25 %; this is due to avoid the reaching of the lower explosion limit by the gas impurity [48]. A similar reason is explained by Ursua et al, but in this case a minimum partial load is imposed in order to prevent the formation of potentially flammable mixtures of hydrogen and oxygen due to the diffusion of these gases through the membranes when the operating current is relatively low. In this study, a fix value of 25 % respect to the nominal load is selected as lower operating limit [49]. Another study of Ursua et al is considered, but in this case the lower operating limit range is higher, between 25÷40 % [47]. A different fix value is also selected by Tractebel and Hinicio in their report, that is equal to 15 % in 2017 but can become 10 % during the next year until 2025 [43]. In conclusion, a precautionary operating range of 25÷100 % respect to the nominal electrolyzer power is chosen for this study.

For the PEM electrolyzer instead, Stolten et al. study that offers a wide performance range respect to the alkaline one but with a sacrifice in its performance, but they doesn't mentioned any values [51]. From the report of Tractebel and Hinicio we can find that the operating range considered is very wide, between 5÷160 % of the nominal load; the minimum operating load value can also became 0 % during the next until 2025 [43]. But this range decreases for the Raggovidda energy analysis report, that selected for the PEM electrolyzer

dynamic operation a range of 12÷130 % [44]. Instead, in one of the previous deliverable report of REMOTE project, we can find that a minimum operating load of 10 % is fixed [28]. The reason to don't work at very low partial load in this case is not given to a safety reason as for the alkaline electrolyzer, but to avoid a too low PEM electrolyzer efficiency during the operation [51]. So, a precautionary operating load range of 10÷130 % of the nominal electrolyzer power is selected for this study.

In the following table, all the operating range assumptions are summarized for each electrochemical component.

Table 7 Operating range assumptions and their references

	Operation load range	**References**
PEM fuel cell	10÷110 %	[44]
Alkaline electrolyzer	25÷100 %	[49], [51]
PEM electrolyzer	10÷130 %	[28], [44]

4 Modeling and methodology

To understand in detailed the behavior of our system, an annual energy simulation is done with an energy management strategy (EMS), to prove the effectiveness of the RES+P2P system proposed by the remote project to meet all the local electrical demand. Two energy storage systems are used initially: battery, as a short-term ESS that absorb/provide electricity as first option, and hydrogen tank as long-term ESS that operates only when the battery reaches its minimum or maximum operation limits. In the following figure, we can see the effectiveness of using an energy storage system in a typical day of July for Demo 3.

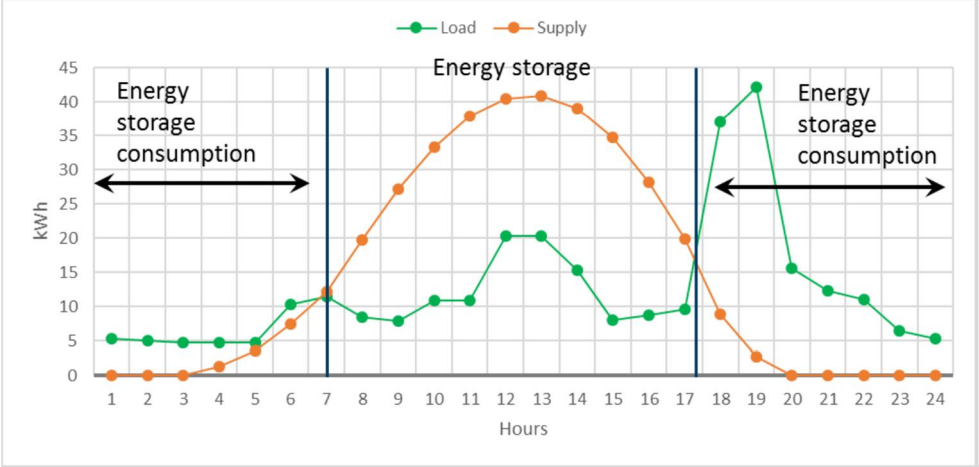

Figure 16 Modelled energy supply (PV) and load and potential for utilization of energy storage for a representative day in July (Ambornetti) [30]

In the EMS, the main key decision factors are the battery State Of Charge (SOC) and the hydrogen tank Level Of Hydrogen (LOH). After the evaluation of maximum and minimum battery SOCs, we can now understand when fuel cell and electrolyzer switch on or off; when RES supply is higher than the electrical load, only when battery SOC lies between its operational range the electrolyzer can produce hydrogen to fill up the tank. Same reasoning for the fuel cell, that can start to produce electricity (when RES supply is lower than electrical load) only if the battery SOC is in the operational range. Instead, considering the hydrogen tank LOH, the electrolyzer can work until the H_2 tank is full and the fuel cell can operate only if enough hydrogen is present in the container. Also the fuel cell and the electrolyzer have an operational range, and depends on the technology under study (as we as seen in a

previous chapter); but a maximum load of 100 % is considered for all the technologies in order to avoid a component undersizing [28].

The computational time step is defined as 1 hour in this current study and is defined as ∆t. It is used to computed different parameter during the simulation, as the battery SOC with the equation below.

$$SOC(t+1) = SOC(t) + \frac{P_{BT,c}(t)\cdot\Delta t\cdot\eta_{BT,c}}{C_{BT}} - \frac{P_{BT,d}\cdot\Delta t}{\eta_{BT,d}\cdot C_{BT}} \qquad (12)$$

where $P_{BT,c}$ and $P_{BT,d}$ represent the battery charging/discharging power, C_{BT} is the nominal battery capacity and $\eta_{BT,c}/\eta_{BT,d}$ stand for the battery charging/discharging efficiency. We have to control the battery charging/discharging power in order to avoid the overshoots of the limits range. Similarly, we can evaluate the storage tank LOH with the following relation.

$$LOH(t) = LOH(t-1) + \frac{P_{EL}(t-1)\cdot\Delta t\cdot\eta_{EL}}{C_{H2}} - \frac{P_{FC}\cdot\Delta t}{\eta_{FC}\cdot C_{H2}} \qquad (13)$$

where P_{EL} and P_{FC} correspond to the electrolyzer/fuel cell operating power, C_{H2} stands to useful capacity of the hydrogen storage tank and η_{EL}/η_{FC} represent the electrolyzer/fuel cell efficiency. As for the SOC before, the maximum electrolyzer/fuel cell working power is controlled to not allow to go above/below the LOH limits.

During an energy supply surplus, as in the first logical block diagram below, the part of energy produced in excess is first used to charge the battery. When the maximum SOC is reached, if there is other energy surplus, it is supplied to the electrolyzer to produce H_2 to fill the storage tank; the electrolyzer works only between its operational range, so within a minimum and maximum working power. When a LOH equal to 1 is reached, that means a completely filled hydrogen vessel, the remaining energy excess produced by RES is curtailed.

Different behavior instead during an energy supply deficit, as shown in the second logical block diagram below. The energy request to satisfy the load completely is provided by the battery and the fuel cell, depending on the battery SOC; first, the battery is used but when the minimum SOC is reached, the fuel cell is activated to prevent the battery over-discharging. Also the fuel cell, as the electrolyzer, works between its minimum and maximum operating limits, but only if enough hydrogen is contained in the storage tank. When the electrical load in excess is lower than the minimum fuel cell power, the EMS forces the fuel cell to work at its minimum point, and the energy produced surplus is used to charge the

battery or curtailed. Instead, when the electrical load to cover with the fuel cell is higher than its maximum working power, an external power source is required to satisfy the power deficit.

In the following figures, charging and discharging logical block diagrams are shown to better understand how the system works. The hydrogen required for the mobility part of the total load is not considered in the diagrams but is studied in the new system configuration, as also explained in antecedent chapters.

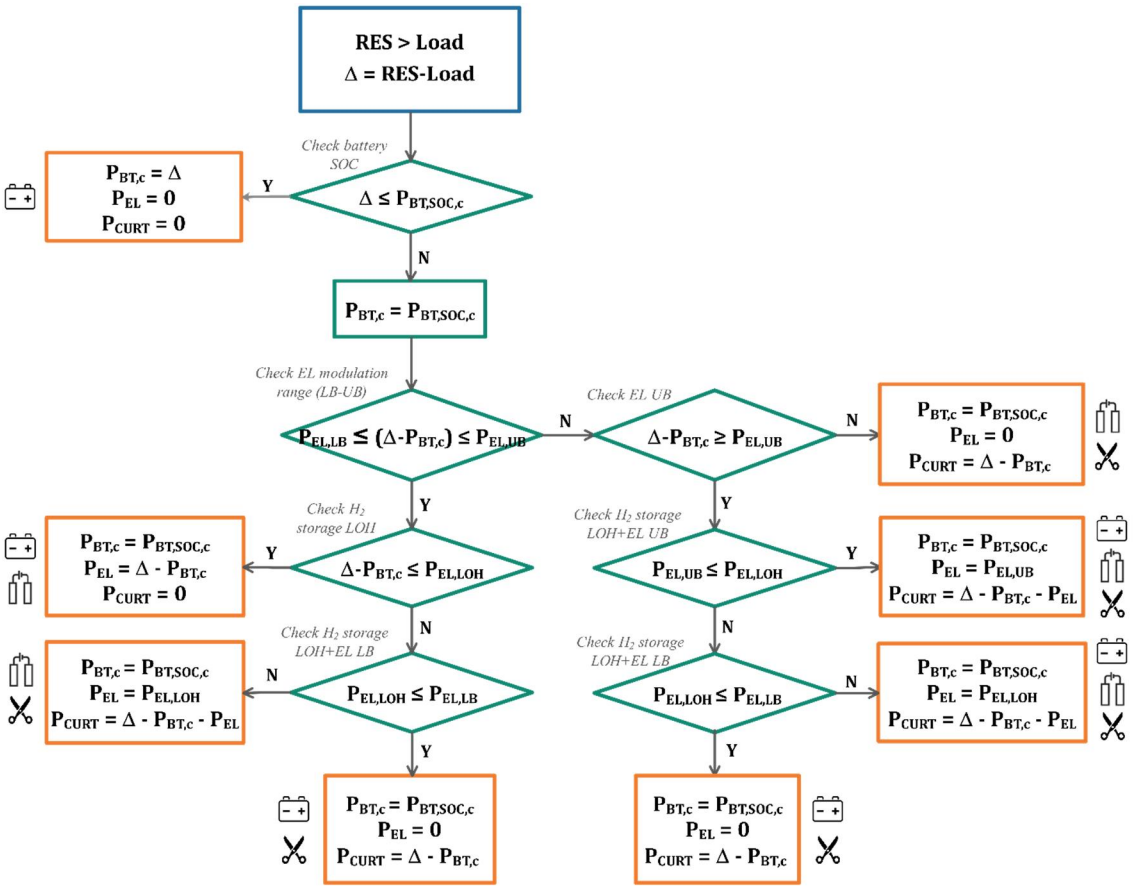

Figure 17 Logical block diagram for the charging case (RES higher than load) [31]

To find the optimal configuration of the system, an optimization algorithm is applied, as explained in a following chapter. To avoid the utilization of external source to satisfy the electrical load in excess (as a diesel generator), the bond of maximum percentage external power is controlled; configurations with a LPSP (Loss of Power Supply Probability) higher than its maximum value are not considered.

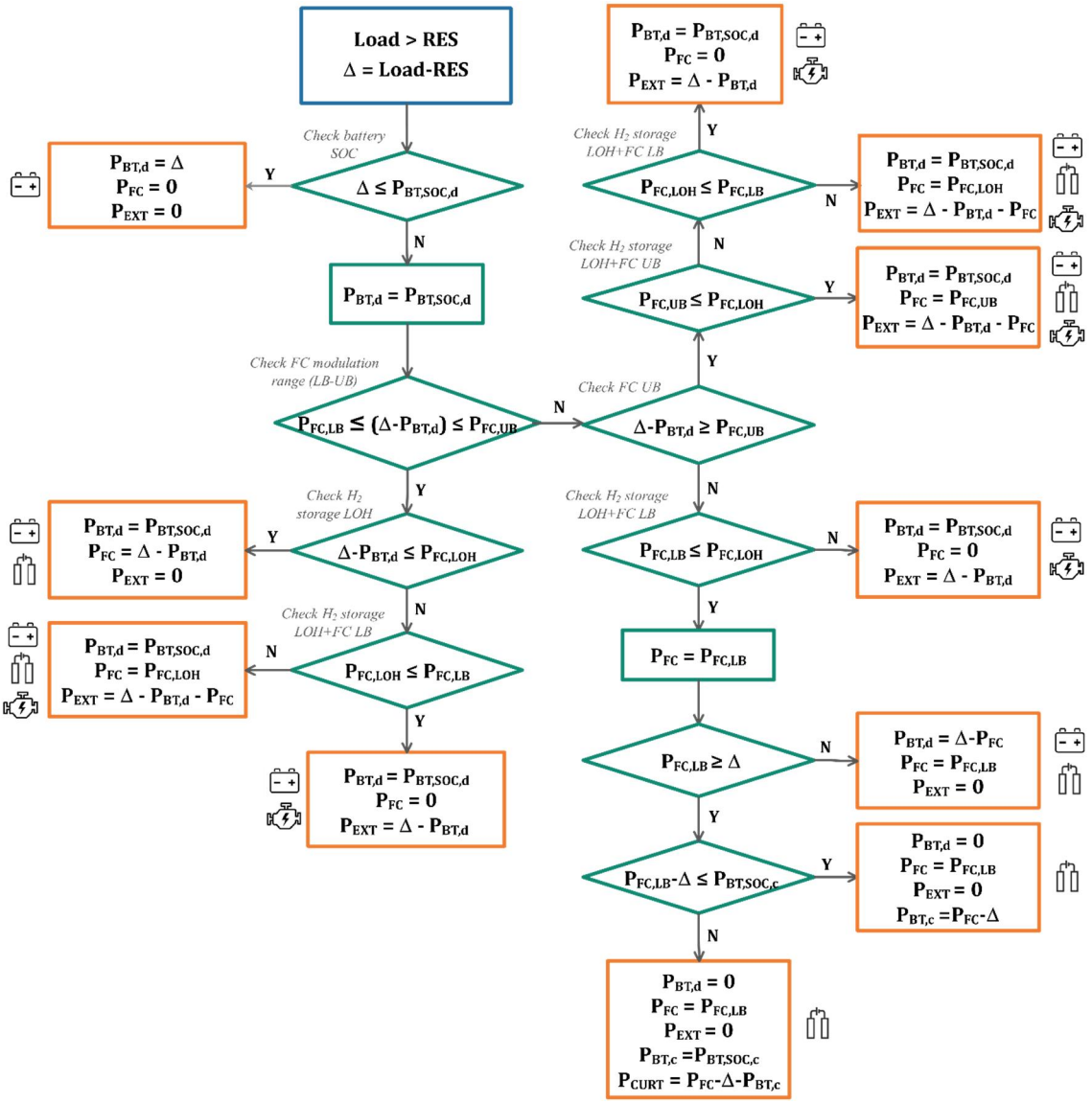

Figure 18 Logical block diagram for the discharging case (RES lower than load) [31]

4.1 System configuration

In the initial system configuration, all the components considered in the two figures (17) and (18) are studied. In the following subchapters, each single component is explained.

4.1.1 Electrical load

As we as seen in a previous chapter, Ambornetti is a remote hamlet of the Italian Alps with a local residential electrical load to be satisfy. The annual energy demand required by this

village is around 348 MWh and no relevant variation during the year can be found [31]. In the graph below, a typical energy variation during the day for each month is shown.

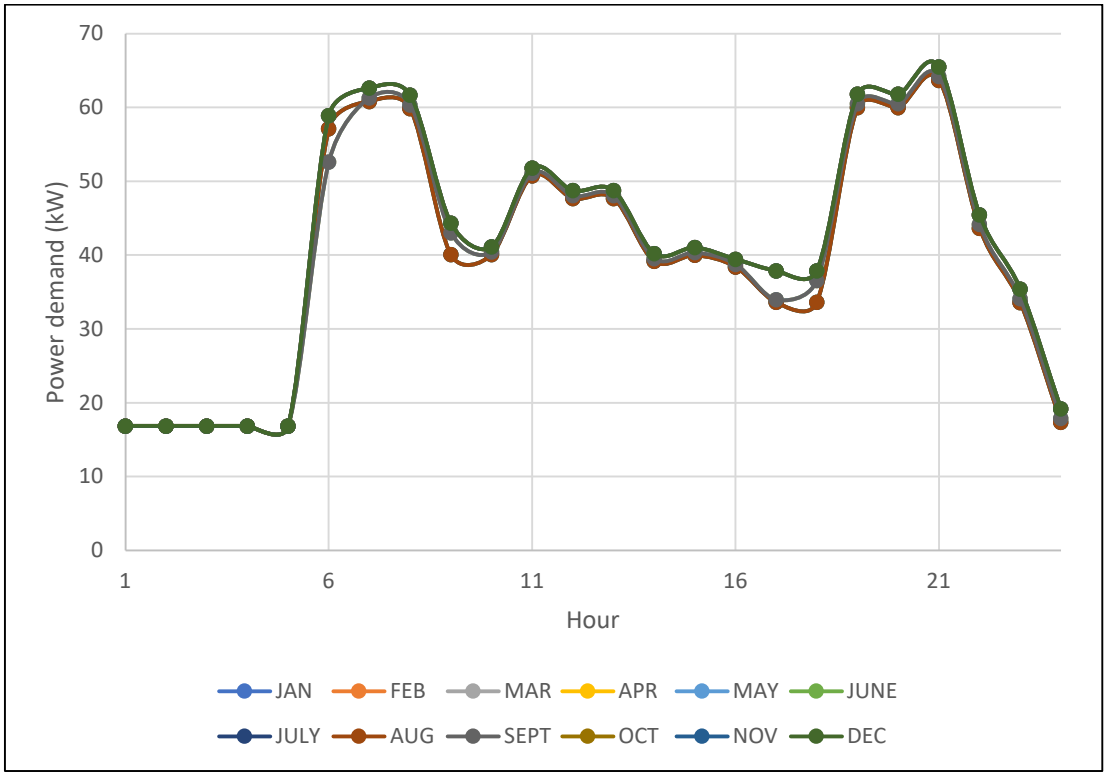

Figure 19 Typical daily variation of power demand for each month

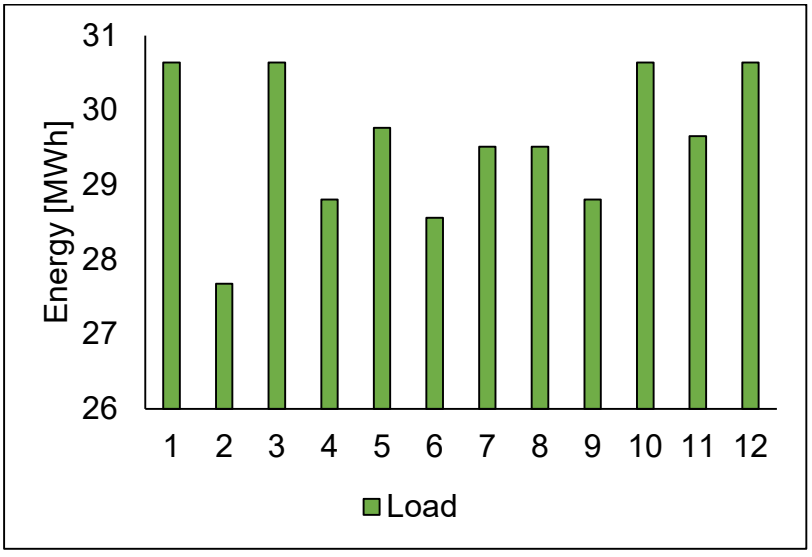

Figure 20 Monthly distribution of Ambornetti's electrical load

Instead, in the second graph above, an average monthly energy demand is explained, to better understand the neglecting variation. The main variations are due to the less days number of the month, as we can see from the February energy requirement; instead, during winter, for month with the same days number a very little increase of energy demand can be seen.

4.1.2 PV system

All the RES data are taken from PVGIS software [52]; in this site it's possible to take the TMY, typical meteorological year, that is a .csv file with the hourly data of the following parameter for an entire year:

- T2m: 2-m air temperature (degree Celsius)
- RH: relative humidity (%)
- G(h): Global irradiance on the horizontal plane (W/m2)
- Gb(n): Beam/direct irradiance on a plane always normal to sun rays (W/m2)
- Gd(h): Diffuse irradiance on the horizontal plane (W/m2)
- IR(h): Surface infrared (thermal) irradiance on a horizontal plane (W/m2)
- WS10m: 10-m total wind speed (m/s)
- WD10m: 10-m wind direction (0 = N 90 = E) (degree)
- SP: Surface (air) pressure (Pa)
- W wind: Power that can be produce by the wind (W)

So, starting from the G(h) and the WS10m the energy produced by a photovoltaic system and a wind turbine can be evaluated.

The geographical information to add in the PVGIS software are tabulated below:

Table 8 Geographical information

Location	*Borgata Ambornetti, Ostana (CN)*
Latitude (decimal degrees)	44.708
Longitude (decimal degrees)	7.177
Elevation (m)	1587.0

The relation to calculate the power produced by a photovoltaic panel is the following

$$W_{PV} = G \cdot A \cdot \eta_{st} \cdot PR \qquad (14)$$

where G is the global irradiance on the horizontal plane, A is the area of the photovoltaic plant, η_{st} is the standard efficiency of a photovoltaic panel and PR is the performance ratio.

The global irradiance varies hourly during the year, instead the plant area and the standard efficiency are constants and equal to the values, respectively, of 357.14 m^2 and 0.21. This value of area is related to a 75 kW plant; considering a standard irradiation G_{st} of 1000 W/m^2 and the following equation the value of area can be calculated

$$A = \frac{W_{nom}}{G_{st} \cdot \eta_{st}} \quad (15)$$

Different things instead for the performance ratio. PVGIS site provides a monthly average for this parameter, that is evaluated with the equation below

$$PR = \frac{E_M}{H_M} \qquad (16)$$

where E_M is the monthly energy output from fix-angle PV system and H_M is the monthly in-plane irradiation for fixed angle. In the following table are shown the PR values for each month, considering a free-standing PV plant on PVGIS software.

Knowing all this data values, we can evaluate the total energy production in one year, that is the sum of the power at which our plant work for each hour; so, in Borgata Ambornetti, a 75 kW PV plant produce 71.69 MWh, that means 956 equivalent hours.

But a more detailed model is selected for the PV energy produced evaluation, considering also the real cell temperature and the real total irradiance over a tilted surface, taking the optimal panel slope from the PVGIS site of 41° in the Ambornetti location [52].

Table 9 Performance Ratio monthly average values (free-standing plant)

	E_M	H_M	PR
January	70.1	80.47	0.871132
February	77.33	89.81	0.86104
March	97.91	116.16	0.842889
April	100.53	121.96	0.824287
May	110.8	137.4	0.806405
June	107.74	136.32	0.790346
July	122.03	156.26	0.780942
August	114.99	146.71	0.783791
September	99.16	123.9	0.800323
October	86.71	104.49	0.82984
November	70.86	83.4	0.84964
December	69.15	79.68	0.867846

For the cell temperature, the following relation is considered, in accordance with different previous studies [53]–[57].

$$T_{cell} = T_a + \frac{G}{800} \cdot (NOCT - 20) \qquad (17)$$

where T_a is the ambient temperature, G is the solar irradiation over a tilted surface (in W/m^2) and NOCT corresponds to the Normal Operating Cell Temperature, that is taken equal to 45 °C.

Then, to find the real total irradiance for an inclined panel, different solar geometrical parameters must be found. The following equation can be applied to evaluate the angle of incidence of beam solar radiation on the surface whatever oriented and tilted:

$$cos(\theta) = \cos(\beta) \cdot cos(\theta_z) + \sin(\beta) \cdot sin(\theta_z) \cdot \cos(\gamma_s - \gamma) \qquad (18)$$

where β is the optimal panel slope, θ_z is the zenith angle, γ_s represent the solar azimuth and γ corresponds to the surface azimuth; all the parameters are calculated in decimal degrees. If the θ angle is higher than 90°, it means that the sun is behind the surface.

To evaluate the zenith angle, the equation below is used.

$$cos(\theta_z) = cos(\Phi) \cdot cos(\delta) \cdot cos(\omega) + sin(\Phi) \cdot sin(\delta) \quad (19)$$

where Φ is the latitude, δ represents the earth declination (evaluated with the equation (20) as a function of the ordinal day of the year n) and ω corresponds to hour angle (relation (21)).

$$\delta = 23.45 \cdot sin\left(360 \cdot \frac{284+n}{365}\right) \qquad (20)$$

$$\omega = (h - h_{culm}) \cdot \frac{360}{24} \qquad (21)$$

where h is the standard time and h_{culm} is the noon time, that is the time when the sun is at its highest point above the horizon (crosses the local meridian); The hour angle represents the angle between the observer meridian and the sun meridian plane (and it is positive towards east). To find the noon time, the following relation is considered as a correction to the standard noon time at 12 a.m.

$$h_{culm} = 12 + \frac{L_{loc} - L_{ref}}{15} - \frac{EOT}{60} + DST \qquad (22)$$

where $L_{loc} - L_{ref}$ is the difference in longitude between the observer's meridian and the longitude of the meridian for the local time zone (longitude is supposed positive towards West), EOT represents the Equation Of Time in minutes (expressed in the relation (23)) and DST is the Daylight Savings Time, equal to 1 (and not 0) only when it's in force.

$$EOT = 229.2 \cdot (0.000075 + 0.001868 \cdot cosB - 0.032077 \cdot sinB - 0.014615 \cdot cos2B - 0.04089 \cdot sin2B) \qquad (23)$$

considering B a value expressed in the equation below.

$$B = (n - 1) \cdot \frac{360}{365} \qquad (24)$$

Instead, for the solar azimuth the arccosine of the following equation is used.

$$cos(\gamma_s) = \frac{cos(\theta_z) \cdot \sin(\Phi) - \sin(\delta)}{sin(\theta_z) \cdot \cos(\Phi)} \qquad (25)$$

The range value of γ_s is between -180°÷180° and has the same sign of the hour angle.

So, knowing the corrected slope of the surface θ, the following relation of the total irradiance over a tilted surface is selected, with the value expressed in W/m^2 (as all the other irradiation variables).

$$G_t = G_{b,n} \cdot cos(\theta) + G_{d,h} \cdot F_{c\_s} + G_{t,h} \cdot \rho_g \cdot F_{c\_g} \qquad (26)$$

where $G_{b,n}$ corresponds to the direct normal irradiance, $G_{d,h}$ is the diffusive irradiance on the horizontal surface and $G_{t,h}$ is the total irradiance on the horizontal surface (all taken frm PVGIS site [52]). The others are dimensionless parameters, corresponding to the albedo of ground for ρ_g (considered as a recommendation equal to 0.2 in average when no more

information are available [58], [59]), the collector sky view factor for F_{c_s} and the collector ground view factor for F_{c_g}. The lasts two parameters can be evaluated by the equations below as function of the panel slope β.

$$F_{c,s} = \frac{1+\cos(\beta)}{2} \qquad (27)$$

$$F_{c,g} = \frac{1-\cos(\beta)}{2} \qquad (28)$$

After the evaluation of the real cell temperature and the total irradiance over a tilted surface, the following equation to find the PV power produced can be applied, in accordance with a high number of previous studies [55]–[57], [60]–[63].

$$P_{PV}(t) = f_{PV} \cdot P_{PV,rated} \cdot \frac{G}{G_{STC}} \cdot \left(1 + \gamma \cdot \left(T_{cell} - T_{cell,STC}\right)\right) \qquad (29)$$

where f_{PV} is the derating factor (taken equal to 82% [60]), $P_{PV,rated}$ is the nominal power of the PV plant, G_{STC} is the standard tests condition irradiation (equal to 1 kW/m^2), γ represent the temperature coefficient (considered equal to -0.003 1/K [64]) and $T_{cell,STC}$ is the standard tests condition cell temperature, equal to 25 °C.

With these hypotheses, the total energy production by a 75 kW PV plant in Borgata Ambornetti is reduced from 71.69 MWh to 69.01 MWh, with an equivalent hours value of 920.

4.1.3 CHP system

A CHP supply system is also considered in the initial isolated microgrid configuration, but, in this way, although it can be treated as a renewable solution, the energy production system will not be completely CO_2-free. To partially compensate this problem, biomass will be supplied from surrounding forests management and local agricultural waste, with the aim of maximizing the same CO_2 absorbed during the life of the biomass used. The CHP generator taken into account is the Biomass CHP HKA 49 of the Spanner Re² GmbH company; this is because the initial size of 49 kW [65].

This type of system is able to work up to 8500 h in one year, although require a maintenance work that is schedule every 300 hours. In particular, the CHP considered provides a constant useful electric power of around 41 kW, because the remaining 8 kW are self-consumed for the generator operation [31]. The main advantage of the CHP utilization respect to a

photovoltaic system is the more predictable and stable energy production, also considering the maintenance but neglecting possible failures during the operation.

4.1.4 Others component

Also other components are required in the system that are fuel cell, electrolyzer, hydrogen storage system and battery. They have already been explained in detail previously, so, only a little description is done. The fuel cell is used to convert hydrogen into water and electricity, in order to meet all the local load when an energy deficit from RES occurs. The hydrogen required by fuel cell is store in a compressed hydrogen storage system; this choice is done because of the more market presence of this storage system typology respect to liquefaction process and chemi/phisy-soprtion. To fill up the storage system, an electrolyzer is used; the operation is the opposite than a fuel cell, so water and electricity are used to produce hydrogen. The electricity is taken from RES when an energy surplus occurs; in this way, energy waste is avoided and the energy supply reliability increase. Instead, the battery system is recharged only when both electrical load and hydrogen storage are satisfied; this system is mainly used for plant start-up and transient, not acting therefor as energy buffer.

4.2 New configuration

In this study, a new system configuration is considered respect to the previous one of the REMOTE project, to take into account also the hydrogen mobility load required by the hydrogen refueling station. In the HRS, an extra electrical supply is needed, in order to guarantee the compressor operation; this electrical energy is added to the electrical load of Borgata Ambornetti. Also a new energy supply system is studied: a production evaluation of a wind turbine is done to understand a possible alternative or supplementary solution to the photovoltaic system. Instead, the auxiliary battery system is not considered in the simulation but only in the economic analysis, because of its little use only for fast transient of electrical load. With these new components, a new sizing optimization must be done to find the optimal system configuration, considering, in this case, also a second optimization bond: LHSP (Loss of Hydrogen Supply Probability), that represents the hydrogen for the mobility load provided by an external source. An initial simulation LOH value different than zero must be considered when a completely RES-based system without CHP is studied; this is because

during the first hours of the year, a minimum electrical load different than zero must be satisfy and a PV-system can't produce during night without solar irradiance. So, only the fuel cell can meet the load required but with a completely empty hydrogen storage tank it cannot produce the energy needed. In the case instead of a PV-CHP hybrid system, the initial electrical load can be satisfied by biomass.

During the charging operation of the system, the logical block diagram changes; in this case, the battery is not considered, so the energy surplus is directly used to produce hydrogen through the electrolyzer. The limits are the same as before, and so the electrolyzer operating range and the maximum and minimum LOH of the storage tank. Instead during the discharging operation, the fuel cell is immediately activated to meet the energy deficit, always respecting its working range and the LOH. But a new energy load is added at the system, that is represented by the hydrogen refueling station; during the day, in a certain period of time an amount of hydrogen is required from the storage tank. The energy load is not electrical as for the residential ones in Ambornetti but is in hydrogen form; this is because the minibus used is a FCEV (Fuel Cell Electric Vehicle) and produced energy from hydrogen with a fuel cell. Only if the storage tank LOH is between is operational range we can provide the hydrogen to the HRS; otherwise, an external hydrogen source is required.

In the following subchapters, all the new components considered in the study are explained.

4.2.1 Wind turbine

First of all, a wind turbine model must be selected, because for each type of turbine there are different power curves. A power curve is a function that describe the power generated by a turbine with different wind speed. From the web, the Wind Energy Solution BV turbine is taken [66]; this is because their turbines have a low cut-in velocity, that is the wind speed at which the turbine starts to rotate. in more detailed, the chosen turbine is the WES50, and so a turbine with a nominal power of 50 kW. In the Fig. 21 and Fig. 22, there are its general technical specifications and power curve [67].

To improve at maximum the wind speed, the maximum tower height is selected, equal to 30 m. The wind speed increase with the height, and the relation to take it into account is

$$v_Z = v_0 \cdot \left(\frac{z}{z_0}\right)^{\alpha} \qquad (30)$$

where v_Z is the wind speed at the height we want to study (30 m), v_0 is the wind speed at the reference height (10 m), z and z_0 the two heights considered and α is the Helmann coefficient.

Life expectancy:	Minimum 20 years
Rated power:	50 kW
Cut in Wind speed:	< 3 m/s (6.7mph)
Cut out Wind speed:	25 m/s (56mph)
Rated wind speed:	9,5 m/s (21mph)
Survival wind speed:	52,5 m/s (117mph)
Wind class:	III
Yawing:	Active
Passive power regulation:	Blade-angle adjustment
Active power regulation:	Fully variable back-to-back IGBT system
Towers heights:	24 m, 30 m (31 m lattice)
Number of blades:	2
Rotor diameter:	20 m
Noise emission at 8 m/s:	45 dB(a) at 100 m
Operating temperatures:	from -20°C up to + 40°C

Figure 21 General technical specifications of WES50 wind turbine

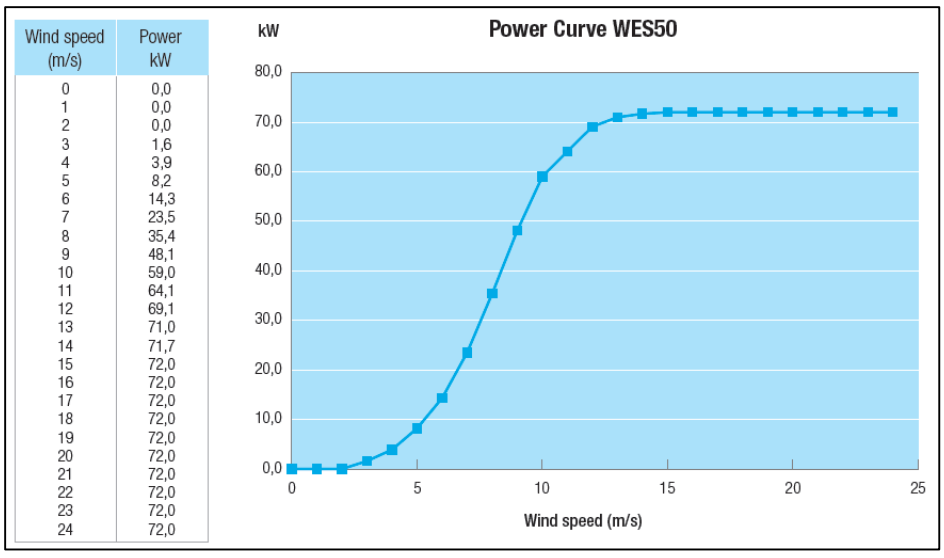

Wind speed (m/s)	Power kW
0	0,0
1	0,0
2	0,0
3	1,6
4	3,9
5	8,2
6	14,3
7	23,5
8	35,4
9	48,1
10	59,0
11	64,1
12	69,1
13	71,0
14	71,7
15	72,0
16	72,0
17	72,0
18	72,0
19	72,0
20	72,0
21	72,0
22	72,0
23	72,0
24	72,0

Figure 22 Power curve of WES50 wind turbine

Now, the Helmann coefficient is required; in a mountain location as Borgata Ambornetti, it's not easy find a constant coefficient. So, in literature, the Justus empirical law is chosen [68] to obtain a value of α for each hour of the year:

$$\alpha = \frac{0.37 - 0.088 \cdot \ln(v_0)}{1 - 0.88 \cdot \ln\left(\frac{z_0}{10}\right)} \qquad (31)$$

where v_0 and z_0 are the reference wind speed and height (in my case 10 m from PVGIS).

So, calculating the wind speed value at 30 m we can evaluate also the power produced by the WES50 turbine using an easy MATLAB program. Summing all the hourly power, we find the energy produced in one year, that is 2.95 MWh. It's a very low value, because it means 59 equivalent hours; obviously it's not acceptable, but probably this is because a closed mountain valley like Po valley is not so windy.

4.2.2 Hydrogen refueling station

For the refueling of the hydrogen minibus considered in the study, we need a hydrogen refueling station. As explain by the EVTC study [69], the components that we need are the following:

- Water tank (comprising of deionizer and purifier for the water)
- Electrolyzer
- Hydrogen storage tank
- Compressors
- Dispenser (including air dryer and filters)

The electrolyzer doesn't need a Pressure Swing Adsorption (PSA) or other purifier for the hydrogen produced because, respect to the steam methane reforming case, it already has a fairly high quality. Anyhow, we could assume that all the H_2 purification components are included in the electrolyzer.

The delivery pressure for mobility application is usually around 350 bar; but two standard pressure for the hydrogen storage in the vehicles are considered: 350 bar for heavy-duty vehicles as buses or trucks, and 700 bar for conventionally light-duty vehicles as cars [43], [70].

The EVTC study also assume that for stations in remote areas with a constant and a small demand are best suited for onsite H_2 production, as our case of Borgata Ambornetti.

Moreover, it considers that a water electrolysis plant has a small capacity respect to the others type of production, in the range of 30-100 kg_{H2}/day [69].

In literature, different studies on an HRS for heavy duty vehicles as buses are found, but in most of them the hydrogen is only use for automotive. Instead in our case, the hydrogen is also used to produce electricity, through a fuel cell, when the energy demand from the load is higher than the energy produces by the RES plant. In figure 23, a typical HRS for heavy duty vehicles is represent; as we can see, the hydrogen is stored at high pressure (between 400 to 450 bar), so all the H_2 produced is compressed to reach it. In the figure, we can also observe the technical information about each plant components from the study of Ulleberg et al. [21]. Also in other two studies, Viktorsson et al. and Nistor et al., consider a storage at the pressure of 450 bar [71][23]. Another study (Weinert et al. [72]) also consider a high pressure storage of 432 bar for heavy duty vehicles, and the water electrolysis solution considers a H_2 production of 30 kg/day. A similar pressure value of 438 bar is considered also in the Wong report [73]. Instead in the studies of Bongjin et al. and Monforti Ferrario et al. [74][75], the hydrogen storage is carried at the pressure of 400 bar.

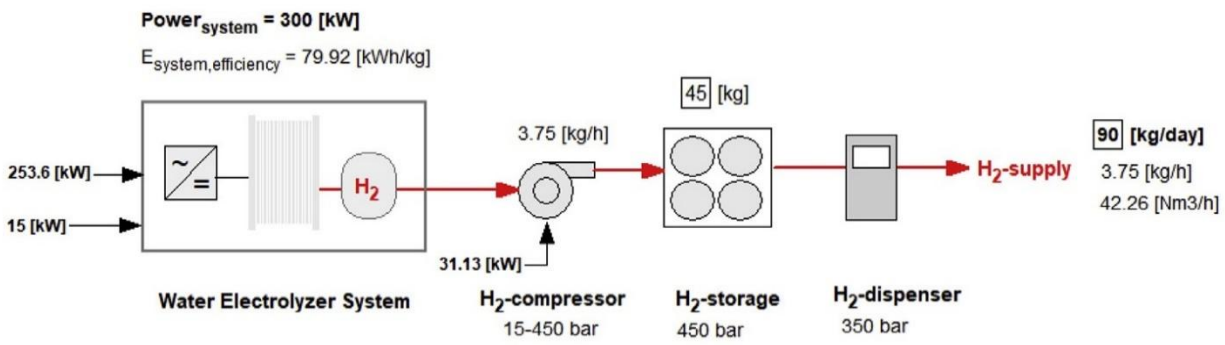

Figure 23 Typical HRS configuration for heavy duty vehicles [21]

In the next figure instead, it's represented the initial HRS configuration in the case of Ambornetti's system (the part about the electrical load was not considered). It's better store the hydrogen at lower pressure and only when it's required from the minibus compress it in the delivery station; this is because if we compress all the hydrogen produced we spent too much energy, because with a high portion of it we can work at lower pressure in the fuel cell.

The only motivation to use a high pressure storage is that minimize the storage volume. In the figure below, some technical information are not yet present.

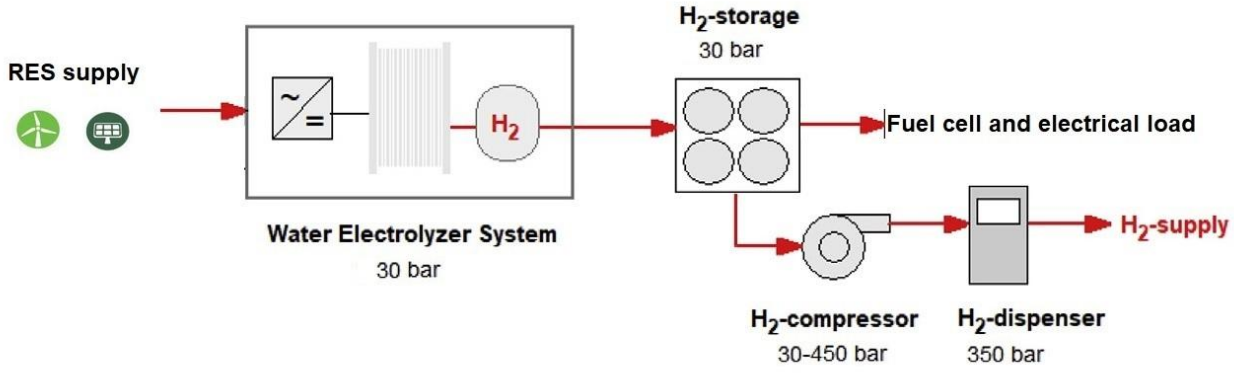

Figure 24 Ambornetti's initial HRS configuration

As explained in a previous chapter, working under pressure at 30 bar for an electrolyzer increase the voltage and so the energy required, but decrease the energy required to compress it before the dispenser of the refueling station.

To reduce the specific work required by the compression, we can perform the electrolysis under pressure reducing the compression ratio [42], as we can see from the equation below.

$$l_C = \frac{c_{p,H2} \cdot T_{in}}{\eta_{is,c}} \left(\beta^{\frac{k-1}{k}} - 1 \right) \qquad (32)$$

where $c_{p,H2}$ is the specific heat at constant pressure (for H_2 is assume around 14000 J/kg/K), T_{in} is the inlet hydrogen temperature, $\eta_{is,c}$ is the compressor isentropic efficiency (assume equal to 0.7), β is the compression ratio and k is the isentropic exponent (assume equal to 1.408 for H_2). So, increasing the inlet pressure the compression ratio is reduced.

But a pressurized configuration of electrolyzer is not a free choice, because from the Open Circuit Voltage (OCV) equation below we can observe that working under pressure generates a Nernstian effect, as seen in the previous electrolyzer subchapter.

From literature, we can also find some studies that use electrolyzers under pressure. For example, in the work of Santarelli et al [37], the electrolyzer pressure is around 20 bar, that are also the relative hydrogen storage pressure. Instead in the study of Zhao et al., that propose a system configuration similar to the Ambornetti's plant (water electrolysis + fuel

cell + HRS), consider an electrolyzer that work at the pressure of around 14 bar (≈ 200 psi) but the hydrogen produced is than compressed at higher pressure (not specified but lower than 350 bar) and stored in a tank [76].

The refueling duration change during the years, and we can say that a time between 10 to 30 minutes can be considered. In particular, the report of Dispenza et al. selects a refueling of 30 min [77]; instead in the Fuel Cells and Hydrogen Joint Undertaking report, it's studied that the required refueling time has dropped from 25 min to below 10 min on average [78].

4.2.3 HRS state-of-the-art

As just seen before, hydrogen as energy carrier for green mobility application is one of the potentially sources, with electricity and biofuels [79]. The IEA Technology Roadmap 2015 reported that an increase in the future in the FCEVs number is expected, but the diffusion of hydrogen refueling station infrastructures is a crucial element for hydrogen vehicles development [80]. It can be very interesting mainly in an almost completely RES-based European energy system, as promoted by the EU climate and energy policy, because of the possible overcapacity energy produced by RES. A very important role in this future energy-integrated design, maximizing efficiency, sustainability and reducing cost can be played by hydrogen technologies, because of the transformation in hydrogen of the energy surplus during the day [81]. The European initiatives and studies for hydrogen fuel and technologies are described by the Fuel Cell and Hydrogen Joint Undertaking (FCH JU); this organization does not only considered initiatives with hydrogen as mobility fuel, but also as electricity production system. The FCH JU also provided funds for the Hydrogen Mobility Europe project (H2ME), a set of the different European and hydrogen mobility partners, as H2 MOBILITY Deutschland, Mobilité Hydrogène France, Scandinavian Hydrogen Highway Partnership and UK H2 Mobility [82]. Always from the FCH JU, to extend environmental benefits well beyond zero local emissions, a possible fuel cell electric buses system for the public transportation is supported, because of the best productivity and operational flexibility compared to other zero emission concepts. Obviously, the costs can be an initial problem for the hydrogen mobility diffusion, but they are expected to drop significantly and become increasingly competitive [78].

But the first institution that works very hard in the hydrogen mobility development, is the California State, or USA in general; from the H_2 station map of the North America, we can

see that most of the hydrogen refueling stations are located in California, because of its policies adopted to foment the use of hydrogen as a fuel [83]. As also explain by the H_2 station map site, there are different typologies of hydrogen delivery: gaseous or liquid delivery (so the production site is in a different location respect to delivery site and hydrogen is transported by trucks in gaseous or liquid form), pipeline transport (so the delivery site is not so near the production site) and on-site production (where production and delivery location are the same). The California Fuel Cell Partnership (CaFCP) joins car manufacturers, fuel cell producers, energy providers, and government agencies in the largest partnership for the fuel cell vehicles promotion [84]. Different support initiatives and incentives have been provided for the entrance of the FCEVs in the transportation sector market. The strategy adopted by hydrogen car manufacturers to promote this mobility technology, is offered directly to the customers; for example, different manufacturers, as Toyota and Hyundai, offered in the US free fuel for three years.

Figure 25 Example of a Hydrogen Refueling Station [85]

In the planning of a new hydrogen infrastructure, industries and governments find two main challenges [72]:

- the lack of accurate data on current station costs;
- the need to find cost-effective infrastructure development strategies.

At the beginning of 21th century, few reports provide an accurate HRS cost database ([86], [87]), but during the last decade different studies try to find a possible solution. As explained by the EVTC report, several efforts conducted by different entities have developed several models to estimate the cost [69]:

- the Hydrogen Analysis (H2A) model developed by the US Department of Energy's Fuel Cell Technologies Office;
- compendium of hydrogen refueling equipment costs or CHREC, developed by University of California, Davis (UCD);
- Hydrogen Station Cost Estimation (HSCE) developed by the NREL;
- recent hydrogen station installation estimates in California, that offer invaluable real-world data of the hydrogen fueling station costs.

The H2A model was developed with input and deliberation from industrial stakeholders such as American Electric Power, BOC Gases, British Petroleum, Chevron, ExxonMobil, etc; there are different example analysis, as reference [88]. CHREC model were conducted by collecting inputs from multiple stakeholders, with the supervisor of the CaFCP; it was developed for use in calculating the cost of stations in California for the Hydrogen Highway Initiative (2005) [72]. The HSCE model, developed by NREL (agency of the United States government), was provided by expert stakeholders who participated in the Hydrogen Infrastructure Market Readiness workshop held in National Harbor, in Maryland. They also published a list of codes and standards applicable for U.S. hydrogen infrastructure projects, explained better in the next subchapter [89].

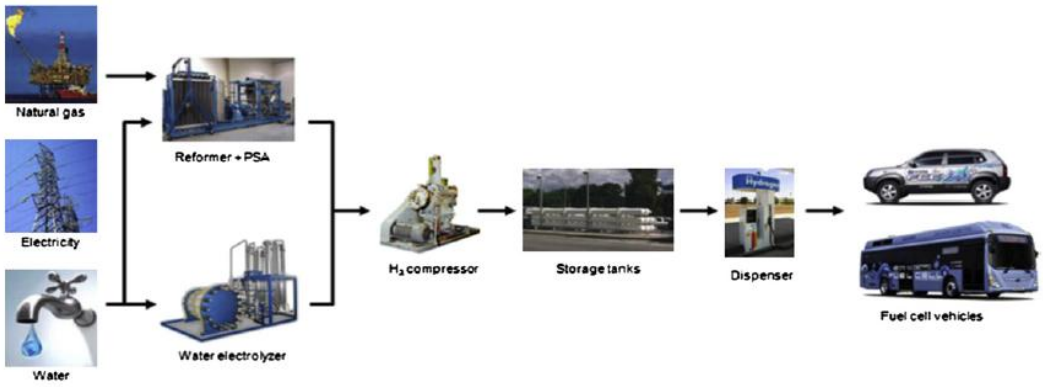

Figure 26 Basic structure of an on-site hydrogen refueling station [74]

4.2.4 Refueling protocol

In most of the literature review before, for the dispensing part, the current regulation is followed. For a hydrogen refueling station, the more used standards are the Society of Automotive Engineers (SAE) J2601 ([69],[21],[23],[88],[90]) and ISO 2011 international ([90]). The principle problem during the refueling is the temperature increase due to the expansion of hydrogen inside the FCV's storage tank. So, Nistor et al. find that the surface tank temperature must be below a limit temperature for the dispenser of 85 °C to remain in a safety condition and ensure a more complete fill [23].

As we can see from the SAE standard J2601 ("Fueling Protocols for Light Duty Gaseous Hydrogen Surface Vehicles", last version of December 2016), it includes the fuel delivery temperature, the maximum fuel flow rate, the rate of pressure increase and the ending pressure that are affected by different factors, as ambient temperature, fuel delivery temperature and initial pressure of the vehicle tank. This standard contains protocols that can be applicated for the two common pressure classes of a FCV (350 and 700 bar) with different fuel delivery temperatures and different compressed hydrogen storage system sizes; as a general rule, we can find that for higher fuel delivery temperature and higher ambient temperature, fueling time may be longer to avoid the overheating of the tank surfaces [91]. As explain by Nistor et al. in their work and also by the standard analyzed before, we can specify for each type of dispenser, target pressure and cooling temperature (as shown in table 10) a table that contain the minimum refueling time accordingly to the ambient temperature and to the initial pressure of the vehicle (example in table 11).

Table 10 SAE TIR J2601 dispenser types [23]

Dispenser type	Target pressure (bar)	Min. precooling T (°C)
A70	700	-40
A35	350	-40
B70	700	-20
B35	350	-20
C35	350	0
D35	350	Ambient

Table 11 Example of the lookup table method used to identify the minimum fueling time for a dispenser of Type B [91]

Input: 330 bar

Input: 26°C

Type B-70 1-7 Kg		Actual Fuelling Times (min)										
		Initial Tank Pressure, P_0 (bar)										
		20	50	100	150	200	300	400	500	600	700	>700
Ambient Temperature, T_{amb} (°C)	>50	-	-	-	No	fuelling	-	-	-	-	-	-
	50	41	39	36	33	30	24	18	13	7	1	-
	45	29	28	25	23	21	17	13	9	5	1	-
	40	21	20	19	17	16	13	10	7	4	1	-
	35	16	16	14	13	12	10	7	5	3	1	-
	30	13	12	11	10	10	8	6	4	2	-	-
	25	11	10	9	9	8	6	5	3	1	-	-
	20	9	8	8	7	6	5	4	2	1	-	-
	10	5	5	4	4	2	1	1	2	1	-	-
	0	5	5	4	3	2	1	1	1	0	-	-
	-10	5	5	4	3	2	1	1	1	0	-	-
	-20	5	5	4	3	2	1	1	1	-	-	-
	-30	5	5	4	4	3	2	1	0	-	-	-
	-40	5	5	4	4	3	2	1	0	-	-	-
	<-40	-	-	-	No	fuelling	-	-	-	-	-	-

Obviously, this precooling requires additional energy and equipment that must be considered in the techno-economic analysis of the system. But Ulleberg et al. study in more detailed the precooling condition starting from the SAE standard J2601, and find that for a slow refueling of hydrogen at 350 bar (heavy duty vehicles) the precooling system is not necessary, so inside the tank there is no overheating of the walls [21]. We consider a slow H_2 refueling when the flow rate is ≤ 1.8 kg/min; in our case, the minibus contains 300 liters of hydrogen, and at 350 bar and ambient temperature means a total of 8.6 kg_{H2}. So, to avoid the use of the precooling system, we can maintain the flow rate under the threshold of 1 kg/min and a refill time of about 12 minutes that is acceptable for our system assumptions.

Another study (Monforti Ferrario et al.) specify a fast filling 350 bar dispenser, but without any kind of precooling system or other additional components; in the report also, no trace of the SAE standard J2601 is found, so we can hypothesize that it was not taken into consideration [75].

4.2.5 Compression stage number

The number of compression stages is an important part to determine in the HRS design, in order to avoid a too high increase of hydrogen temperature, because of the following compression work equation

$$l_c = c_{p,H2} \cdot (T_{out} - T_{in}) = c_{p,H2} \cdot T_{in} \cdot \left(\frac{T_{out}}{T_{in}} - 1\right) \quad (33)$$

Knowing that the temperature ratio is equal to the first relation and that the isentropic efficiency is equal the second equation below, a different reason can be made.

$$\frac{T_{out}}{T_{in}} = \left(\frac{p_{out}}{p_{in}}\right)^{\frac{m-1}{m}} \quad (34)$$

$$\eta_{is,c} = \frac{l_{c,is}}{l_c} = \frac{\beta^{\frac{k-1}{k}} - 1}{\beta^{\frac{m-1}{m}} - 1} \quad (35)$$

where m is the exponent of the real polytropic transformation. So, from the compression specific work we can also evaluate the H_2 outlet temperature by the inverse of relation (33).

Applying more than only one compression stage allow to add one intercooler for each stage to cool down the gas before compressing it again. Obviously, all the heat exchangers must be considered in the economic analysis of the system. Each compressor has the same compression ratio, that is define by the following calculation.

$$\beta_{opt} = \left(\frac{p_{final}}{p_{initial}}\right)^{1/n} \quad (36)$$

where n is the number of compression stages.

In most of the literature review, there are only two types of compressor used for increasing the hydrogen pressure: reciprocating and diaphragm.

As we can see from the Wong report [73], two reciprocating compressors in parallel (to obtain a 100 % redundancy) are used, and each of them is four stages air-cooled to reach the pressure of 438 bar. Also in the work of Nistor et al. is used a reciprocating compressor, but in this case only two stages in order to feed a 450 bar storage tank [23]. The last study that use a reciprocating compressor is the work of Monforti Ferrario et al., with the intention of reach 400 bar, but in this case the number of stages are not specified [75].

Other reports instead indicate that the compressor is diaphragm, as the NREL technical report [88] that to compress the hydrogen from 20 to 350 bar use two stage. Also in the Allen Master Thesis use a diaphragm compressor to increase the pressure from 13 to 430 bar, but in this case is only a one-stage [92]. A one-stage diaphragm compressor is as well used in other two studies to reach the pressure of 450 bar from the electrolyzer pressure of 15 bar, and are the works of Viktorsson et al. and of Ulleberg et al. [71][21]. The last study

considered (Weinert et al.), doesn't specify the exact number of diaphragm compressor stages utilize to reach 432 bar, but we can understand from the report that are more than one [72].

According to the cost function explain in a following chapter and the utilization of a MATLAB program, an optimal compression stage number is defined firstly considering only the investment cost and then also the operational cost during work.

4.2.6 Other possible HRS configuration

A possible other solution respect to figure 24 can be the following HRS configuration. In this case we have two storage tanks: the first at 30 bar and the last at 450 bar. The recharge of the second tank can be done in the previous 5 hours between two minibus recharge, instead of the previous 10 minutes as considered for the initial configuration; in this way, the hydrogen flow rate in the compressor and in the intercooler is lower. A lower flow rate may mean so a lower size of the two components: a techno-economic analysis must be done to understand the difference of the two configurations under analysis but also the optimization algorithm must be applied to find the optimal one in economic terms.

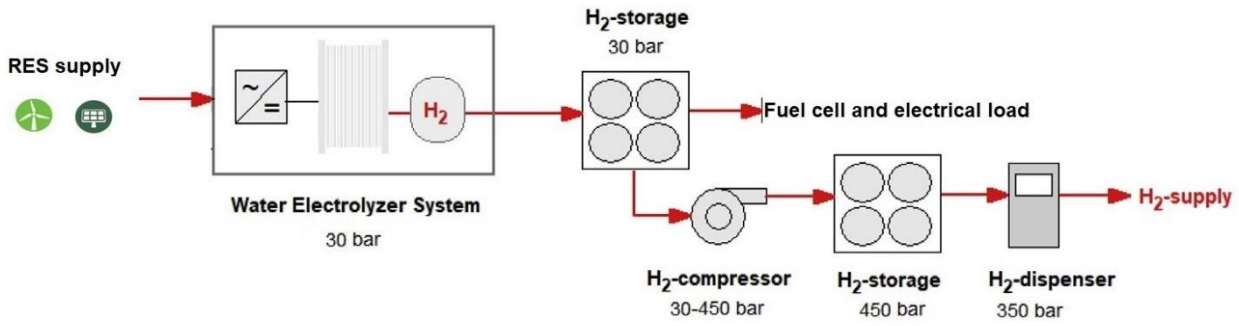

Figure 27 Possible other solution to Ambornetti's HRS configuration

4.3 Mobility scenarios

Initially, three different mobility scenarios have been selected. The first is Ostana-Ambornetti, and so only the connection between the two mountain village is considered. The

second is Paesana-Ambornetti; Paesana is the village at the beginning of Po Valley, so it can be interesting linked Ambornetti with the principle village of the valley. The last is Paesana-Ambornetti-Pian del Re; Pian del Re is a mountain plateau at the end of the valley. So, this scenario considers a minibus line for all the Po Valley, with Ambonetti village as refueling place, where our system is installed.

In the next table all the results are summarized.

Table 12 Mobility scenarios

Route	km/trip	km/day	km/y
Ostana-Ambornetti	4.5	36	13140
Paesana-Ambornetti	13.5	108	39420
Paesana-Ambornetti-Pian del Re	28.1	224.8	82052

At the end, only the first and the last scenarios are considered; this is because we want to evaluate a system configuration for a long trip minibus line and for a short trip one.

Knowing the liters of hydrogen consumed per day, we also know how many times we have to refill the minibus (considering the 300 liters storage). With the initial hypothesis of 4 travel roundtrip per day, a total 8 travel is obtained; we can see that a single travel lasts 1 hour, so the starting hour can be at 6 a.m. from Paesana for the first trip, and finish with the last at 8 p.m. from Pian del Re (considering two hours between each travel). The three supplies from the HRS can be make every 3 travels each day, and so during the first at 6 a.m., the fourth at 12 a.m. and the second-last at 6 p.m. In the next subchapter, also the total hydrogen volumes required per day and per year are evaluated.

4.4 Automotive study (minibus choice)

For the automotive part, there are two solutions that avoid the CO_2 production during the transport phase, that are the Fuel Cell Vehicle (FCV or Fuel Cell Electric Vehicle, FCEV) and the Electric Vehicle (EV). In the following section, the two possibilities are considered and the primary energy consumption is evaluated for each of them.

An FCE vehicles has a lower technologic increase respect to the Electric Vehicle, but, more than others, the Asian automotive manufacturers, as Toyota and Hyundai, have produced some models. The FCVs are considered mostly for the heavy transportation sector, as trucks or trains, because of the high range that can reach; but they are also studied for the others automotive opportunities.

In our case, a fuel cell electric minibus is considered. First, in literatures the average H_2 storage size of a minibus must be found. In the report of Napoli et al., it's studied a minibus supplied by a Hydrogen Refueling Station (HRS) that works with a PV plant and an auxiliary battery to produce the hydrogen through an electrolyzer [93]. They assume a minibus with a storage that contains 296 liters of H_2 at the pressure of 350 bar. As we can see from the work of Muller et al., the standard pressure for the H_2 storage is around 350 bar for buses and 700 bar for cars [70]. Also in the study of Dispenza et al. they use a minibus with two storages of 150 liters, for a total of 300 liters. The hydrogen is delivered through a solar powered hydrogen refueling station [77]. If we control in more detailed the reports, we can see that both use a minibus designed by the Italian manufacturer Dolomitech SRL. In the minibus datasheet they tell us that the storage can contain 7 kg of hydrogen [94].

Now, assuming a minibus with 300 liters of storage at 350 bar, we can evaluate the daily and annual automotive H_2 consumption. First, the typical consumption per km of a fuel cell bus must be considered. In the work of Viesi et al., the Italian mobility scenario is studied and in 2020 for a FC economic bus the fuel consumption is 0.086 kg_{H2}/km [81]. Also in the Fuel Cells and Hydrogen Joint Undertaking report of September 2015 provides that the fuel efficiency is increased significantly, and the consumption decreases from 25 kg_{H2} to 8-9 kg_{H2} every 100 km during previous years [78]. Before evaluating the annual hydrogen consumption, the density value of the H_2 inside the storage is calculated. With the hypothesis of ideal gas, we can use the following ideal gas law

$$p \cdot V = n \cdot R \cdot T \qquad (37)$$

where p is the gas pressure, V is the gas volume, n is the mole number of the gas, R is the ideal gas constant (equal to $8.314472\ \frac{kJ}{mol \cdot K}$) and T is the gas temperature. The ideal gas constant can be also written as $R^* = \frac{R}{MW_{H2}}$, and equal to $4157\ \frac{J}{kq \cdot K}$ for hydrogen, that represent the specific gas constant for the hydrogen. In this way the relation changes

$$\frac{p}{\rho} = R^* \cdot T \qquad (38)$$

where ρ is the gas density, and so the inverse of the specific volume.

Knowing that, considering a pressure storage of 350 bar and a temperature of 20 °C, the gas density is equal to $28.73\ {}^{kg}/_{m^3}$. So, the fuel consumption (in liters), is 2.99 l_{H2}/km.

Table 13 Hydrogen consumption and energy content

Route	*km/day*	*km/y*	*l_{H2}/day*	*l_{H2}/y*	*MWh_{H2}/y*
Ostana-Ambornetti	36	13140	107.7	39332	37.7
Paesana-Ambornetti-Pian del Re	224.8	82052	672.8	245614	235.1

The last column indicates the energy contained in the hydrogen used for the automotive part in one year (with the hypothesis of a H_2 LHV of 119.96 MJ/kg_{H2}).

Also, the minibus range of km considering the tank full can be evaluated, and with the gas density and fuel consumption values defined before, we obtain a range of around 100 km. It's not an important value, but probably is due to the fact that we consider a minibus, and so not a big vehicle as a truck or a big bus that can reach 450 km of autonomy (starting from 60 km and then 300 km), as introduced by Fuel Cells and Hydrogen Joint Undertaking report [78].

4.4.1 FCV-EV comparison

As alternative to the FCV/FCEV, we can use an EV minibus. First, some average main characteristics of an EV minibus must be found in literature, that are the electric consumption per km, the autonomy range in km and the battery capacity in kWh. In the DPMB (Brno Public Transport Company) analysis, they consider a typical minibus with a capacity of 30 passengers, that has an electric energy consumption of 0.5 kWh/km and a range of 150 km [95]. Considering also a usable percentage of the battery of 80 % (from 15 % to 95 % as present by Felix in his report [96]), the resulting battery capacity is of about 93.75 kWh. Also in the report of Felix et al. mentioned before, the electric energy consumption is contained in the range between 0.416 and 0.546 kWh/km, but consider an average of 0.5 kWh/km [96]. In this case the battery capacity is only 45 kWh, but a minimum range of 100 km is guaranteed. The last check is from the Baronti et al. work, that study a minibus with an

average consumption of 0.5 kWh/km and two 72 V 585 Ah lead-acid batteries, that means a battery capacity of around 84 kWh [97]. In this case, considering the usable percentage of 80 %, the range is of 135 km.

We can also check this dataset with a real EV minibus. From the EPIC Motiv Electric manufacturer, a minibus with 30 passengers of capacity has a capacity between 106 to 127 kWh and a range between 137 to 191 km (depends on the minibus model) [98]. So, the relative electric energy consumption, declared by the company, is around 0.62 kWh/km.

In the following table are summarized the results for the EV minibus analysis, considering the average electric energy consumption of 0.5 kWh/km.

Table 14 Electric and primary energy consumption

Route	*km/day*	*km/y*	*MWh_{el}/y*	*MWh/y*
Ostana-Ambornetti	36	13140	6.57	12.0
Paesana-Ambornetti-Pian del Re	224.8	82052	41.03	75.1

The last column represents the primary energy consumption, with the hypothesis that the EV minibus is recharge from the national grid; from the ISPRA report, the average efficiency of the Italian national thermoelectric park is around 54.6 % [99]. We can see that the primary energy consumption of the EV minibus is more than 3 times lower respect to the FCV minibus (considering the hydrogen fuel as primary energy). But different is if we consider the recharge time, because as Felix et al. study, a normal charge at 230 V requires 12 hours, instead a fast charge can be done in maximum 1 hours (although fast recharges in long term are harmful to the battery) [96].

In literature, different studied can be found as a comparison between battery electric vehicles and fuel cell vehicles. For example, in a comparative analysis it has been found that in 2030 scenario both BEV and FCEV have significantly lower lifecycle costs, similar to a gasoline-fueled internal combustion engine; moreover, they find that BEV and FCHEV are not sensible to electricity cost, but FCV and FCHEV are sensible to hydrogen cost. So, they found that the best path for a future development of FCEVs is the FCHEV [100]. A Tuscany case study instead compared hydrogen and electric vehicles by a life cycle assessment; for the hydrogen production, electrolysis from wind turbine and biomass or direct separation

from biomass gasification syngas are considered. Better performance are founded in environmental impact terms when RES are used both to produce hydrogen and electricity than the use of Italian national energy mix, and a worse performance in the hydrogen scenario is obtained; this is probably due to the lower efficiency in the H_2 production [101]. In the Ajanovic et al. review, we can see that both BEV and FCEV have several advantages and disadvantages; the main advantage of BEV respect to FCEV is the lower current capital cost, instead FCEV have higher driving range (comparable with conventional cars), shorter refueling time and higher lifetime. Both of them has significant lower WTW emission respect to conventional cars, but depends on the energy supply mix; obviously a high investment in research and a supporting economic policy can help the two vehicle types to be more competitive on the market [102]. Also in the Granovskii et al. report is represented that the environmental impact competitiveness of an electric vehicle compared to a hybrid one is obtained only if the electricity comes from RES, and not from fossil fuels. The fuel cell technology instead has some economic disadvantages, mainly due to the hydrogen price for the vehicles utilization [103]. Different WTW (Well To Wheel) analysis were made to compare conventional cars, electric vehicles and fuel cell vehicles. In the study of Bicer et al., three different environmental impact fields are considered: global warming, human toxicity and ozone layer depletion.

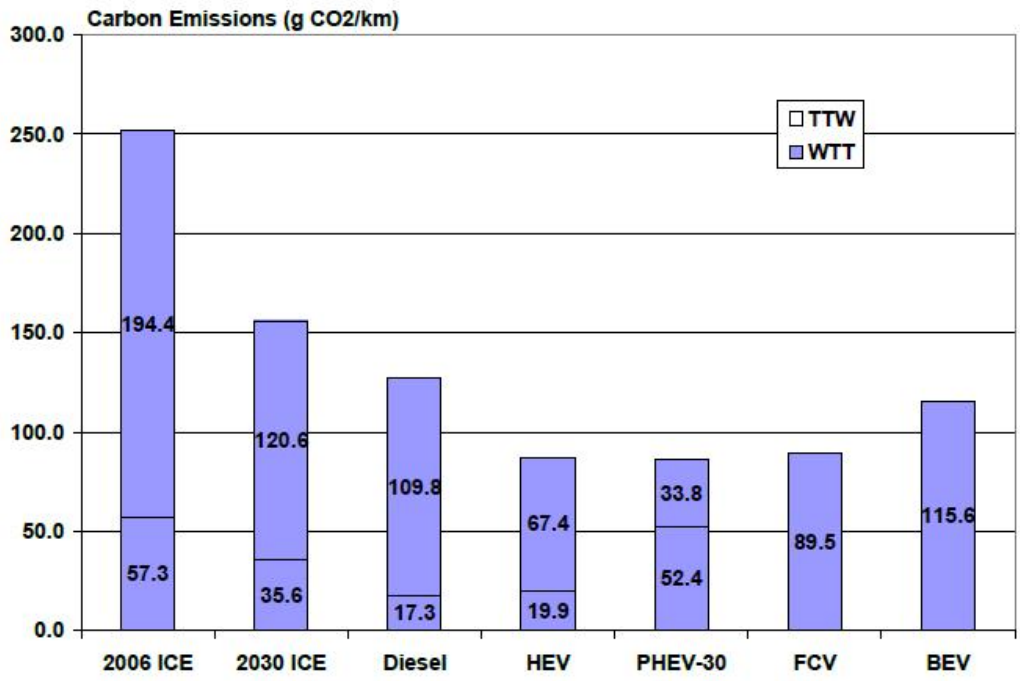

Figure 28 Well-to-wheels (WTT) and Tank-to-wheels (TTW) analysis of carbon emissions for conventional and advanced vehicles [104]

We can see that hydrogen-based vehicle have a GWP (Global Warming Potential) three times lower than the other vehicle typologies under study; it is also shown that electric vehicles yield higher human toxicity values due to the respective manufacturing and maintenance stages [105]. In a similar study instead, it was found that adopting new hydrogen production energy-based pathways (utilization of RES) for a FCEV, can achieve the same WTW as a battery electric vehicle; and this efficiency could also be higher if a solid oxide electrolyzer cell is used, supplied by a solar-thermochemical system or even by a nuclear plant [106]. In the previous figure, taken from a technical report, a comparison of CO_2 production through a WTW analysis is shown, to better understand the environmental benefit both of BEVs and FCEVs.

Also the IEA has done a comparative study between the different mobility solution technologies [80], finding the WTW carbon dioxide emission and compare it with the vehicle range, one of the main characteristic for automotive sector; in the following figure the results are summarized. An important key point is found in this study: FCEVs can achieve a mobility service compared to today's conventional cars at potentially very low WTW carbon emissions.

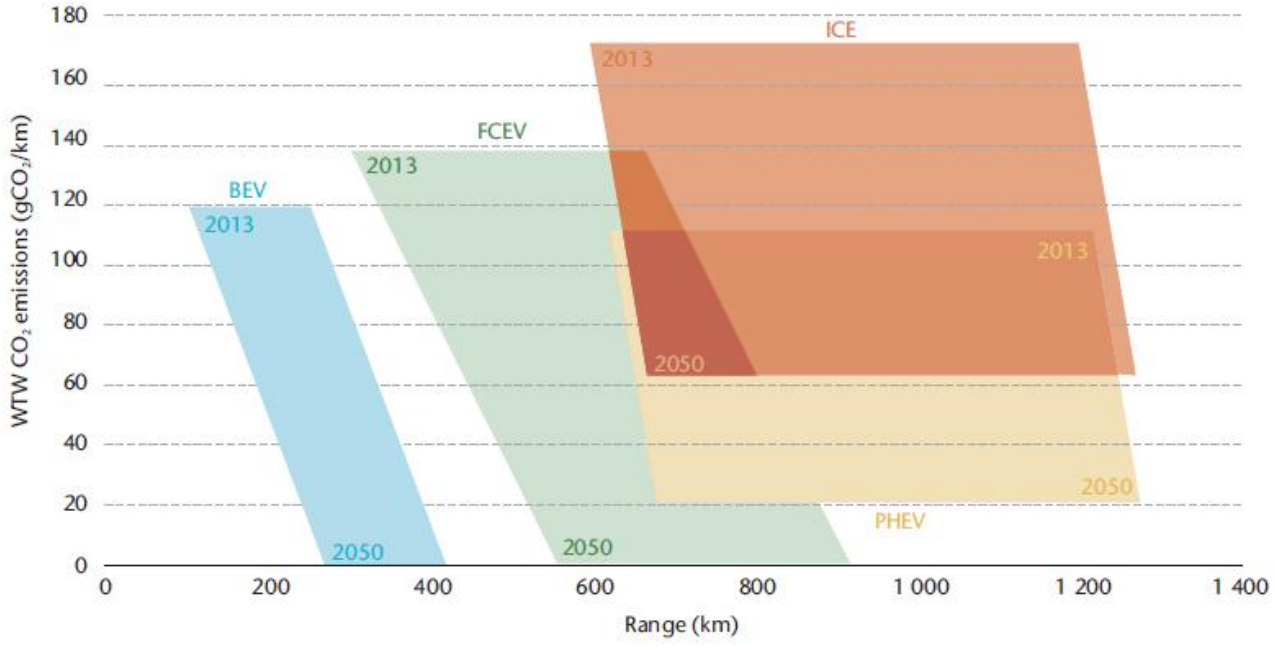

Figure 29 Well-to-wheel (WTW) emissions vs. vehicle range for several technology options [80]

4.5 Optimization algorithm

An optimization algorithm is computed in order to find the optimal configuration of the system for a specific scenario. The chosen parameter to be optimized is the Net Present Value at the end of the system lifetime (in the base scenario 20 years), with the constraints to be respected for finding the optimal point that are the LPSP and LHSP. The LPSP is the Loss of Power Supply Probability, and represent the external energy source required to satisfy the electrical load. Instead, the LHSP is the Loss of Hydrogen Supply Probability and provide a value of the external amount of hydrogen used to satisfy the mobility load. To change the NPV parameter, 4 (or 5 depending on the system configuration) variables are chosen; these variables are the size of the main system components, and so PV system, fuel cell, electrolyzer, low pressure hydrogen storage tank and, when required, CHP system. As we can see from the results, not always the configuration with the lowest NPV has also the lowest LCOE or LCOH; this is because on the different fraction of the energy production used for electricity load and mobility load but also on the system operation during the total lifetime. The algorithm used for the optimization is the Particle Swarm Algorithm (PSA), a computational method that optimizes a candidate solution through different iterations, part of a series on the evolutionary algorithm. This algorithm simulates the movement of a swarm of particles (midges) that move to the optimal point through tests (to find food). In this method, also a quality weight can be applied to the optimization variables considered; but in our case, all the components have the same importance.

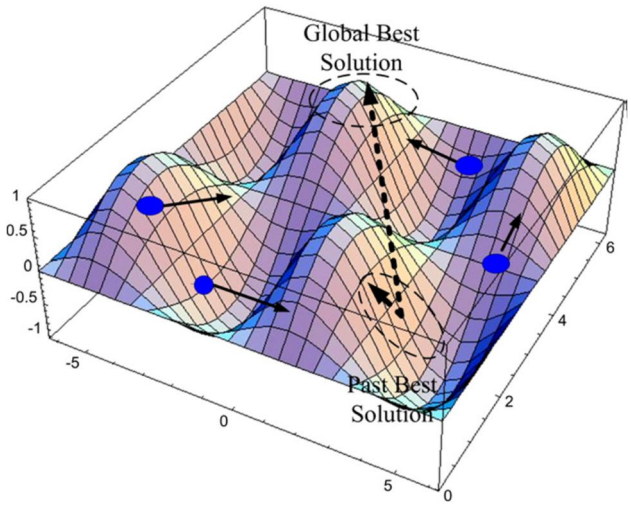

Figure 30 Search concept of particle swarm optimization [107]

5 Economic analysis

To complete the techno-economic analysis, a literature review is done to evaluate the economic information (investment cost, replacement cost, operational cost and lifetime) of each single component. For some of them, these information are taken directly from component company producer.

5.1 Component cost

5.1.1 PV system

For the photovoltaic system, the economic data are taken directly by the village administrators, as we can see form the Marocco et al. report of the REMOTE project [31]. This information are used for the LG NeON® R solar module, taken from the LG site; the module is a N-type monocrystalline cell, and each module has a maximum power of between 350÷365 W depending of the model with an efficiency of around 21 % [108]. The PV inverter is included in the module cost but has a lower lifetime than it, equal to 10 years respect to 25. But also, other studies are considered to obtain a confirmation of the data selected and are summarized in the following table.

Table 15 PV system economic information

CAPEX [€/kW]	REPL. [€/kW]	OPEX [€/kW/y]	LIFETIME [y]	REFERENCES
1547	760	24	25 (10 for inv.)	[31], [108]
1700	1700	28	30	[109]
1670	1330	50(3% CAPEX)	20	[17]
1100	-	-	-	[110]
1785	1785	9	20	[15]
1785	1785	9	30	[22]

The information of 4th row is taken by the IRENA report of 2018 and is a global average investment cost.

5.1.2 Wind turbine

As explained in the previous chapter, the turbine selected is the WES50, but we don't have economic information about this type. So, a literature review is done to obtain an average investment cost to use in this study as summarized in the table below.

Table 16 Wind turbine economic information

CAPEX [€/kW]	REPL. [€/kW]	OPEX [% CAP]	LIFETIME [y]	REFERENCES
1175	-	3	20	[31]
1300	800	450 [€/kW]	20	[109]
900	-	4	-	[44]
1330	-	-	-	[110]
1400	-	2	20	[111]
900	900	2	30	[22]
1100	800	3	25	[24]
1477	-	-	-	[25]

In this study, the same economic information of the first reference analyzed are considered with a replacement cost equal to the capex, but a cost increase of 15 % due to equipment transport and installation must be taken into account. The information examined in the Boussetta et al. study ([109]) are taken by the wind power statistics in Europe report edit by the IEA, International Energy Agency, of the 2012, but now a 2019 update is done [112]. Instead in the 4th row, the wind turbine capex is a global average cost deliberated by the IRENA [110].

5.1.3 Fuel cell and electrolyzer

A single subchapter is written for fuel cell and electrolyzer, because they have similar information that in literature are very varied due to the assumption made.

Both PEM and alkaline electrolyzers are considered in this master thesis in two different technology scenarios. The lifetime of the PEM electrolyzer is just selected in a previous

chapter in a more detailed study and is around 40000 operating hours but with also a 5000 on/off cycles [43][44]; instead for the alkaline one, the maximum operating hours are 76923 and 7500 on/off cycles [43][49]. Also for the PEM fuel cell the life has already been studied, with 30000 operating hours and an addition of three hours in the real operating life for each on/off cycle [16], [18], [19], [31].

For the PEM electrolyzer specific investment cost, a cost function is selected and is explained below, taken from the study of Proost [113], according also with the value obtained by the study of Gracia et al. [17].

$$c_{spec,PEM} = 23364 \cdot P_{nom}^{-0.404} \qquad (39)$$

where $c_{spec,PEM}$ is the specific cost of the PEM electrolyzer expressed in €/kW and P_{nom} is the PEM electrolyzer nominal power. In this way the cost variation of the size selected is also considered.

The same is done for the alkaline electrolyzer, but the cost function depending on the equipment size is more similar to the functions analyzed by the Turton's book [114]. The following equation, considered also in the Marocco et al. report, are explained by the final report of the P2G Roadmap for Flanders [31][115]. A specific investment cost of 2000 €/kW is selected for a reference size of 312 kW with a cost exponent equal to 0.7 (seven-tenth rule) in according with previous studies [109].

$$c_{spec,ALK} = 2000 \cdot \frac{312}{S_0} \cdot \left(\frac{S_0}{312}\right)^{0.7} \qquad (40)$$

where S_0 is the size selected in the study, in kW.

A similar equation as before is considered for the PEM fuel cell, always used in the REMOTE project mentioned before. In this case, a specific investment cost of 3947 €/kW is chosen for a reference size of 10 kW, taken from the Battelle Memorial Institute report that studied the manufacturing cost of a PEM fuel cell [116]. The cost exponent value is the same of the alkaline electrolyzer.

$$c_{spec,FC} = 3947 \cdot \frac{10}{S_0} \cdot \left(\frac{S_0}{10}\right)^{0.7} \qquad (41)$$

where S_0 is the size selected in the study, in kW as before. The above expression is in accordance with the economic information contained in different references; for example in the study of Gracia et al. and in another report of the Battelle Memorial Institute, always for

the manufacturing cost analysis of the PEM fuel cell but with a wider range of power [17][117]. But also, in the Rullo et al. and in the Zoulias et al. studies a similar value of capex is obtained [18] [20].

A separate discussion must be made for the evaluation of the replacement investment cost both for the fuel cell and electrolyzer. An initial percentage of the investment cost equal to 35 % is selected by Marocco et al., taken by the Tractebel and Hinicio report [31][43]. Instead, for the PEM fuel cell, in the REMOTE project is considered a value of 46 %, according with the value explained by the Tractebel report mentioned before. But a different method is described in the Raggovidda energy analysis but also in the study of Shehzad et al. and is selected for this master thesis [44][118].

$$c_{repl} = \frac{2 \cdot 0.4}{3} \cdot c_{capex} \quad (42)$$

where c_{repl} is the replacement cost and c_{capex} is the initial investment cost. A similar fraction of the CAPEX is also considered in the Kalinci et al. report (replacement percentage of around 27 % than investment cost) [16].

Also for the operating and maintenance cost a more detailed study is done. Initially, the value considered by Marocco et al. in the REMOTE project are, respectively for PEM electrolyzer, alkaline electrolyzer and PEM fuel cell, equal to 3 %, in accordance with the study of Gracia et al. [31][17]. Another work that use the value of 3 % as O&M cost is Menanteau et al [111]. But in the Tractebel and Hinicio report, the O&M cost is not all fix, but a function of the yearly real operating hour of the fuel cell or the electrolyzer; we can see that they consider a total fraction of 4 % than the investment cost of the electrochemical equipment, and then 1/3 of it is fix and the remaining 2/3 are variable and depend on the ratio between the real operating hours during one year and the total year hours (8760) [43]. This reasoning can be translated in the following equation.

$$O\&M = 4\% \cdot \left({}^{1}/_{3} + {}^{2}/_{3} \cdot \frac{hour_{real}}{hour_{tot,year}} \right) \cdot capex \quad (43)$$

where ${}^{1}/_{3}$ is the O&M fix part, ${}^{2}/_{3}$ is the O&M variable part that depend on the real operating hours of the component in one year ($hour_{el,real}$) and on the total hours in one year ($hour_{tot,year}$). In this way, also the fact that both the fuel cell and the electrolyzer could work not continuously is considered.

In the following table, all the assumptions for the three electrochemical equipment are summarized in the order: PEM electrolyzer, alkaline electrolyzer and PEM fuel cell.

Table 17 Fuel cell and electrolyzer economic assumptions

CAPEX [€/kW]	REPL. [€/kW]	OPEX [% CAP]	LIFE [h+cycle]	REFERENCES
Eq. 39	Eq. 42	Eq. 43	40000+5000	[31], [43], [44], [113]
2000 (312 kW)	Eq. 42	Eq. 43	76923+7500	[31], [43], [44], [49], [115]
3967 (10 kW)	Eq. 42	Eq. 43	30000	[19], [31], [43], [44], [116]

5.1.4 Hydrogen storage tanks

Different articles are taken into account for the low pressure storage tank. In the following tables all the references investment costs are summarized, starting from the report of Marocco et al. of the same REMOTE project.

Table 18 Literature cost for a low pressure hydrogen storage tank

30 bar storage tank literature investment cost

CAPEX [€/kg]	REPL. [€/kg]	OPEX [€/kg/y]	LIFETIME [y]	REFERENCE
470	-	2% CAPEX	35	[31]
470	-	2% CAPEX	35	[43]
470	-	-	15	[18]
353	353	3% CAPEX	20	[17]
600	-	-	-	[12]
513	513	Negligible	20	[16]
450	450	2% CAPEX	20	[15]
430	-	0.5% CAPEX	20	[20]
535	350	0.5% CAPEX	25	[22]
550	-	-	-	[25]

So, an average specific investment cost of 500 €/kg is choosing, with a replacement cost equal to capex, an operating and maintenance (OPEX) cost equal to 2% of capex and a lifetime of 20 years.

Instead, the table below represent the summary of literature review for the high pressure hydrogen storage tank (450 bar). In this case, no other REMOTE studies considered an HRS connected to the plant and, so, we don't have any information about this storage type.

Table 19 Literature cost for a high pressure hydrogen storage tank

450 bar storage tank literature investment cost

CAPEX [€/kg]	REPL. [€/kg]	OPEX [€/kg/y]	LIFETIME [y]	REFERENCE
1043	-	-	-	[72]
1000	-	1% CAPEX	-	[75]
900	-	4% CAPEX	-	[21]

The first investment cost considered, from the work of Weinert et al., is evaluated by the following relation [72].

$$CAPEX = \frac{1000}{1.12} \cdot {m_{H2,stor}}^2 \quad (44)$$

An average capex of 1000 €/kg is studied, with the same value as replacement and an opex equal to the 2% of capex and a lifetime of 20 years (as the low pressure hydrogen storage tank).

5.1.5 Compressor and intercooler

For compressor and intercooler the economic information are taken from Turton cost functions; from this book, we know that the specific cost of a component is higher for lower size, due to the value of the cost exponent under than 1 [114]. A more detailed MATLAB program has been compiled with the evaluation of the investment cost (CAPEX) and the specific energy consumption for a system from one to five stages of compression to understand the optimal stage number.

From the Turton book, we can assume that the equipment purchased cost (C_{p0}), at ambient operating pressure and using carbon steel construction, can be evaluated with the following equation.

$$C_{p0} = 10^{K_1 + K_2 \cdot log_{10}(A) + K_3 \cdot (log_{10}(A))^2} \qquad (45)$$

where K_1, K_2 and K_3 are coefficient taken from a table of Turton's book and differ with the equipment under study and A is the capacity or size parameter of the equipment. But this formula can be applied for a specific component only in a certain validity range (as we can see underneath for compressor and intercooler). If the size parameter is out of this range, we could apply the cost exponent to find the new equipment purchased cost, starting from a reference one; usually as reference size is take the lower boundary of the validity range if the size is smaller of it and vice versa if the size is higher than the higher boundary of the validity range. As we can see in the equation below, we need a cost exponent n that change for each type of equipment; but, if we don't have more information as for the intercoolers, we could use a value of 0.7 (seven-tenth rule). This value is also in agreement with previous studies [109].

$$C_{p,0} = C_{p,0,ref} \cdot \left(\frac{S_0}{S_{0,ref}}\right)^n \qquad (46)$$

Now, we have to take into account the bare module factor to find the bare module cost of the equipment; this factor considers the real construction material and also the pressure under which the equipment works in the plant, and it's multiply with the purchased initial cost. The bare module factor equation is different for compressors and heat exchangers as explained by the following equations, respectively.

$$C_{BM,c} = C_{p0} \cdot F_{BM,c} \quad (47)$$

$$C_{BM,i} = C_{p0} \cdot F_{BM,i} = C_{p0} \cdot (B_1 + B_2 F_M F_P) \qquad (48)$$

where $F_{BM,c}$ and $F_{BM,i}$ are the bare module factors of compressor and heat exchanger, respectively, B_1 and B_2 are coefficient taken from a Turton's book table for a specific type of heat exchanger, F_M is the material factor and F_P is the pressure factor; obviously, the factor for a compressor depends only by the construction material, because the pressure change inside it. The material factor is taken by tables (the base case is carbon steel), instead, for the intercooler, the pressure factor is evaluated by the equation below.

$$F_P = 10^{C_1 + C_2 \cdot log_{10}(P) + C_3 \cdot \left(log_{10}(P)\right)^2} \qquad (49)$$

where C_1, C_2 and C_3 are coefficient taken by Turton's book table for a specific type of heat exchanger and P is the intercooler working pressure. Also this relation has a validity range that depends on the intercooler considered. All the equations above are taken by the Turton's book and represent the Turton cost function [114].

Now, the investment cost must be discount at the year of the study, because using the Turton cost function, a 2001 investment cost is obtained. To discount the compressor and intercooler capex it's used the CEPCI, Chemical Engineering Plant Cost Index; this is an index evaluated in average for each year that follow the market trend. In the 2001 the CEPCI index has a value of 394.0 that increase at 607.5 in the 2019; the index values are taken from the Chemical Engineering site [119]. As we can see from the index higher value, the cost will increase during the century because also the market trend rises. With the following relation, the cost discounting is considered.

$$C_{BM,2019} = C_{BM,2001} \cdot \frac{CEPCI_{2019}}{CEPCI_{2001}} \qquad (50)$$

To evaluate the final investment cost for a certain component is the monetary exchange dollar-euro, because the from the Turton cost function cost in USA dollar is obtained. For the 2019, the year in which the costs were discounted, the average monetary exchange of the year was 1.12 $/€. For the compressor, the rotary type is taken; this is due to the validity range of the Turton cost function, as we can see from the figure below.

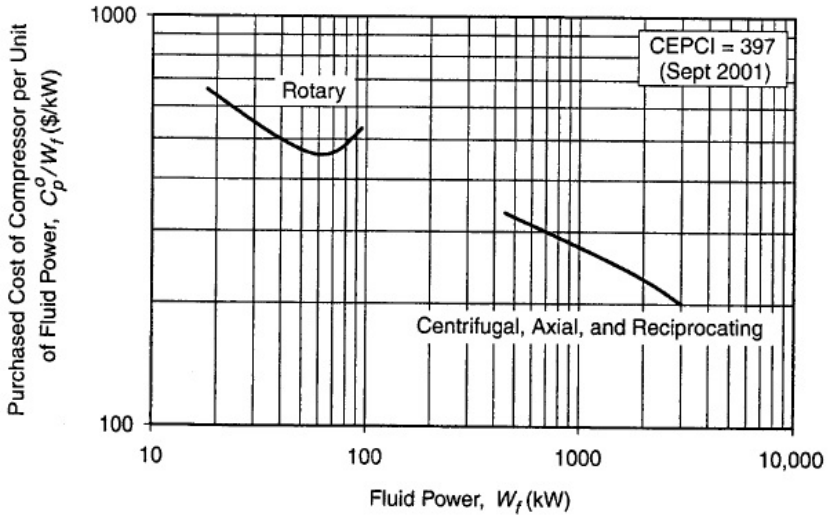

Figure 31 Specific purchased cost for a compressor respect to the fluid power [114]

Knowing that the size of the compressor used is certainly lower than 200 kW, the rotary compressor was chosen. As we can see from the figure above, the size parameter of a compressor is the fluid power, evaluated by the product between specific energy consumption and hydrogen flow rate in kg/s. In the following table, the information for a rotary compressor are summarized, with the hypothesis of a carbon steel compressor.

Table 20 Rotary compressor cost function characteristics [114]

Rotary compressor	
K_1	5.0355
K_2	-1.8002
K_3	0.8253
F_{BM}	2.4
n	0.84

Instead for the intercooler, the air cooled and the spiral tube types are both considered, because of the operating pressure at which they can work. The validity range of the two different type of intercoolers are 10÷10000 m^2 and 1÷100 m^2, respectively.

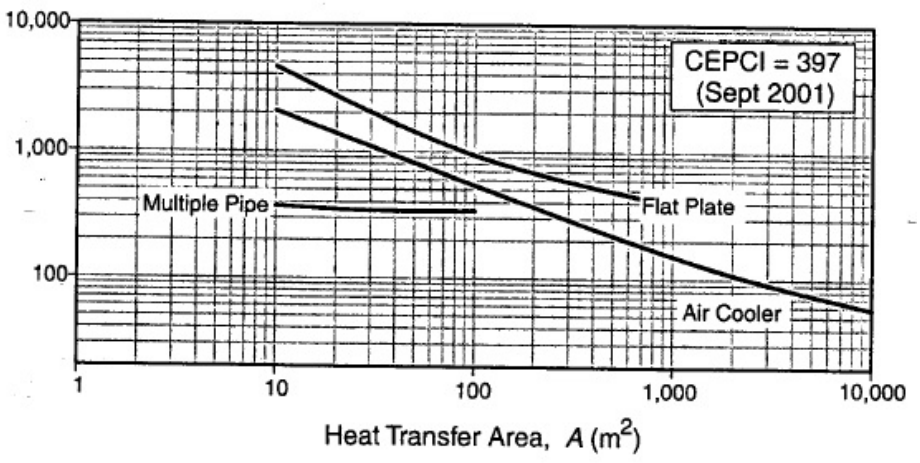

Figure 32 Specific purchased cost of an air cooled HE respect to its area [114]

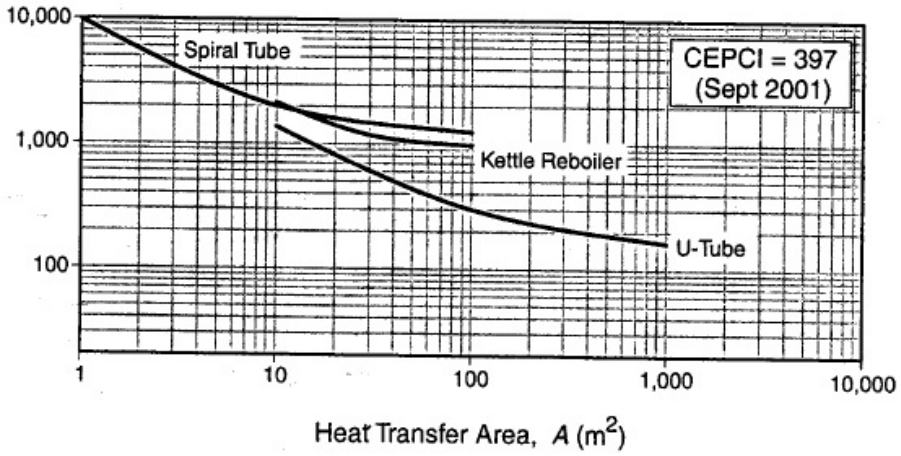

Figure 33 Specific purchased cost of an spiral tube HE respect to its area [114]

As explained in the figures above, the size parameter of a heat exchanger is the area. To evaluate it, some hypothesis must be done; the first is the air temperature to cool down the hydrogen after a compression at the inlet and outlet of the intercooler, than a value of the heat transfer coefficient must be consider and last is the outlet temperature of the hydrogen after a heat exchanger with the hypothesis that the pinch point of it is at the outlet section. All these hypotheses are useful to evaluate the heat exchange and after the area of the intercooler and are summarized in the following table.

Table 21 Heat exchanger characteristics

Heat exchanger characteristics	
$\boldsymbol{T_{in,air}}$ $(°\boldsymbol{C})$	20
$\boldsymbol{T_{out,air}}$ $(°\boldsymbol{C})$	30
$\boldsymbol{U}$ $\left(\boldsymbol{W/_{m^2 \cdot K}}\right)$	50
$\boldsymbol{\Delta T_{pp}}$ $(°\boldsymbol{C})$	10
$\boldsymbol{T_{out,H2}}$ $(°\boldsymbol{C})$	$T_{in,air} + \Delta T_{pp}$

First, the compressor outlet temperature is evaluated by the inverse of the equation (33); in this way we know the temperature of hydrogen at the inlet of the heat exchanger. Then,

knowing the hydrogen flow rate and the outlet temperature of it from the intercooler, the heat exchange is calculated by the equation (51) and last the area of the intercooler is determined by the inverse of the equation (52) that we can see below.

$$Q_{int} = c_{p,H2} \cdot \left(T_{out,H2} - T_{in,H2}\right) \cdot \dot{m}_{H2} \qquad (51)$$

$$Q_{int} = U \cdot A_{int} \cdot \Delta T_{log} \qquad (52)$$

where $\dot{m}_{H2}$ is the hydrogen flow rate, U is the heat transfer coefficient hydrogen-air and ΔT_{log} is the logarithmic mean value difference of the intercooler, that is considered in countercurrent, so from one side enter the hydrogen and the air goes out and vice versa for the other side. In the following relation, ΔT_{log} is defined for a countercurrent heat exchanger.

$$\Delta T_{log} = \frac{\left(T_{in,H2} - T_{out,air}\right) - \left(T_{out,H2} - T_{in,air}\right)}{\log\left(\frac{T_{in,H2} - T_{out,air}}{T_{out,H2} - T_{in,air}}\right)} \qquad (53)$$

After the evaluation of the intercooler area, we can apply an economic analysis using the Turton's book. In the table below, all the coefficients needed are summarized for the different type of heat exchangers considered.

Table 22 Air cooled and Spiral tube heat exchanger cost function characteristics [114]

	Air cooled	**Spiral tube**
$\boldsymbol{K_1}$	4.0336	3.9912
$\boldsymbol{K_2}$	0.2341	0.0668
$\boldsymbol{K_3}$	0.0497	0.2430
$\boldsymbol{B_1}$	0.96	1.74
$\boldsymbol{B_2}$	1.21	1.55
$\boldsymbol{F_M}$	1 (CS)	1.7 (Cu sh&tu)
$\boldsymbol{C_1}$	-0.125	-0.2155
$\boldsymbol{C_2}$	0.15361	0.09417
$\boldsymbol{C_3}$	-0.02861	0

With the assumption that in other literature reports compressor and intercooler are considered together, a single total capex is used in the final economic analysis for the plant. So, also a common replacement cost, operational & maintenance cost and lifetime is found. A replacement cost equal to the initial investment cost, a 2 % of the capex O&M cost and a 20 years lifetime are taken into account in the works of Gökçek and of Ferrero [22][37]; also in this study we consider the same economical information.

5.1.6 Dispenser (350 bar)

From literature, there are very different value of investment cost for a hydrogen dispenser, but a function cost similar to the one used by Turton's book is selected. This function (explain below) is provided by Tractebel and Hinicio report, with an investment cost of 750 k€ for a reference size of 200 kg/day of hydrogen delivered by the hydrogen refueling station. In this case, a particular value of 0.66 is applied as cost exponent (instead of the seven tenth rule) [43].

$$C_{disp} = 750 \cdot 10^3 \cdot \left(\frac{S_0}{200}\right)^{0.6\ 6} \qquad (54)$$

where S_0 is the selected size in the study, in kg/day. Considering an average value of 20 kg/day, the capex obtained by the equation above is in accordance with the values considered in different other studies, summarized in the following table containing also other economic information about a 350 bar dispenser.

Table 23 Literature cost for a 350-bar dispenser

CAPEX [k€]	REPL. [k€]	OPEX [% CAP]	LIFE [y]	REFERENCES
130	130	-	-	[21]
135	135	-	-	[120]
57÷135	-	-	10	[85]
218	-	4 %	20	[71]
Eq. 54	Eq. 54	4 %	10	[43]

So, for this study, the selected economical information have been taken by the Tractebel and Hinicio report.

5.1.7 CHP system

The CHP system is not considered for all the simulations done in this Master Thesis, but also some optimization with it can be done to understand the difference taking into account a continuous and more predictable energy production system.

To obtain a total investment cost for a CHP, we have to consider each single main component cost. As we can see from the datasheet of the company producer, in a CHP system there are dryer, gasifier, reformer and motor; also transport and installation costs are still taken into account [65]. These components must be studied separately, because of the different operational costs and lifetimes, that are shown in the next table.

Table 24 Economic information of CHP components [31], [65]

Component	CAPEX [€/kW]	REPL. [€/kW]	OPEX [€/kW/y]	LIFE [y]
Dryer	2041	1225	0.004348	20
Gasifier	3673	2204	0.009662	20
Reformer	41	41	0.009662	3
Motor	204	204	0.009662	3
Transp. & inst.	357	388	/	/

But respect to other components, also a biomass cost due to CHP operation must be considered. Initially, a biomass specific consumption is defined and is taken from the company producer datasheet, with a value of 44 kg/h at the maximum power, equal to 49 kW; this means a specific consumption of 0.898 kg/kW [65]. Then, a specific biomass cost is selected; from the AIEL, an Italian association specialized in agroforestry energies, for the type P31S - M25, with about 35% of relative humidity, a cost of 0.1 €/kg can be chosen. Also considering biomass transportation of 0.02 €/kg and 10% of VAT, a final biomass cost of 0.13 €/kg is obtained [121]. Knowing the equivalent hours of the system, a yearly biomass consumption and cost can be evaluated; this cost is considered as an additional operational cost of the CHP.

5.1.8 Other auxiliary equipment

In the economic analysis of the plant, other auxiliary components must be taken into account in order to make a more detailed study. For example, in our case, an auxiliary battery and water tank are also incorporated; but they are only included in the economic analysis and not in the yearly plant simulation, because we suppose that all the main equipment are not damaged and/or malfunctioned of any kind during the plant lifetime (only the normal replacement is considered).

Different studies in literature also contain an auxiliary battery in their plant, so an economical review is done. But initially, we have to understand what its size is and above all its task within the plant; the fact that the fuel cell and the electrolyzer are not fast enough to compensate sudden change of load is knew (although PEM technology is faster than alkaline), so the battery can be used for this reason but also for other more dynamic behavior as the plant start-up. Knowing the battery assignment, we can design its size assuming an autonomy of 0.5 hours considering the greater electrical load required by Ambornetti. So, making sure that the greater electrical load of the village is 65.534 kW, a precautionary battery size of 33 kWh is taken. The battery assignment and also its size are similar to the battery selected in a previous REMOTE project report, the Deliverable D2.2; so, it's corrected consider a similar battery size (in the previous report the size is 30 kWh) [28]. Considering a Li-ion battery, in the following table are summarized the economic information explained by the different studies analyzed.

Table 25 Auxiliary battery economic assumptions

CAPEX [€/kWh]	REPL. [€/kWh]	OPEX [€/kWh/y]	LIFE [y]	REFERENCES
550	550	10	10	[31]
600	600	10	3500 cycles	[109]
550	550	0	10	[17]
800	-	-	10÷15	[122]

In this study, the same information about batteries of the first row are considered and are in accordance with all the other data contained in literature.

Instead, the auxiliary water tank has the task of not interrupting the supply of water for the electrolyzer in case of malfunctioned, failure or maintenance in the water supply system. To

allow the maintenance, a water volume of 12 hours of autonomy is selected. Starting from the total water consumption in one year by the electrolyzer (evaluated knowing that the average water volume required to produce 1 kg of hydrogen is equal to 15 liters [43]), we can estimate the water tank volume with the equation below.

$$V_{H2Otank} = V_{H2O,year} \cdot \frac{12}{8760} \qquad (55)$$

where $V_{H2Otank}$ is the water tank volume, $V_{H2O,year}$ is the volume of water required in one year of plant operation, 12 are the autonomy hours needed and 8760 are the hours in one year. Then, to evaluate the investment cost of the water tank, the following relation is used.

$$c_{spec,H2O} = 5941.7 \cdot V_{H2Otank}^{-0.389} \qquad (56)$$

where $c_{spec,H2O}$ is the specific cost of the water tank in €/m^3; this formula is a cost function taken from the report of public water services assets in Portugal, and consider also a replacement cost equal to the capex, a O&M cost of 1 % respect to the capex and a 20 years lifetime [123].

5.2 Additional costs

A more detailed review is done to understand the increase in capex for each plant component due to equipment transport and installation (except for the PV system because is already considered by the LG information and for the CHP system).

5.2.1 Transport & installation cost

For the transport and installation cost, an average value of 10 % is selected for all the plant in the Norwegian case study of Ulleberg et al. [21]. Instead, in the Rome case study analyzed by Monforti Ferrario et al., a cost increase of 20 % is considered to take into account all the plant integration [75]. Also in the life cycle cost analysis of Viktorsson et al. is considered a general integration cost, and is selected a value of 11 % of the total plant CAPEX [71]. In the report of Weinert et al., the installation cost is evaluated around 13 % for the on-site electrolysis plant with a hydrogen production of 30 kg/day [72]. The last reference examined is the book of Peters et al., “Plant Design and Economics for Chemical Engineers”, where the installation cost is evaluated in the range between 6÷14 % and the shipping transport of

around 10 % (but depends on the equipment type and the plant location) [124]. So, a precautionary average value of 15 % is selected for all the plant equipment.

Table 26 Plant economic information summary (excluded additional costs)

COMPONENT	CAPEX	REPL.	OPEX	LIFETIME	REFERENCES
PV system	1547 €/kW	760 €/kW	24 €/kW/y	25 (10 inv.)	[31], [108]
WT system	1175 €/kW	1175 €/kW	3 %	20	[31], [109]
CHP system	6316 €/kW	245 €/kW (3 y)	0.0333 €/kWh/y + 5.28 €/h	Depends on component	[31], [65], [121]
PEM EL	Eq. 39	Eq. 42	Eq. 43	40000+5000 (h+cycles)	[31], [43], [44], [113]
ALK EL	2000 €/kW (312 kW)	Eq. 42	Eq. 43	76923+7500 (h+cycles)	[31], [43], [44], [47], [48], [115]
PEM FC	3967 €/kW (10 kW)	Eq. 42	Eq. 43	30000 h	[19], [31], [43], [44], [116]
Battery	550 €/kWh	550 €/kWh	10 €/kWh/y	10	[17], [31], [109]
Water tank	Eq. 56	Eq. 56	1 %	20	[123]
Low p H2 t	500 €/kg	500 €/kg	2 %	20	[15]–[17], [31]
High p H2 t	1000 €/kg	1000 €/kg	2 %	20	[15], [21], [72], [75]
Compr & int	Turton	Turton	2 %	20	[22], [37], [114]
Dispenser	Eq. 54	Eq. 54	4 %	10	[43], [71], [85]

5.3 Economic assumption

To complete the economic analysis, some economic and financial assumption must be done to understand the electricity and hydrogen value during the system lifetime of 20 years. Only one scenario is considered in this study, that is the literature-based RES one; it correspond to renewable P2P solution with the cost information taken from literature (usually expressed as target data for technology) [31]. In the following pages, before the Net Present Cost

method are explained and then two different methods to evaluate the real interest rate are analyzed, with very similar results.

5.3.1 Net Present Cost

To understand the cost of a certain plant during the analysis period (in this case the system lifetime), we have to discount all the cost for each year because of the market change; so, we have to apply the NPC method that is computed as follows.

$$NPC = CAPEX_0 + \sum_{j=1}^{n} \left[\frac{OPEX_j}{(1+i)^j} + \frac{REPL_j}{(1+i)^j} \right] \quad (57)$$

where NPC is the Net Present Cost at the year selected, j is the year counter, $CAPEX_0$ is the total investment cost of the plant performed at the beginning of the analysis and includes also transport and installation costs, $OPEX_j$ are the operational and maintenance costs for each component in the j -th year, $REPL_j$ are the replacement costs (including also transport and installation costs) performed at the end of a specific component life to maintain the system operation, n is the system lifetime (so, the analysis period in years) and i is the real discount rate. Also the NPV (Net Present Value) can be evaluated, when we want to estimate the total economic gain obtained by the selling of all the electricity and the hydrogen produced by the plant with a specific financial structure and assumption, considering the net cash inflow-outflows for each single year [125].

Knowing the total NPC, also the levelized cost of electricity (LCOE) and the levelized cost of hydrogen (LCOH) can be estimated; for the first parameter the Net Present Cost of only the equipment part that is used to produce electricity is considered and is divided by the electricity produced in the analysis period. The same for the second parameter, but in this case the equipment part that is used to produce hydrogen is considered, and the denominator is the total mass of hydrogen produced during the plant lifetime provided to mobility load. Both electricity and hydrogen delivered in the 20 years must be discounted considering the discount rate i, as we can see in the equations below.

$$LCOE = \frac{NPC_{el}}{\sum_{j=1}^{n} \frac{Electricity\ delivery_j}{(1+i)^j}} = \frac{CAPEX_{0,el} + \sum_{j=1}^{n} \left[\frac{OPEX_{j,el}}{(1+i)^j} + \frac{REPL_{j,el}}{(1+i)^j} \right]}{\sum_{j=1}^{n} \frac{Electricity\ delivery_j}{(1+i)^j}} \quad (58)$$

$$LCOH = \frac{NPC_{H2}}{\sum_{j=1}^{n} \frac{Hydrogen\ delivery_j}{(1+i)^j}} = \frac{CAPEX_{0,H2} + \sum_{j=1}^{n} \left[\frac{OPEX_{j,H2}}{(1+i)^j} + \frac{REPL_{j,H2}}{(1+i)^j} \right]}{\sum_{j=1}^{n} \frac{Hydrogen\ delivery_j}{(1+i)^j}} \quad (59)$$

But some of the system components must be taken into account for both the energy production, so we have to divided the investment cost, operational and maintenance cost and the replacement cost (when required), in two fraction that consider the hydrogen energy and the electric energy respect to the total energy produced (the sum of the two energy). So, two different NPCs have been evaluated, and the sum is the total NPC of the equation (57). Both the NPC and the LCOE or LCOH can be calculated over different time horizons. The meaning of these LCO is the price of electricity or hydrogen that if sold we obtain an economic gain equal to 0. The following relations are used to take into account the electricity part for the LCOE.

$$fr_{el,RES} = \frac{\frac{L_{RES}}{\eta_{LOAD}} + \frac{L_{FC}}{\eta_{LOAD} \cdot \eta_{D1} \cdot \eta_{FC} \cdot \eta_{EL} \cdot \eta_{D2}}}{\frac{L_{RES}}{\eta_{LOAD}} + \frac{L_{FC}}{\eta_{LOAD} \cdot \eta_{D1} \cdot \eta_{FC} \cdot \eta_{EL} \cdot \eta_{D2}} + \frac{M_{SYS}}{\eta_{EL} \cdot \eta_{D2}}} \qquad (60)$$

$$fr_{el,OTH} = \frac{\frac{L_{FC}}{\eta_{D1} \cdot \eta_{FC}}}{\frac{L_{FC}}{\eta_{D1} \cdot \eta_{FC}} + M_{SYS}} \qquad (61)$$

where L_{RES} represents the load portion satisfy by RES, L_{FC} is the load portion satisfy by the fuel cell, M_{SYS} provides the mobility load satisfy by the system and all the η represents all the efficiency of the system components. The first fraction, $fr_{el,RES}$, is considered for the energy produced by the RES, because both the energy directly supplied to the electrical load and stored as hydrogen and reused in the fuel cell are produced by them; instead the second one, is for all the other components, considering only the fuel cell contribution. The rest portion of NPC of each single shared component, is considered to evaluate the LCOH.

But also the electricity provided to compressors must be taken into account in the separation between electricity and hydrogen, because it is used for the mobility part, so it must be considered for the LCOH evaluation. The compressor energy portion is calculated with the following relation, where L_{COMP} is the yearly energy consumption of the compressors.

$$y_{COMP} = \frac{L_{COMP}}{L_{RES} + L_{FC}} \qquad (62)$$

In this way, two different values of LCOE and LCOH are evaluated, with the equations below.

$$LCOE_{real} = \frac{NPC_{el} \cdot (1 - y_{COMP})}{(L_{RES} + L_{FC} - L_{COMP})_{actualized}} \qquad (63)$$

$$LCOH_{real} = \frac{NPC_{h2} + NPC_{el} \cdot y_{COMP}}{M_{SYS,actualized}} \qquad (64)$$

Obviously, L_{RES}, L_{FC}, L_{COMP} and M_{SYS} at denominators must be actualized at the end of the system lifetime (in this initial case 20 years).

5.3.2 Real discount rate and WACC

The first method to calculate the real discount rate is the one that is used also in other REMOTE project reports, as the work of Marocco et al. and the Deliverable 2.1 [31][30]; the formula is written in the following relation.

$$i = \frac{d-ir}{1+ir} \qquad (65)$$

where i is the real discount rate (also called corrected discount rate), d correspond to the nominal discount rate and ir represent the inflation rate. The value of d and ir are, respectively, 7 % and 2 %, according to the information explained in the reports mentioned before, to obtain a real discount rate value equal to 4.9 %.

Another method is the WACC, acronym of the Weighted Average Cost of Capital, that can be taken as real discount rate assuming different financial parameter considering the performance of the stock market [126]. In the equation below, the formula of the WACC is represented.

$$WACC = \%E \cdot K_e + \%D \cdot K_d \qquad (66)$$

where $\%E$ and $\%D$ represent, respectively, the equity and debt percentage of the capital investment, K_e is the equity cost and K_d is the debt cost. To assume real values for the equity and debt percentages, we have to apply some hypothesis on the financial structure of the investment. Assuming that this is a high risk project with a IPP type of developer/owner structure (Independent Power Producer), from the NETL cost estimation methodology, we can find an equity percentage value of 40 % and a debt percentage value of the remaining 60 % [127]. In this case, a negligible corporate tax rate is assumed. Instead to find the cost of equity we have to apply the following equation.

$$K_e = R_f + premium \qquad (67)$$

where R_f is the systemic risk discount rate (risk “free”) and the premium is the increase in risk for our investment. As risk free the mean value of the 10 years government bond performance can be taken, because they are consider the investment with the lowest risk in the market; in Italy, the government bond is the BTP, and the value is obtained from

Sole24Ore site [128]. The value changes every day, so we have to evaluate all our parameter in the same day to obtain a reasonable WACC. The premium equation is represented below.

$$premium = R_s + \beta \cdot (R_m - R_f) = R_s + \beta \cdot EMRP \qquad (68)$$

where R_s is the small stock premium, and so considers the liquidity of the investor, β is the average yield variance compared to the market (sensitivity respect to a market modification), R_m is the average economic return of the market and the $EMRP$ is the Equity Market Risk Premium. Assuming that we are not a little investor, so some liquidities are available, the small stock premium value is considered equal to 0. Instead for β, the same variation of the market yield is accepted, so with a value equal to 1. For last, the $EMRP$ can be found from the KPMG research summary every 3 months, but the March 2020 report has not been published; this is due to the pandemic crisis caused by the coronavirus that interrupted the work of any statistical institute as KPMG (acronym of the initial letters of the organization founders) [129]. As we can see from their site, the December 2019 research summary can be used also for the first 2020 quarter, so a value of 6.0 % can be used [130].

The cost of debt must be also evaluated, with the following formula.

$$K_d = IRS + spread \qquad (69)$$

where IRS correspond to the Interest Rate Swap, that is the value of the interest rate applied to a fixed rate loan, and $spread$ represents the rate that guarantee a gain for the bank, it depends on the investor type and on the investment risk. Also the value of the IRS can be taken from the Sole24ore site [131], instead for the spread value, considering an investor with a stable economic, we can assume also a lower value (less investment risk for the bank).

In the following table, all the economic and financial assumptions for the WACC estimation are summarized, and is also represent the WACC value evaluated at the 9th April 2020.

As we can see, the $WACC$ value is not so different respect to the real discount rate obtained with the first method. Finally, in this study a real discount rate equal to the Weight Average Cost of Capital is considered.

In literature, a very wide range of i values can be found; some studies consider the nominal discount rate equal to 7÷8 % or even more (as [13], [23], [72], [74]), but also other studies consider a value more similar to us, around 5 % (as [22], [24], [25], [71]).

Table 27 Economical and financial information to evaluate the WACC

WACC evaluation

Equity %	40	**Debt %**	60
$\boldsymbol{K_e}$ **[%]**	7.729	K_d [%]	2.56
$\boldsymbol{R_f}$ **[%]**	1.729	$\boldsymbol{IRS}$ **[%]**	0.06
$\boldsymbol{premium}$ **[%]**	6	$\boldsymbol{spread}$ **[%]**	2.5
$\boldsymbol{R_s}$ **[%]**	0	$\boldsymbol{WACC}$ **[%]**	4.6276
$\boldsymbol{\beta}$ **[%]**	1		
$\boldsymbol{EMRP}$ **[%]**	6		

Table 28 Economical and financial plant assumptions

Economic and financial plant assumptions

System lifetime (n)	20 years
Real discount rate (i)	4.6276 %
Developer/owner structure	IPP
Investment risk	High
Liquidity stock	High ($\boldsymbol{R_s} = 0$ %)
O&M costs	Depends on component
Transport and installation costs	15 % (except than PV and CHP systems)

6 Results and discussions

6.1 CO2 avoided

Using a hydrogen storage system linked to a RES supply, a high amount of CO_2 can be avoided during the energy production and public transport. In the following sections, the CO_2 value for the different utilities is evaluated.

6.1.1 Energy production

To produce energy, a standard engine used for isolated users is the stationary diesel engine. An engine at least equal to the maximum electrical load required from Borgata Ambornetti must be taken; from the load data (month average data) we can see that the maximum load is 65.534 kW, and this value is reached in more than one month. To be sure that the engine can satisfy the electrical load, a 66 kW diesel engine is selected.

Now, the fuel consumption of the engine must be evaluated; from the work of Dufo-Lopez et al. and the work of Maleki et al. [132][133], a linear relation depending on the diesel engine nominal power and on the power at which the engine work in the moment consider is used:

$$Cons_{fuel} = B_G \cdot P_{N,G} + A_G \cdot P_G \qquad (70)$$

where A_G and B_G are the coefficients of the consumption curve, measured in l/kWh, $P_{N,G}$ is the nominal power of the diesel engine and P_G is the output power of the diesel engine. The two constant coefficients can be taken by the study of Skarstein and Ulhen [134], equal respectively to 0.246 l/kWh and 0.08145 l/kWh.

So, from this relation, the total fuel consumption in one year is 135940.5 liters of diesel. In literature, we can find different value of CO_2 production knowing fuel consumption; in the report of Jakhrani et al., several studies are considered [135]. In the work of Alsema, the coefficient is hypothesized in the range 2.4-2.8 kg_{CO2}/l; in detailed, the value of 2.63 kg_{CO2}/l is selected, as expressed in the report [136]. Instead, for Fleck and Huot the emission factor from a diesel generator is 3.15 kg_{CO2}/l, but considering only the diesel combustion part (and not the part of the fuel and generator production, for a Life Cycle Analysis), the emission decreases to 2.86 kg_{CO2}/l [137]. The last work considered provide an emission of around

2.7kg of CO_2 for a consumption of one liter diesel [138]. Knowing all these emission factor, we can say that the annual emission of CO_2 is in the range 358-389 tons.

Another possible solution to evaluate this factor is to consider the real chemical reaction. The diesel fuel is a mixture of different hydrocarbons, but we can consider in the reaction for a common diesel fuel an average hydrocarbon, that is $C_{12}H_{24}$ (Cyclododecane); the hydrocarbons present approximately differ between $C_{10}H_{20}$ to $C_{15}H_{28}$ [139]. From the reaction, we can see that from 2 moles of $C_{12}H_{24}$, we obtain 24 moles of CO_2

$$2C_{12}H_{24} + 36O_2 \rightarrow 24CO_2 + 24H_2O \qquad (71)$$

Now, assuming an engine efficiency of 40% [140], an LHV of 42.7 MJ/kg and the molecular weight of the cyclododecane and carbon dioxide respectively 168 g/mol and 44 g/mol, we obtain that in 1 year the fuel consumption is around 122 tons of diesel and so the annual CO_2 emission is 383 tons. We can observe that this value is contained in the range evaluated before using the emission factor found from literature.

As alternatives to the diesel generator, we can try to understand the CO_2 avoided due to the connection to the national electric grid. This solution is not so reasonable because the plant location, as explained at the beginning, is inside “Parco del Monviso”, a protected mountain area and so it’s difficult to take the authorization for starting the connection work. From the ISPRA report [99], in the 2016 the Italian gross energy production is around 289.8 TWh, with a CO_2 production to the energy production of 92.6 Mton. This means an emission factor of 0.32 kg_{CO2}/kWh and considering the annual electrical load of Borgata Ambornetti, the CO_2 avoided is 113.4 ton. The value is very lower respect to the emission of a diesel generator; this probably is due to the high fraction of RES plants (that has null or at most very low emission considering a LCA study) present in the Italian national grid.

Now, a similar CO_2 evaluation is done also for a CHP system; not all the configurations studied in this Master Thesis consider this type of system, because of the not completely CO_2-free solution. It can be considered a renewable energy source, because of using local biomass that can regenerate during the years; the utilization of local biomass is an important factor because of the possibility of emits the same or also lower amount of carbon dioxide absorbed by the biomass during its life. Not yet knowing the quantity of biomass (in energy form) consumed by the CHP system, because depends on its size that is selected by the optimization algorithm, we can calculate the possible carbon dioxide emission considering that the annual electricity load is completely satisfy by CHP. Initially, a biomass CHP

emission factor must be found from literature; in the PFPI report, an emission factor of 213 lb_{CO2}/MMbtu is considered, equal to, in the IS, around 0.329 kg_{CO2}/kWh and knowing the total energy consumption of 354.83 MWh, we obtain 116.98 ton_{CO2} as total emission [141].

6.1.2 Mobility

For the automotive part, a traditional diesel minibus is assumed. As fuel consumption we can take an average of 0.21 l/km [142], instead as emission factor per km per person the average of a UK analysis in the public transport sector is estimated of around 0.055 kg_{CO2}/km in the case of a diesel minibus [143]. So, with an average number of 15 passengers as hypothesis, the CO_2 production per liter of diesel is around 3.93 kg_{CO2}/l.

The routes considered for the minibus line are two, and for all the distance (also in one day and in one year assuming 4 travel per day roundtrip), the daily and annual fuel consumption and the CO_2 production per day and year are evalated. In the next table all the results are summarized.

Table 29 Automotive CO2 production per year

Route	*km/day*	*km/y*	*l_{fuel}/y*	*ton_{CO2}/y*
Ostana-Ambornetti	36	13140	2759.4	10.8
Paesana-Ambornetti-Pian del Re	224.8	82052	17230.9	67.7

The amount of CO_2 avoided is very lower respect to the energy production case, because for this part we consider only one minibuses that runs 8 times along the Po Valley; considering the two loads, a total amount of 368.8÷456.7 ton_{CO2} are avoided.

6.2 Scenarios under study

6.2.1 Base scenario

The base scenario studied in this Master Thesis has the following characteristics:

- Only photovoltaic and wind energy production system (no CHP);
- PEM electrolyzer and PEM fuel cell;

- Paesana-Ambornetti-Pian del Re trip;
- Two storage tank options at different pressure;
- 12-minutes refueling;
- 3 refueling per day;
- 4 roundtrip travels per day.

First, the optimal number of compression stages must be verified, to obtain the best economic configuration considering investment cost but also operational cost. As we can see from the plot below, for the 20 years system lifetime simulation two compression stages is the best economic solution. So, for all the next scenarios, a 2-stages compression is considered.

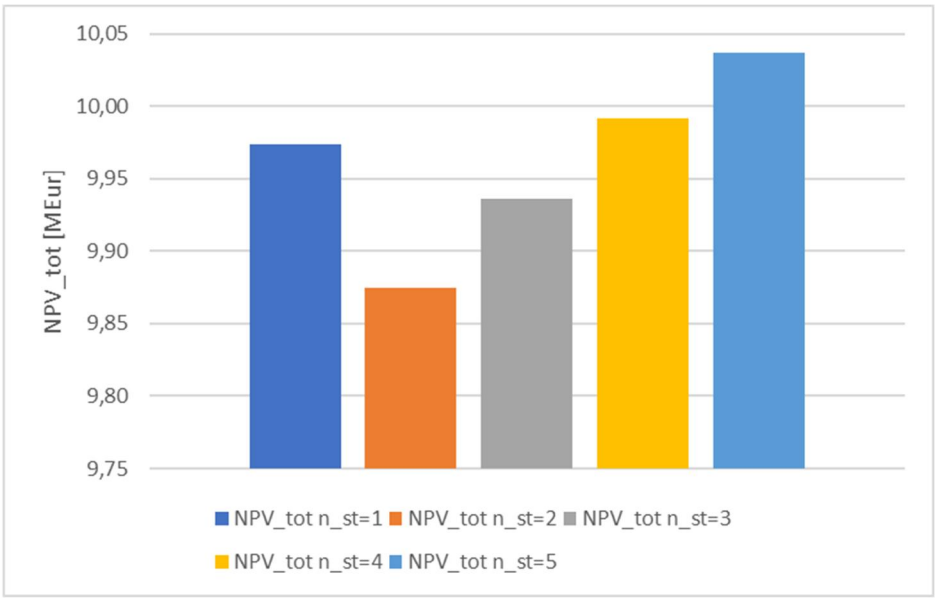

Figure 34 NPV variation for different compression stages number

In a completely CO_2-free scenario, all the electrical and mobility load must be satisfied using RES coupled with a fuel cell technologies; this means that there is not a system able to work as base load and also with a predictable and constant source of energy, with the risk of oversizing RES and storage capacity; because first, the RES production is used but when they cannot produce energy, the fuel cell must satisfy the rest of load. In the following figures, the optimal NPV for three different value of LPSP and LHSP are shown, with also the contribution of the different components for the optimal configuration with LPSP and LHSP equal to 1 %.

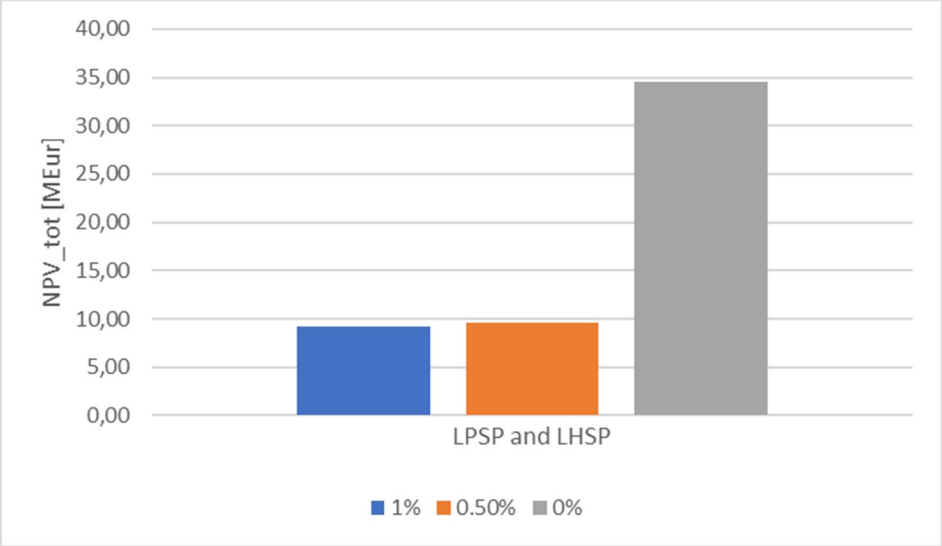

Figure 35 NPV_tot for different LPSP/LHSP values (base scenario)

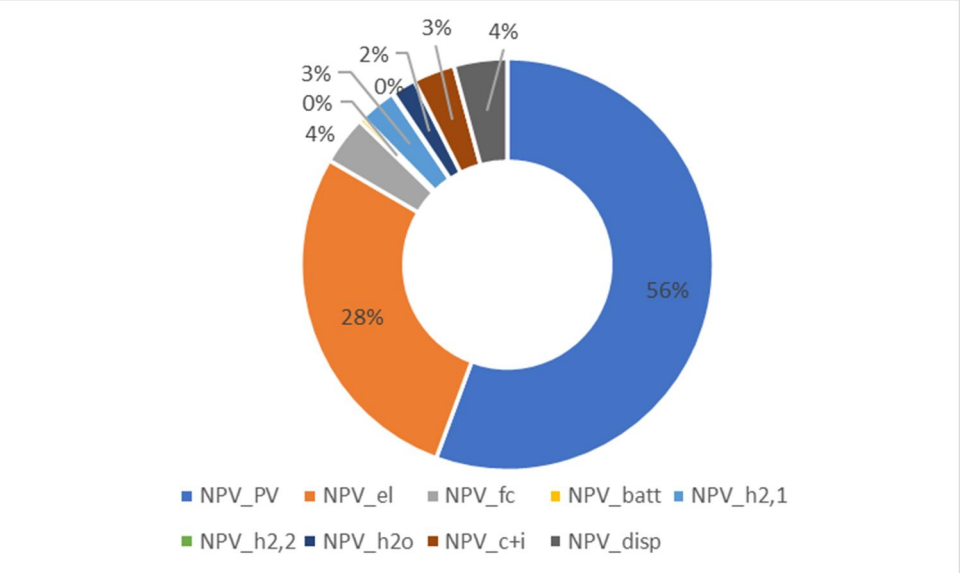

Figure 36 Components contribution on the total NPV (base scenario)

As explained by the second figure above, the more expensive components of the system are the photovoltaic system and the electrolyzer; this is probably due to the necessity of satisfy the load only with the photovoltaic system coupled with a fuel cell. The wind turbine is not present because of the very low production of energy, so, from the optimization algorithm in all the possible configurations, a wind turbine size equal to zero is obtained. The fuel cell investment is not so high because of the limited electrical load required (also

considering the compression portion), instead the electrolyzer must produce the hydrogen necessary to satisfy both electrical and mobility loads. The hydrogen pathway (for energy production) could not intervene every day; but its function is essential as a backup medium to guarantee energy self-sufficiency. The satisfy electricity load is divided in the following way: 42.8 % from RES and the rest 56.2 % from the fuel cell (in case of 1 % of LPSP). A high amount of energy produced by the RES is curtailed; this is probably due to the peak demand, that must be satisfy but only in very few hours during the year happened (45.7 % of the total energy produced). Instead for the 0 % simulation, an incredible energy curtailed value of 91 % is computed; this is obviously due to the system oversizing. The lifetime for fuel cell and electrolyzer systems are also computed in the simulation; respectively, lifetimes of 4.8 and 6.7 years are obtained, according to the information found in literature. In the following table the main component sizes are summarize; the investment for the low pressure storage tank is not so high due mainly to the low specific investment cost of the component, that is lower respect to the PV system and to the electrolyzer. The high value of power installed for the photovoltaic system is due to the fact that it must be able to cover partially the load and produce the hydrogen required by mobility but also by the fuel cell when solar power is not available, and so mainly during night; the same for the electrolyzer and low pressure hydrogen tank, that in this scenario is continuously required for the system operation.

Table 30 Main components size (base scenario)

Components	**Size**
PV system	2685 kW
PEM fuel cell	75.9 kW
PEM electrolyzer	994 kW
Low p tank	12543 kWh

Instead, in the first of the figures in the previous page, an interesting NPV behavior is obtained; for a completely satisfied load (both electric and mobility) a very high NPV value at the end of the lifetime is obtained. Also the LCOE and LCOH increase, from 1.28 €/kWh and 38.29 €/kg to 5.08 €/kWh and 125.74 €/kg; this increase is too high, mainly due to the very higher PV size (around 16.5 MW). So, a more detailed study must be done; to

understand better this behavior, other simulations with different LPSP and LHSP values (from 0.5 % to 0 %) are done, with the following results.

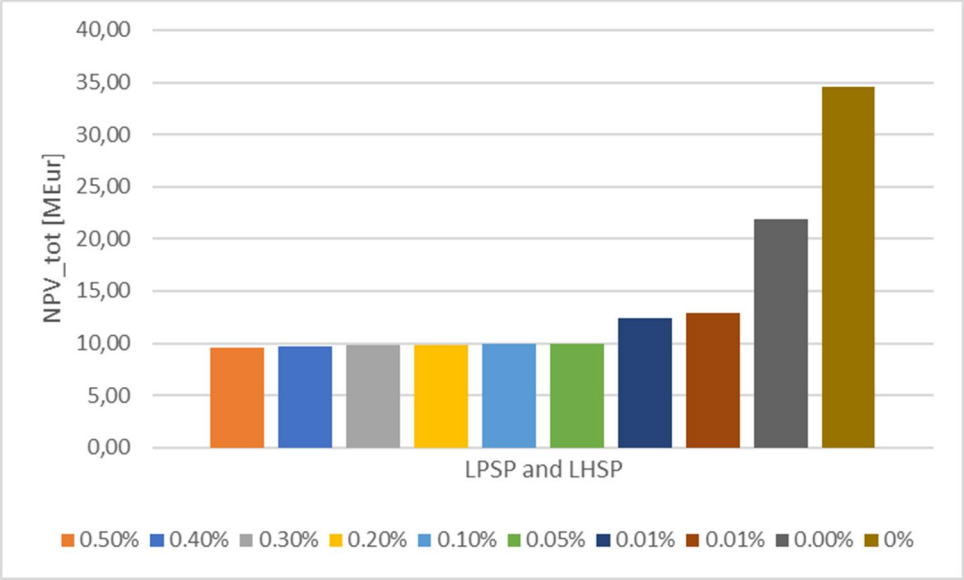

Figure 37 NPV variation for more values of LPSP and LHSP (base scenario)

As explained by the graph above, only for a LPSP and LHSP of 0.01 % a discontinuity can be observed; a LPSP and LHSP of 0.01 % of external source to satisfy the loads is a very low value, that can be considered as acceptable in case of off-grid application as in Borgata Ambornetti. A possible solution to this strange behavior is the lower operating boundary of the fuel cell; in the simulation if the operating partial load of the fuel cell is lower than 10 % (its lower boundary), the FC system cannot work. With the hypothesis of satisfy the portion of the load required and curtail the rest energy produced by the fuel cell operating at its lower boundary and that this peaks of load happen only in a few hours of the year, a new set of simulation is done. As seen from the plot below, considering only a few simulations we can find that the argument explained before is the reason of the NPV discontinuity in the initial configuration; with the new value of fuel cell lower operating boundary, a more linear behavior of the net present value is obtained, allowing to obtain a completely autonomous system without a too high investment expenditure. So, with a LPSP and LHSP between 1 % and 0 %, a LCOE and LCOH in the range, respectively, of 1.28÷1.39 €/kWh and 38.29÷40.73 €/kg are acquired, mainly due to the lower size of PV system (from around 16.5 MW to “only” 3 MW). Considering a literature value of around 18 €/kg for an on-site

electrolysis, the value of LCOH in our case is too high. Also the LCOE is higher than other studies; in a previous report of the REMOTE project, the value for Demo 3 is around 0.55 €/kWh. Only also considering a CHP system in the configuration a similar value can be achieved, as we will see in a following CHP-optimized scenario.

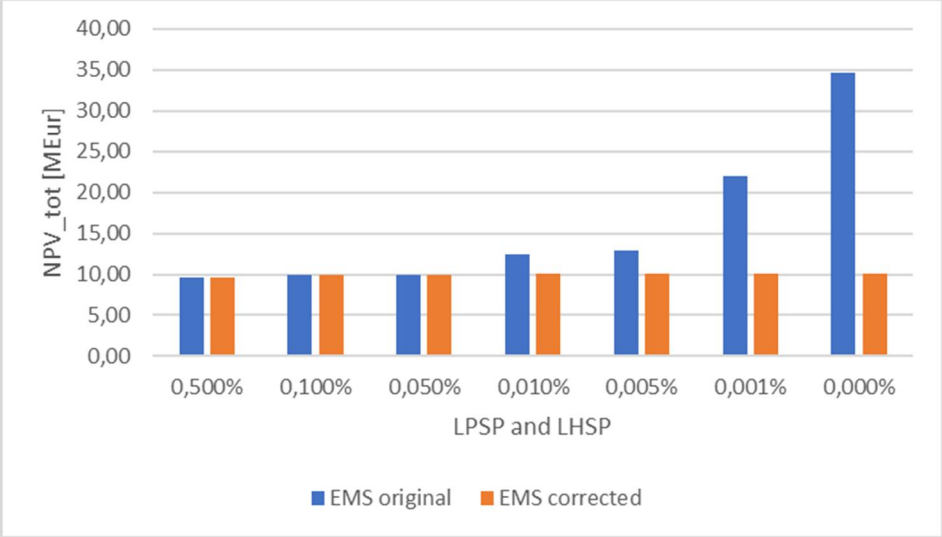

Figure 38 NPV variations with different LPSP and LHSP values for the two fuel cell lower boundary conditions

It should also be noted that possible local utilization of by-products from H2-based devices operation, such as heat and oxygen, has not been taken into account in the present economic analysis. Moreover, environmental advantages are also linked to these types of hybrid energy storage systems since they represent an interesting low carbon alternative to the usage of traditional fossil fuels.

In the next subchapters, only the main differences of the different scenarios respect to the base scenario are shown.

Table 31 Results summary for base scenario

RES production		**Load satisfied**		**Economic info**		**Other information**	
Load	6.6 %	*RES*	43.1 %	*NPV*	9.21 M€	*FC lifetime*	4.8 y
ELY	47.7 %	*FC*	55.9 %	*LCOE*	1.28 €/kWh	*EL lifetime*	6.7 y
Curtailed	45.7 %	*External*	1.0 %	*LCOH*	38.29 €/kg	*CO_2 prod*	0.0 ton

6.2.2 Alkaline electrolyzer scenario

In this scenario, the only difference respect to the base one is the substitution of the electrolyzer technology types: an alkaline electrolyzer is considered instead of a PEM one. As explained in previous sections, alkaline electrolyzers have different characteristics and parameters than PEM electrolyzer, so a different techno-economic analysis is expected to be obtained. The same value of LPSP and LHSP are studied, and the results are summarized in the following figures; in the second one, only the 1 % solution of LPSP and LHSP is considered to find the contribution of each single component for the total net present value.

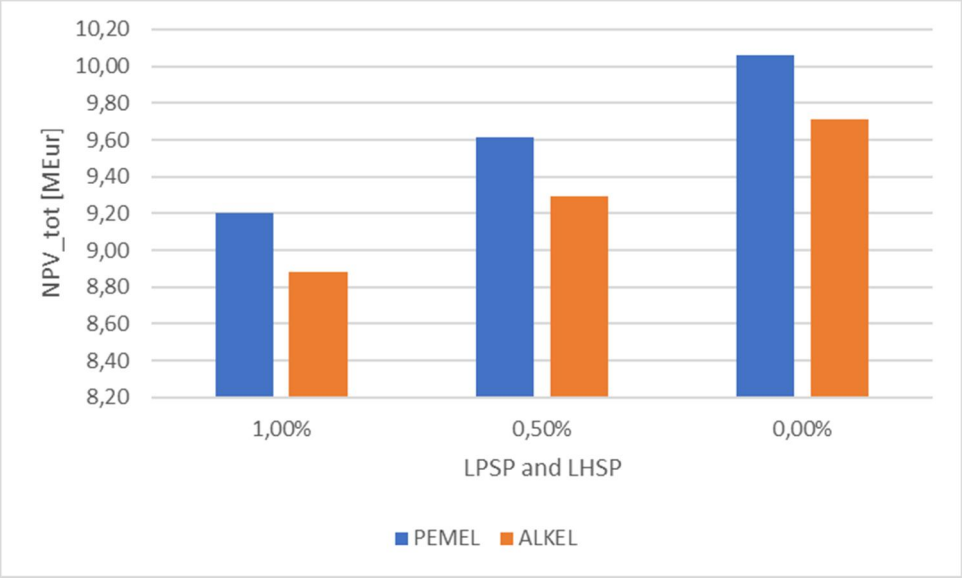

Figure 39 NPV differences between base scenario and ALKEL one for different LPSP and LHSP values

From the graph above we can understand that using an alkaline electrolyzer at the moment is economically better respect to the base scenario using a PEM electrolyzer, with a difference of around 400 k€ for all the simulations. The reasons can be various: the first is the specific investment cost, lower for an alkaline electrolyzer because of the higher level of technology development; another possible reason is the different component lifetime computed by the simulation. Respect to a lifetime of 6.7 years for the PEM electrolyzer, the alkaline one has a lifetime of 10.9 years; in a system with a total lifetime of 20 years this means that alkaline electrolyzer must be replaced only one time instead of two times as PEM electrolyzer.

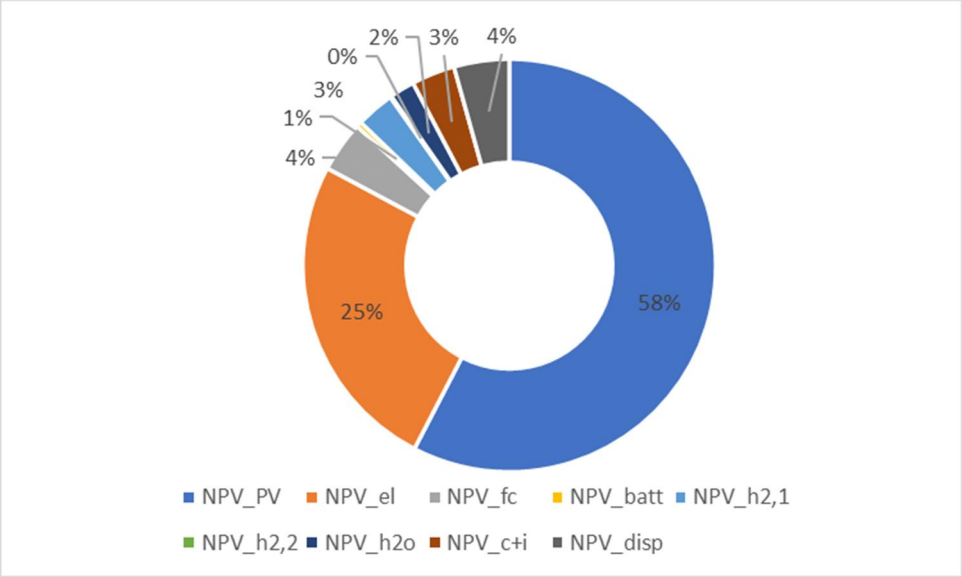

Figure 40 Components contribution on the total NPV (ALKEL scenario)

The fact that alkaline electrolyzer is cheaper than PEM one is explained by the previous figure above, where the electrolyzer contribution is reduced from 28 % of the initial scenario to 25 % of the current scenario. In this way, also the LCOE and LCOH are reduced and, for the 1 % of LPSP and LHSP simulation, become 1.23 €/kWh and 36.96 €/kg; this variation is only due to the different investment of the electrolyzer because no other important variations are obtained.

Table 32 Results summary for alkaline electrolyzer scenario

RES production		**Load satisfied**		**Economic info**		**Other information**	
Load	6.6 %	*RES*	43.1 %	*NPV*	8.88 M€	*FC lifetime*	4.8 y
ELY	47.7 %	*FC*	55.9 %	*LCOE*	1.23 €/kWh	*EL lifetime*	10.9 y
Curtailed	45.7 %	*External*	1.0 %	*LCOH*	36.96 €/kg	*CO_2 prod*	0.0 ton

6.2.3 Ostana-Ambornetti trip scenario

In this case, a different mobility scenario is studied; instead of considering a minibus line for all the Po Valley, only the connection between Ambornetti and Ostana, the nearest inhabited mountain village, is considered as shown also in previous chapters. So, a lower mobility load

is required with a possible increase in the LCOH evaluation, due to the lower hydrogen mass delivered by the refueling station. A lower hydrogen refueling station size is expected, and so a lower investment cost for the hydrogen part but with a possible increase in the LCOH.

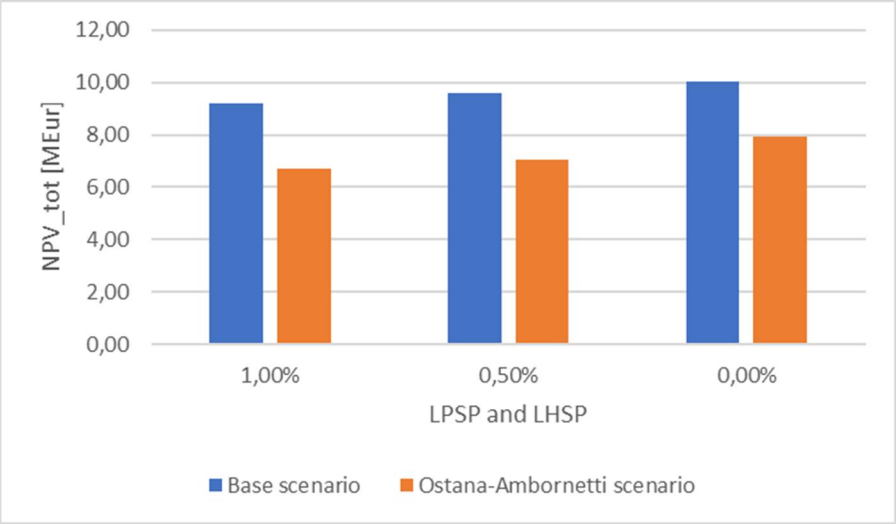

Figure 41 NPV differences between base scenario and Ostana-Ambornetti one for different LPSP and LHSP values

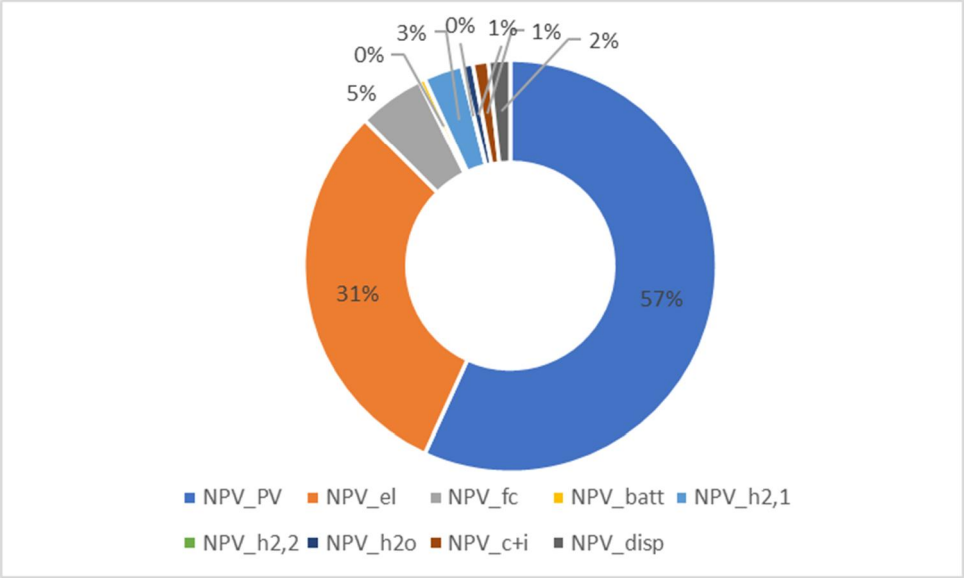

Figure 42 Components contribution on the total NPV (Ostana-Ambornetti mobility scenario)

As represented from the first figure above, the NPV is lower in this different mobility scenario, but the same discontinuity of the base one is always present. The reason of it is the same of the initial configuration, and probably is obtained for all the scenarios without a CHP

system that consider also the electric load of the village. Looking at the size of the main components, they are all lower respect the initial case: reducing the hydrogen mass required by the mobility load, the energy production, hydrogen production and hydrogen storage can be lower. in the following table, all the component sizes are summarized. This may also explain the little difference in the components contribution to the total NPV, because all the system components are affected by the lower load required, unless the fuel cell, that must satisfy the electrical load of Ambornetti. So, a higher FC contribution is obtained. Reducing the PV system size, also the energy produced curtailment does not change: from a value of 45.7 % of the total energy produced, a value of 46.5 % is computed. The main reason is because despite we reduce the energy produce by the system, also the hydrogen production through the electrolyzer is lower because lower hydrogen mass is required by the minibus. Instead, both LCOH and LCOE increase respect to base scenario, with an increase of LCOE content lower compared to the increase of LCOH. In the case of 1 % of LPSP and LHSP simulation, the LCOE and LCOH values are, respectively, 1.34 €/kWh and 46.14 €/kg.

Table 33 Main components size (Ostana-Ambornetti mobility scenario)

Components	**Size**
PV system	2004 kW
PEM fuel cell	68.5 kW
PEM electrolyzer	707 kW
Low p tank	9578 kWh

Table 34 Results summary for Ostana-Ambornetti mobility scenario

RES production		**Load satisfied**		**Economic info**		**Other information**	
Load	8.7 %	*RES*	42.9 %	*NPV*	6.72 M€	*FC lifetime*	4.8 y
ELY	44.9 %	*FC*	56.1 %	*LCOE*	1.34 €/kWh	*EL lifetime*	7.4 y
Curtailed	46.5 %	*External*	1.0 %	*LCOH*	46.14 €/kg	*CO_2 prod*	0.0 ton

6.2.4 5-hours refueling (high pressure tank filling)

A possible different refueling configuration can be considered to try to reduce the hydrogen refueling station investment cost. With an initial reasoning, it is expected that increasing the hours of high pressure tank filling with the same hydrogen amount requested by the minibus,

a hydrogen refueling station of lower size would be acquired; the high pressure tank has the same size (equal to the hydrogen quantity contained in the minibus tank), but compressors, intercoolers and lower pressure tank could probably have a lower size due to a lower H_2 flow rate. Instead the dispenser at 350 bar is not affected by this variation, because the minibus refueling is done always in 12 minutes as the base scenario and it is the high pressure tank filling time that changes. The same value of LPSP and LHSP are studied, and the results are summarized in the following figures; in the second one, only the external 1 % solution is considered to find the contribution of each single component for the total NPV.

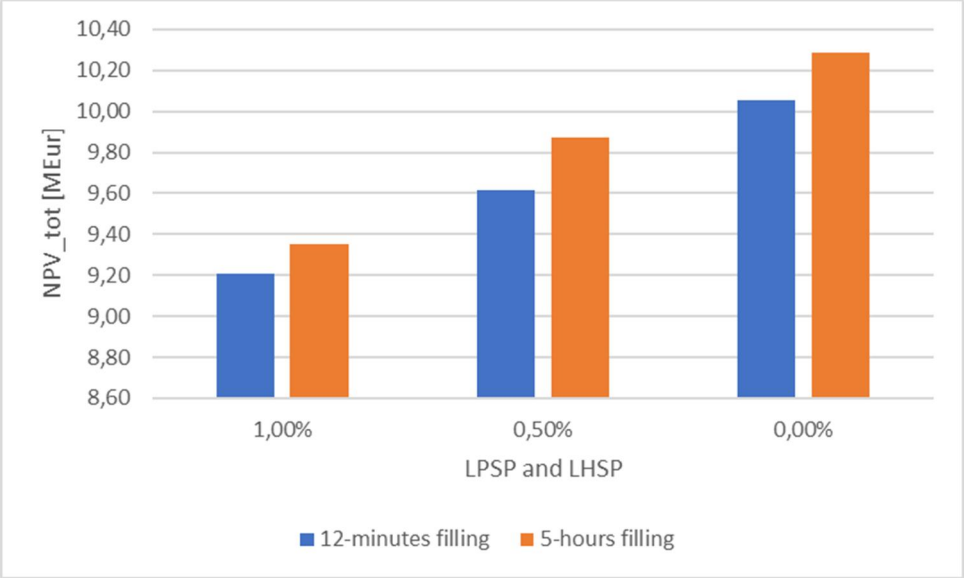

Figure 43 Differences between base scenario and 5-hours filling one for different LPSP and LHSP values

Unlike previously assumed, the economic simulation in this new scenario gives us different results. For LPSP and LHSP values of 1 % and 0.5 %, higher net present values are obtained; instead only in the case of 0 % as LPSP and LHSP the 5-hours filling scenario has a lower NPV respect to the base one. To understand better this behavior, the main component sizes are represented.

As seen from the table below, but also from the component's contribution figure, the main difference with the initial configuration is the low pressure hydrogen storage size. Despite a lower size of the other components, the main economic contribution is given from the low pressure hydrogen storage size that has a more than double size respect the base scenario.

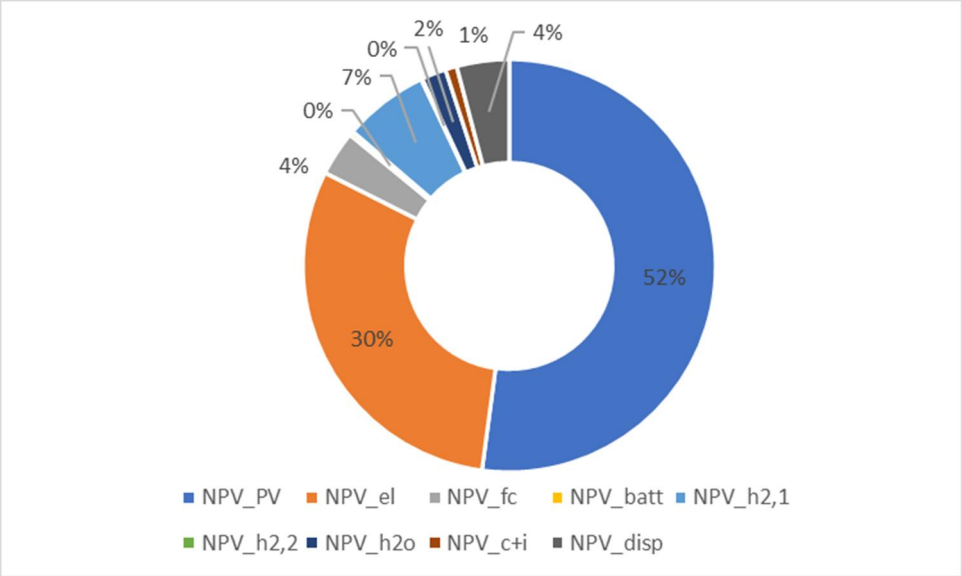

Figure 44 Components contribution on the total NPV (5-hours filling scenario)

Table 35 Main components size (5-hours filling scenario)

Components	**Size**
PV system	2557 kW
PEM fuel cell	68.6 kW
PEM electrolyzer	970 kW
Low p tank	29550 kWh

Also some simulations with an upper size boundary of 13000 kWh have been carried out, in order to understand if the optimal point is reached by the optimization algorithm or not. In this case, the optimal point is reached, so a strange behavior occurs in the system simulation with 5-hours filling. Making sure that the higher NPV values are not due to the lower operating boundary of the fuel cell, this behavior is probably due to a concomitance between electric energy required and hydrogen mobility required. Increasing the filling hour, increase the working hour of the hydrogen refueling station and the mass of H_2 required by the dispenser is divided and a lower flow rate is obtained. But probably a peak load required both from the village and from the HRS occurs, increasing the size of the low pressure hydrogen tank. Very interesting is the LCOH variation: instead of increase, a lower value is obtained, from 38.29 €/kg to 37.71 €/kg. This means that the oversizing of the tank is probably due to an electrical peak load and not to the mobility load. In accordance to this reasoning, the LCOE increase respect to the base scenario from 1.28 €/kWh to 1.32 €/kWh.

Table 36 Results summary for 5-hours filling scenario

RES production		Load satisfied		Economic info		Other information	
Load	7.0 %	*RES*	43.5 %	*NPV*	9.35 M€	*FC lifetime*	4.8 y
ELY	50.8 %	*FC*	55.5 %	*LCOE*	1.32 €/kWh	*EL lifetime*	4.8 y
Curtailed	42.2 %	*External*	1.0 %	*LCOH*	37.71 €/kg	*CO_2 prod*	0.0 ton

6.2.5 CHP scenario (both fixed and optimized size)

Different solutions can be obtained considering also a CHP system to produce energy required to satisfy both loads. These two scenarios, CHP size fixed at 49 kW and CHP size optimized, are not completely CO_2-free because to produce electricity a biomass combustion is required; but, as just said before in the previous chapter, the hypothesis of using only local biomass is done. In this way, we can say that the carbon dioxide produced during the CHP operation is about the same amount absorbed by the biomass during their life. A first fixed size scenario is considered with a 49 kW CHP, because this is in the initial size selected in the REMOTE project, but also an optimized CHP size scenario must be done. Obviously, it is expected that in both the cases the NPVs are lower than base scenario and also the main component sizes are lower because of the continuous predictable energy produced by the CHP system; for this reason, also the LCOE and LCOH values are expected to be lower. Another previous hypothesis to be made concerning the energy curtailment of the system; if at the beginning the value is high (around 46 %), with the CHP system is expected to be lower for not oversizing the photovoltaic panels size. The discontinuity in the NPV behavior when a 0 % of LPSP and LHSP simulation is done, in this case is not expected, because of the contribution of CHP also for the peak loads. The same value of LPSP and LHSP are studied, and the results are summarized in the following figures; in the second one, only the 1 % solution of LPSP and LHSP is considered to find the contribution of each single component for the total net present value.

From the graph, we can see the difference in net present value at 20 years between the two scenarios under study; respect to the base scenario, from an economic point of view a system based both on PV and CHP systems is better than only a PV-based standalone system. This is because, as just said before, a biomass energy source is more continuous and predictable respect to photovoltaic energy.

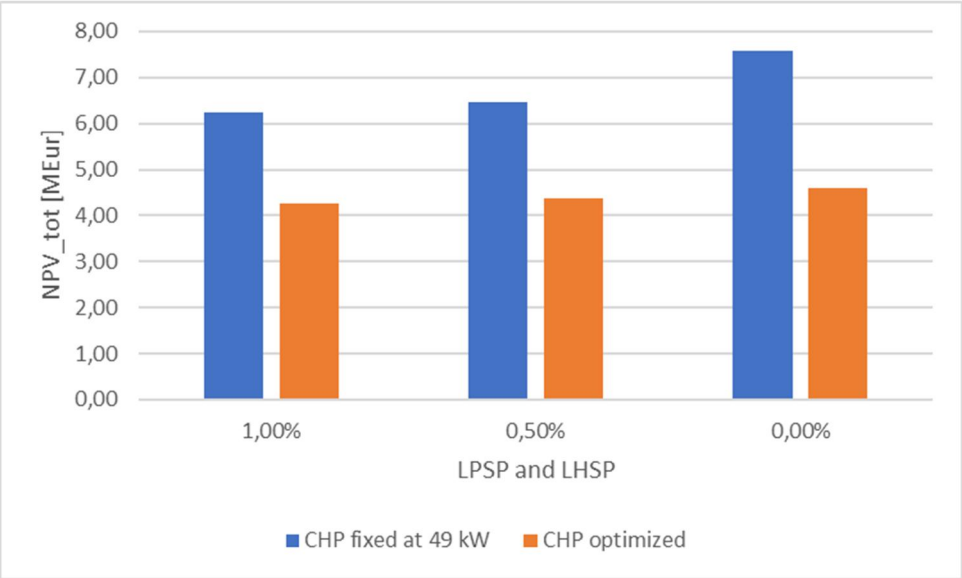

Figure 45 Differences between the two CHP-scenario for different LPSP and LHSP values

In the case of CHP size of 49 kW, the increase in cost between LPSP and LHSP equal to 0.5 % and 0 % is higher respect to the CHP-optimized case; the main reason is the not so high size choice for the CHP, because the higher electrical load requested by the village during one hour is around 66 kW, so also another energy source is needed and the PV system cannot always generate the remaining energy required. For this reason, the PV size for the 0 % simulation in the case of 49 kW CHP, as also shown in the following table for the 1 % case, is around 2 MW, that is very high considering the coupling with CHP system. Instead, in the CHP-optimized scenario for a 1 % simulation a PV size of around 110 kW is required but to reach the 0 % of external energy source contribution, a size equal to zero is needed for PV. So, only the CHP system is needed to obtain a perfectly standalone system. In the following tables, the main component sizes for the two scenarios are shown for the 1 % of external energy contribution simulations.

Table 37 Main component sizes (CHP fixed at 49 kW scenario)

Components	**Size**
PV system	1230 kW
PEM fuel cell	29 kW
PEM electrolyzer	438 kW
Low p tank	5854 kWh

All the component sizes are lower respect to the base scenario, so from this we can understand the utility of CHP system in our location. As expected, also the energy curtailed decrease, with a 37 % of the total energy produced by PV+CHP system in the 1 % simulation. The lower NPV affects also the LCOE and LCOH value for this scenario: respect the base scenario (that has, respectively, 1.28 €/kWh and 38.29 €/kg), a LCOE and LCOH of, respectively, 0.59 €/kWh and 39.97 €/kg are acquired. The main difference is obtained for the LCOE, with a very high decrease, instead for the LCOH there is a little increase. This is probably due to the fact that using a continuous energy source as CHP, a higher investment fraction of it affects the HRS, and so the economic fraction taken into account for the LCOH evaluation is higher respect to LCOE.

Table 38 Main component sizes (CHP-optimized scenario)

Components	**Size**
PV system	112 kW
PEM fuel cell	10.6 kW
PEM electrolyzer	68 kW
Low p tank	857 kWh
CHP system	104 kW

Very different sizes are found for the CHP-optimized scenario; the PV system now has a reasonable size respect to the CHP system, with a considerable decrease in the investment cost. But all the main components are design with lower sizes; the main difference is also obtained with the low pressure hydrogen storage tank size, that now it should not be oversized as the CHP system helps a lot also during night when the PV system does not produce. The energy curtailed percentage reaches now a very interesting value of 6 % respect the total RES production, according to the objective of a standalone self-sustainable system; obviously, this is due to the not oversizing of the system. Now, the values of LCOE and LCOH both decrease and reach interesting values of 0.29 €/kWh and 33.06 €/kg, mainly due to the lower total investment cost respect to the base scenario. Different values of lifetime for all the electrochemical hydrogen technologies are computed in the simulation: for the PEM electrolyzer, a lifetime of 4.2 years is obtained; this is probably due to its lower size, because to fill the low pressure storage required more operating hours than before, despite also the lower size of the storage system. Instead for the fuel cell system, an

incredible lifetime value of 85 years is computed; the main reason is the high investment cost of the system and the very low size (only 10.6 kW), so this technology is only used to cover the annual peak load when the couple PV-CHP system is not able to satisfy it. To reach the completely autonomy and self-sustainability of the system (so, with a LPSP and LHSP values of 0 %), the optimization algorithm shows us that the economical best configuration is with a PV size equal to zero. This means a completely CHP-based system to cover both electrical and mobility loads; probably because of the high reliability of the system. Instead, the other components have higher size, mainly the fuel cell system, because it must cover the electrical load during the maintenance period of CHP system. For this reason, the 300 k€ if investment increase is mainly due to the electricity load, as also shown from the LCOE and LCOH values, respectively, of 0.35 €/kWh and 32.86 €/kg, with a decrease for the mobility part. In the following figures, the components contribution to the total NPV are shown for both the CHP-based scenarios for the 1 % simulations.

As explained by the following graphs, the PV-system contribution decreases with a high contribution of the CHP system; mainly for the CHP-optimized scenario, the CHP system became the higher investment of the system. Despite the size are similar, CHP has a higher NPC at 20 years because of the initial investment and operating cost higher than PV; this is due to the biomass cost required for the CHP combustion and energy production.

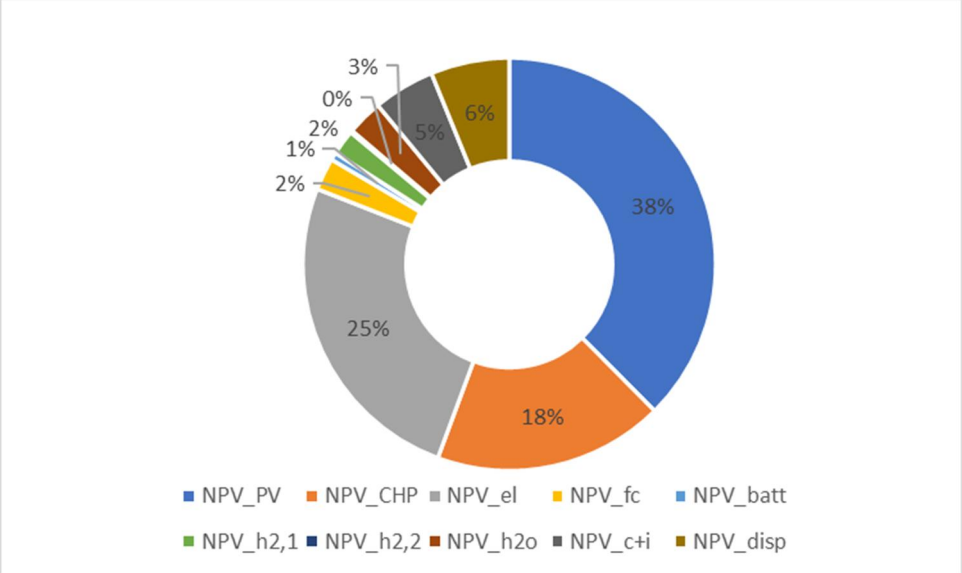

Figure 46 Components contribution on the total NPV (49 kW CHP scenario)

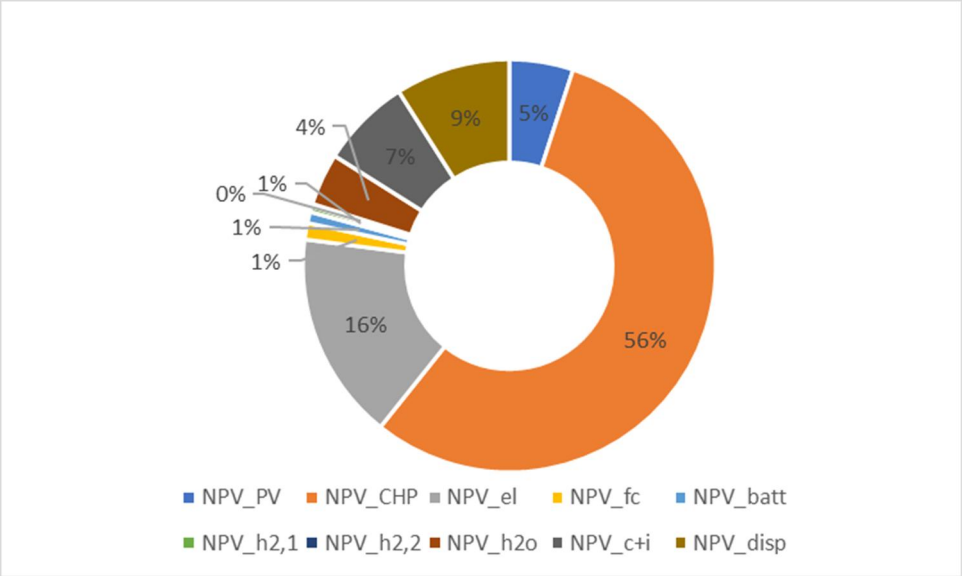

Figure 47 Components contribution on the total NPV (CHP-optimized scenario)

Table 39 Results summary for CHP-fixed scenario

RES production		Load satisfied		Economic info		Other information	
Load	22.0 %	*RES*	85.1 %	*NPV*	6.24 M€	*FC life*	6.5 y
ELY	40.2 %	*FC*	13.9 %	*LCOE*	0.59 €/kWh	*EL life*	6.5 y
Curtailed	37.8 %	*External*	1.0 %	*LCOH*	39.97 €/kg	*CO_2 pr.*	113.5 ton

Table 40 Results summary for CHP-optimized scenario

RES production		Load satisfied		Economic info		Other information	
Load	8.7 %	*RES*	42.9 %	*NPV*	4.27 M€	*FC life*	85.5 y
ELY	44.9 %	*FC*	56.1 %	*LCOE*	0.29 €/kWh	*EL life*	4.2 y
Curtailed	46.5 %	*External*	1.0 %	*LCOH*	33.06 €/kg	*CO_2 pr.*	239.7 ton

6.2.6 Only electrical load scenario

An only electrical load scenario is studied to understand the system configuration, both considering a PV-based system and a PV-CHP-based system. In the first case, a probable higher LCOE is expected, because all the system investment is used for the electricity load; obviously, the hydrogen refueling station components are not considered. Instead, the discontinuity in NPV for a system without any contribution from external source is expected to be obtained as the base scenario, because of the peak electrical load during the year that

an only PV-based system cannot satisfy without an oversizing. In the second case, a very low investment cost is expected because of the coupling of the two energy sources. As in the scenarios before, a lower electrolyzer lifetime is expected because a probable lower size could be obtained from the simulation. Also in this case we can obtain a higher LCOE respect to the CHP-optimized case, but this value will probably be lower than base scenario.

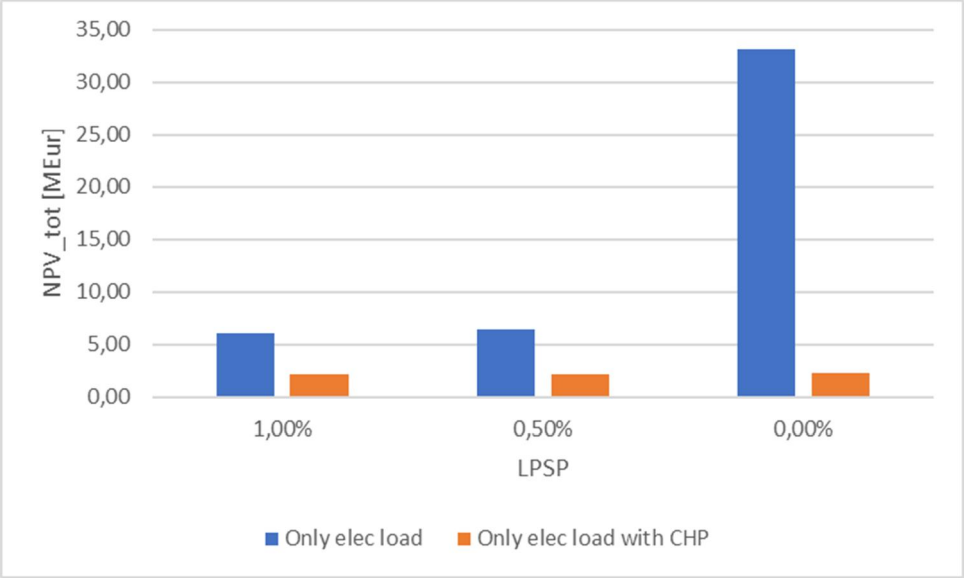

Figure 48 Differences between the two only electrical load scenarios for different LPSP values

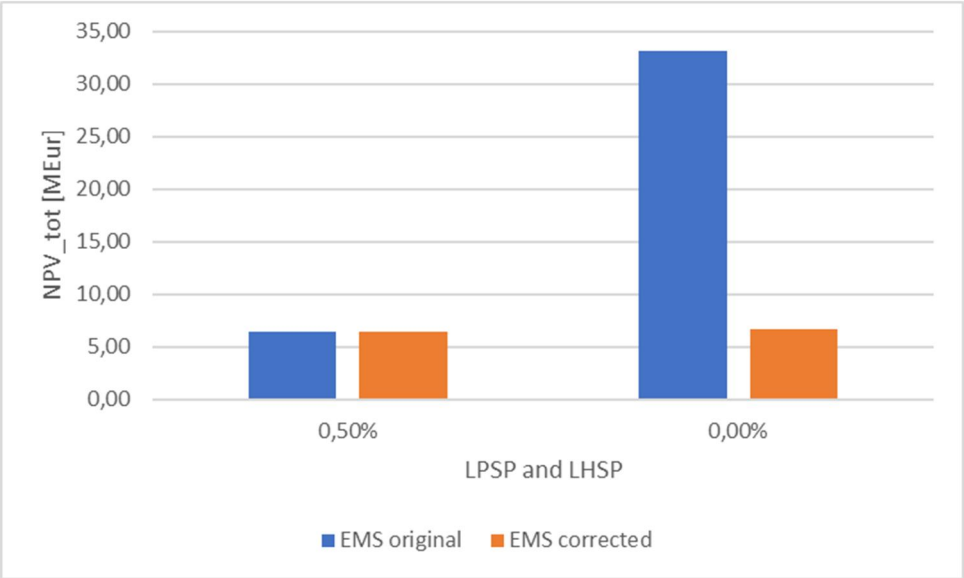

Figure 49 NPV variations for the PV-based only electrical load scenario with different LPSP values for the two fuel cell lower boundary conditions

As expected, the discontinuity in the NPV is due to the electrical peak load during the year; so, a different behavior is expected for the completely PV-based system with only mobility load scenario. Instead, the behavior also considering a CHP system is very different: a very low NPV is obtained, between 2.12 to 2.30 M€ changing the LPSP and LHSP values from 1 % to 0 %. To ensure that the reasoning initially carried out for the base scenario on the discontinuity of the NPV is correct, the same study considering the lower operating load boundary of the FC equal to zero has been made; as expected, the same behavior is computed with the only difference in the 0 % simulation, ensuring the fact that is only due to some peak of electrical load during the year.

In the following tables, the main component sizes are shown for both the scenarios. As just seen for previous scenarios, the sizes for the CHP-optimized with only electrical load scenario are very lower than the other; instead for the first scenario, the main differences are the PV and electrolyzers systems size. This variation is probably due to the lower hydrogen load required from the system neglecting the mobility part. As expected, the LCOE is higher than the base scenario because of the total investment for the electricity part, with a value of 1.35 €/kWh. For the same reason of lower hydrogen load and so lower production from the electrolyzer, a higher lifetime for the PEM technology is computed, with a value around 7.3 years, higher respect to the literature studied; instead for the FC technology, the same lifetime is obtained. A completely different lifetime behavior is computed for the second scenario; as for the CHP-optimized scenario, the PEM electrolyzer size is very lower than the base scenario, so it must probably work more hours to satisfy the hydrogen production required. In this way, a lifetime value of only 3.6 years is computed; instead the fuel cell operates less, only to satisfy some peak loads during the year, so a higher lifetime is obtained than the base scenario. The LCOE is lower as expected, but also a bit higher than CHP-optimized scenario, with a value of 0.47 €/kWh respect to 0.29 €/kWh. Another interesting behavior is the same of the CHP-optimized scenario: the variation of the PV system size for LPSP and LHSP values from 1 % to 0 %. In all the simulations done (1 %, 0.5 % and 0 %), the optimization algorithm gives us some configurations with a PV size equal to zero, but only in the 0 % simulations these configurations are the best economically. For the low pressure hydrogen storage tank, in the case of CHP-optimized only electrical load scenario, a more reasonable size is obtained; to translate in volume the 737 kWh measure, the H_2 LHV and density must be used, obtaining a volume of around 9 m^3 (respect to the 129 m^3 tank required for the only PV and electrical mobility scenario).

Table 41 Main component sizes (only electrical load scenario)

Components	Size
PV system	1812 kW
PEM fuel cell	68.6 kW
PEM electrolyzer	667 kW
Low p tank	10630 kWh

Table 42 Main component sizes (only electrical load with CHP scenario)

Components	Size
PV system	41.5 kW
PEM fuel cell	21.2 kW
PEM electrolyzer	16.2 kW
Low p tank	737 kWh
CHP system	67.3 kW

In the following figures, the components contribution for the two only electrical load scenario are shown; we can see that the two graphs reflect the same behavior of the base scenario for the PV-based electrical load one, and of the CHP-optimized scenario for the PV-CHP-based electrical load one, although the components of the HRS are overlooked.

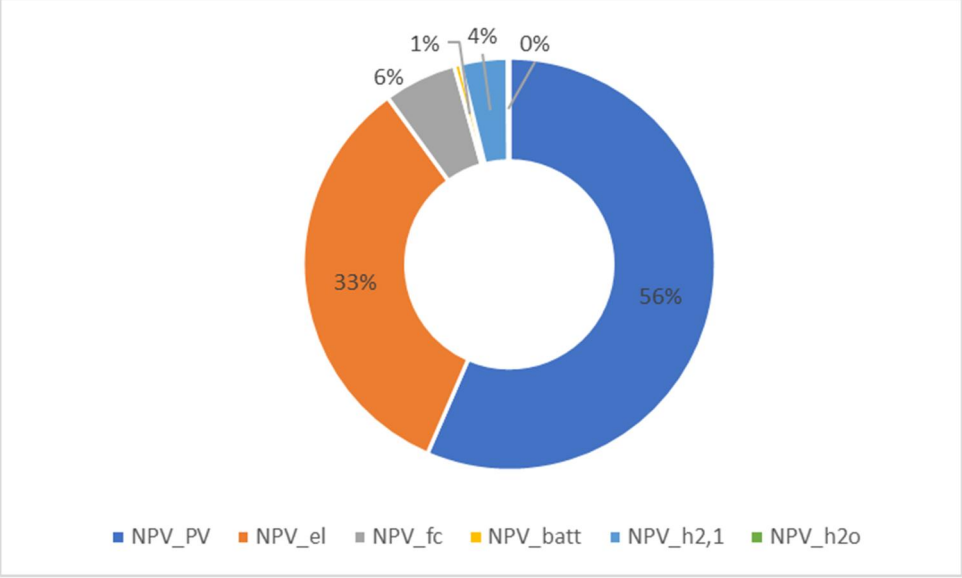

Figure 50 Components contribution on the total NPV (only electrical load scenario)

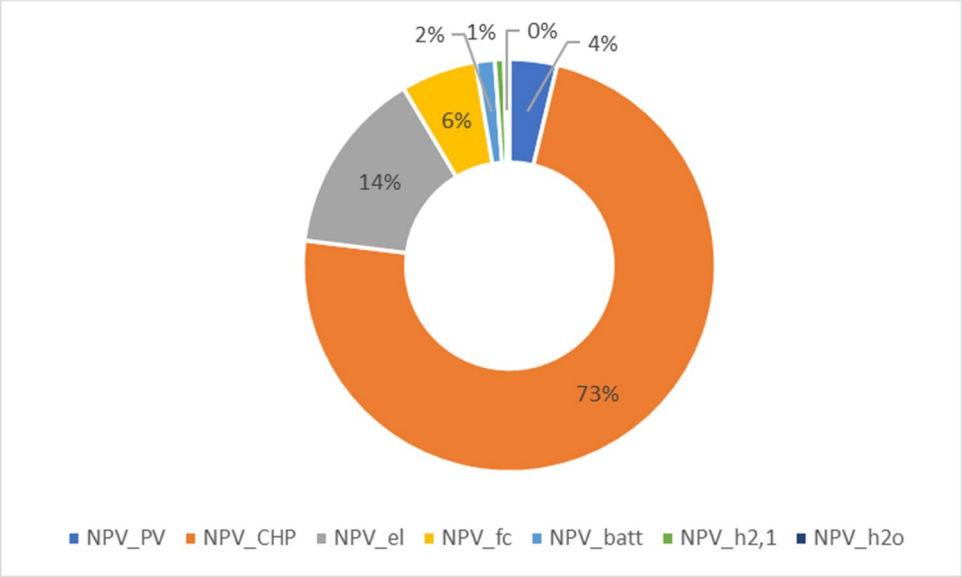

Figure 51 Components contribution on the total NPV (only electrical load with CHP scenario)

Table 43 Results summary for only electrical load scenario

RES production		Load satisfied		Economic info		Other information	
Load	9.5 %	*RES*	42.8 %	*NPV*	6.11 M€	*FC lifetime*	4.7 y
ELY	45.8 %	*FC*	56.2 %	*LCOE*	1.35 €/kWh	*EL lifetime*	7.4 y
Curtailed	44.7 %	*External*	1.0 %	*LCOH*	/	*CO_2 prod*	0.0 ton

Table 44 Results summary for only electrical load with CHP scenario

RES production		Load satisfied		Economic info		Other information	
Load	67.3 %	*RES*	92.8 %	*NPV*	2.12 M€	*FC life*	6.7 y
ELY	16.5 %	*FC*	6.2 %	*LCOE*	0.47 €/kWh	*EL life*	3.5 y
Curtailed	16.1 %	*External*	1.0 %	*LCOH*	/	*CO_2 pr.*	155.8 ton

6.2.7 Only mobility load scenario

In the possible case of only mobility scenario, only the completely RES CO_2-free configuration of the system is studied; this means that the CHP system is not considered, because produce hydrogen individually for the mobility load through a biomass combustion is not a very environmentally sustainable choice. Both the refueling configurations are

computed, in order to find the best HRS configuration; the 5-hours scenario, for the only mobility case, is expected to be the best one, because of the lower size of the refueling system components (due to the lower flow rate) and the probable lower size of the low pressure hydrogen storage system. Respect to the base scenario, the LCOH would be higher, because all the investment is done for the hydrogen mobility load; between the two cases under study, the 5-hours filling one is expected to be the best from a LCOH point of view. The fuel cell system will probably have a lower size, because it's used only for the operation of compressors when RES supply is not available (during the morning refueling and sometimes during the evening refueling); knowing that the 12-minutes filling scenario has a higher flow rate, the FC system will probably have a higher size respect the 5-hours filling one. In the following figure, the NPV variations with the LHSP value is explained, for both the refueling configuration scenarios in the case of only mobility load.

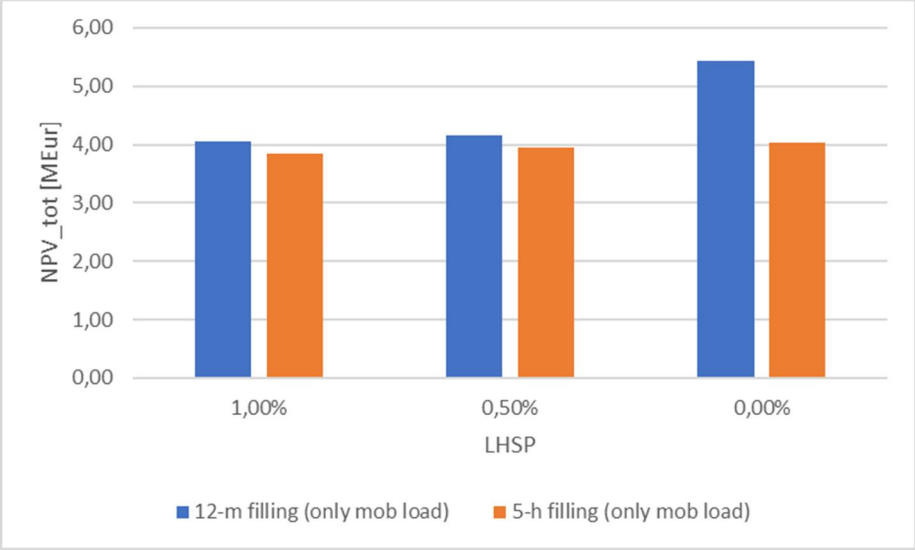

Figure 52 Difference in the NPV between the two filling configurations for only mobility load scenario with different LHSP values

As expected, the discontinuity is not present when we reach the completely autonomy of the system from an energy supply point of view; the increase for the 12-minutes filling for only mobility load scenario between 0.5 % of LHSP to 0 % is higher than the variation between 1 % and 0.5 %, but it's very lower respect to the variation in the base scenario. This means that the main contribution to the discontinuity in NPV is due to the electrical load peaks during the year, as assumed before. Instead for the 5-hours filling case, the variation is really limited, because of the lower but continuous hydrogen load required; in the initial filling

configuration, the hydrogen mass request by the HRS is the same but is required in a shorter period, so it can be seen as a peak load. This is the reason of the higher variation reaching the 0 % of external hydrogen supply. The LCOH values for both the scenarios are, respectively, 45.08 and 42.73 €/kg, with an increase than the base scenario situation; this means, as expected for both the only mobility and only electrical load, that a coupled system is better in terms of LCOE and LCOH, because, although the higher investment, the NPV is divided for the two energy carriers produced. Finally, we can say that for only mobility scenario, the best hydrogen refueling system configuration is the 5-hours filling one, as expected from previous hypothesis. In the following tables, the main component sizes are summarized for both the refueling configurations.

Table 45 Main component sizes (12-m filling only mobility load scenario)

Components	**Size**
PV system	829 kW
PEM fuel cell	15.3 kW
PEM electrolyzer	328 kW
Low p tank	3573 kWh

Table 46 Main component sizes (5-h filling only mobility load scenario)

Components	**Size**
PV system	876 kW
PEM fuel cell	3.2 kW
PEM electrolyzer	307 kW
Low p tank	3184 kWh

The hypothesis done before for the component sizes have been met; the only difference is the higher PV system size required in the second case, but always lower than the base scenario, because of the electrical load neglect. Instead, as expected before, the fuel cell size is only 3.2 kW for the 5-hours filling scenario respect to the 15.3 kW of the 12-minutes one; the reason is the compressors size due to the hydrogen flow rate request by the refueling station, lower if we increase the time period needed for the high pressure H_2 tank filling. Another important difference is the lower size of the low pressure storage tank; the

variation is not so significant, but is enough to understand that divided the hydrogen mass request is better. The differences could be also higher if the HRS was really sized for a 5-hours filling, instead, for a more precautionary choice in case of failures, it was sized for a 1-hour filling. The energy curtailment is almost the same of the base scenario for both the cases under study, because of the less probable directly utilization of the RES energy production and the main utilization to produce H_2. For this reason, also a lower lifetime for the PEM electrolyzer is computed, respectively for the cases of 6.0 and 5.35 years. In the following figure, the contributions of the components are shown for both the scenarios.

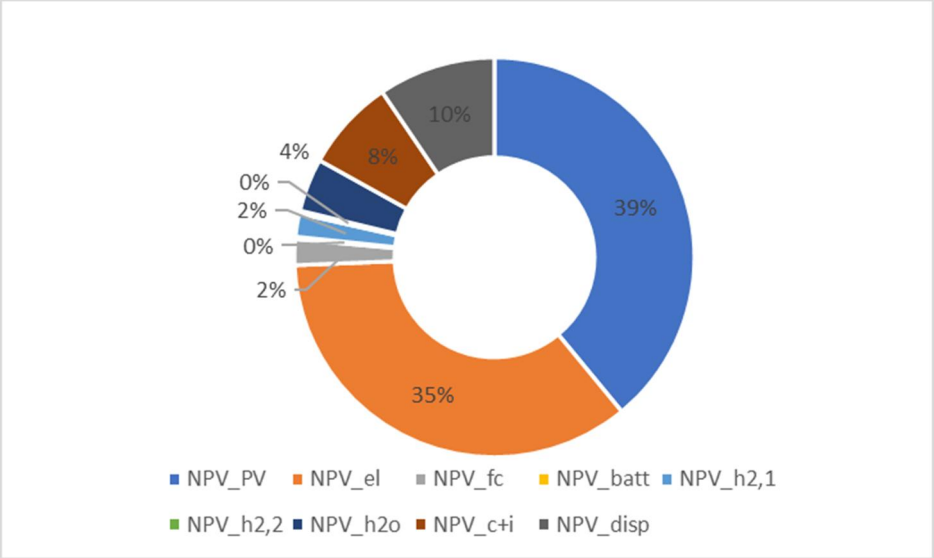

Figure 53 Components contribution on the total NPV (only mobility load 12-m filling scenario)

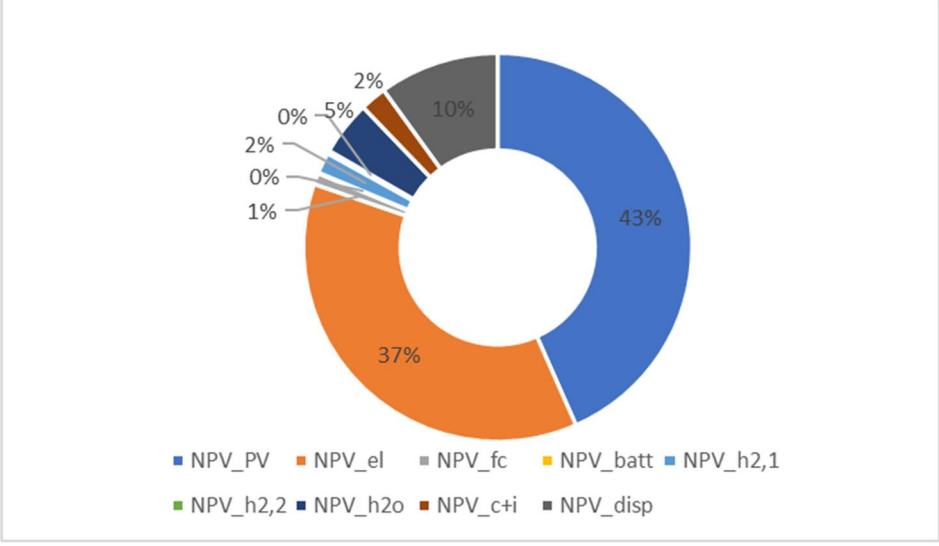

Figure 54 Components contribution on the total NPV (only mobility load 5-h filling scenario)

The main differences between these scenarios and the base one are the higher contribution of the HRS components, that are compressors, intercoolers and 350-bar dispenser, because of the neglecting of electrical load impact for the other components and, in the 5-hours filling scenario, to the lower flow rate required by the HRS that means a lower components size.

Table 47 Results summary for only mobility load

RES production		Load satisfied		Economic info		Other information	
Load	0.5 %	*RES*	42.2 %	*NPV*	4.05 M€	*FC lifetime*	12.1 y
ELY	55.1 %	*FC*	56.8 %	*LCOE*	/	*EL lifetime*	6.0 y
Curtailed	44.3 %	*External*	1.0 %	*LCOH*	45.08 €/kg	*CO_2 prod*	0.0 ton

Table 48 Results summary for 5-hours filling only mobility load

RES production		Load satisfied		Economic info		Other information	
Load	0.7 %	*RES*	55.6 %	*NPV*	3.85 M€	*FC lifetime*	6.2 y
ELY	51.7 %	*FC*	43.4 %	*LCOE*	/	*EL lifetime*	5.4 y
Curtailed	47.6 %	*External*	1.0 %	*LCOH*	42.73 €/kg	*CO_2 prod*	0.0 ton

6.2.8 Results summary

In the following final table, all the main economical and environmental results (Net Present Value at the end of the system lifetime, Levelized Cost Of Electricity, Levelized Cost Of Hydrogen and carbon dioxide production per year) are summarized for each scenario. Obviously, for the scenarios that consider only one of the loads, the LCOE and LCOH are not both evaluated; for the only electrical load scenarios, only the LCOE is computed, instead for the only mobility load scenarios, only the LCOH is computed. To obtain a comparison in environmental terms between these RES-based scenarios and the conventional one based on diesel engine (both for electricity production and mobility), all the values shown in the column CO2 per year must be compared with the total production of 368.8÷456.7 ton_{CO2}. The range consider different way to evaluate the production from a stationary diesel engine for the electricity part and also the two different mobility scenarios. As just explained before more times, the use of renewable and local biomass in the CHP system must be underlined, because of the possibility of a cyclic production and absorption of CO_2.

Table 49 Main results summary for all the scenarios

Scenario	NPV [M€]	LCOE [€/kWh]	LCOH [€/kg]	CO_2 per year [ton]
Base	9.21	1.28	38.29	0.0
ALKEL	8.88	1.23	36.96	0.0
Ost-Amb	6.72	1.34	46.14	0.0
5-h filling	9.35	1.32	37.71	0.0
CHP-fixed	6.24	0.59	39.97	113.5
CHP-optimized	4.27	0.29	33.06	239.7
Only elec load	6.11	1.35	/	0.0
Only elec load with CHP	2.12	0.47	/	155.8
Only mob load	4.05	/	45.08	0.0
Only mob load with 5-h filling	3.85	/	42.73	0.0

6.3 Sensitivity analysis

A sensitivity analysis has been performed on two main parameters to understand how they affect the net present cost: the system lifetime and the hydrogen technologies investment cost. For the first case, three other possible system lifetimes are adopted in addition to 20 years as in the base scenario, that are 15, 25 and 30 years. Instead in the second case, only a possible future scenario is analyzed, when the hydrogen technologies development reaches a good situation with the reduction of the investment to about half of the present value; this could be considered as a 2030-scenario. In the following subchapters, the sensitivity analysis results are described in more detail.

6.3.1 System lifetime

A possible analysis on how the system lifetime affects the economic results can be done in this study. As initial hypothesis, an increase in the net present value is expected because of the higher operational and maintenance cost during the year but also for the higher number of replacements for some components. The main investment increase is probably due to the electrolyzer and fuel cell systems, because of the limited lifetime and the higher initial and

replacement cost; also the dispenser for the hydrogen refueling station is replaced after 10 years, so increasing the lifetime more than 20 years, a second replacement is applied. Other replacements but of lower contribution in the NPV increase for a system lifetime higher than 20 years are the auxiliary battery and some of the CHP equipment, as dryer and gasifier. Instead, a different reasoning must be done for the LCOE and LCOH evaluation; from one side, the NPV increase, so a possible increase can be expected for both the parameters, but also the electricity load satisfied and the hydrogen production for mobility increase, that can result a reduction for them. The behavior of the two parameters can be different, because the increase in NPV can be also due to only one of the two loads considered. In the following figure, the net present value variation is shown to better understand the system behavior; instead, in the next table the variation of LCOE and LCOH is explained.

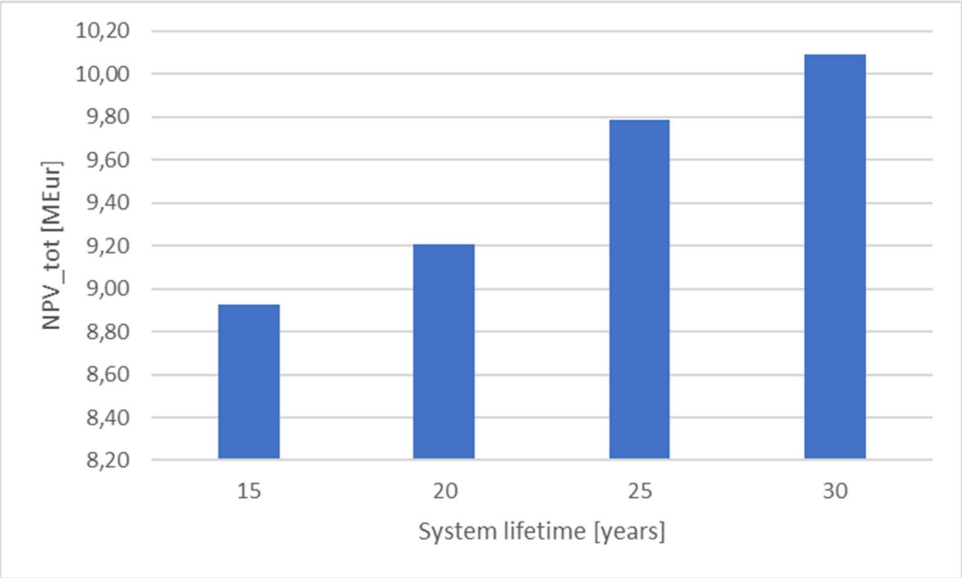

Figure 55 NPV variation respect to system lifetime variation (sensitivity analysis)

Table 50 LCOE and LCOH variations respect to system lifetime variation (sensitivity analysis)

	15 years	**20 years**	**25 years**	**30 years**
LCOE [€/kWh]	1.23	1.28	0.98	0.92
LCOH [€/kg]	56.46	38.29	45.20	42.55

As expected, the NPV increase with the system lifetime for the higher replacements number but also the higher O&M costs; the variation is almost linear, and increasing or decreasing

the system lifetime is expected to follow the same behavior. Considering an average lifetime of 6.7 and 4.8 years respectively for PEM electrolyzer and PEM fuel cell, the replacements are high affected by the system lifetime; for this reason, the NPVs of these systems are two of the main variations.

Instead, a stranger comportment is obtained for the LCOE and LCOH. For the first parameter, both increasing and decreasing the lifetime of the system a lower LCOE is obtained; this means that for a lower lifetime, the main contribution for the electricity part is the lower total NPV, but for higher lifetime instead, the lower value is due to the higher electricity load satisfied during the year. The opposite behavior instead is found for the LCOH, because for the 20 years scenario the minimum value is achieved; decreasing the lifetime, a higher LCOH is due mainly to the lower hydrogen mobility production although the lower total NPV. For higher lifetimes instead, initially an increase is evaluated because of the higher investment but for 30 years there is a reduction, mainly due to the increase in the mobility load satisfied during the years. So, the increase in NPV is mainly due to the mobility part.

6.3.2 Hydrogen technologies costs (future scenario)

Hydrogen-based energy production system at the moment are not developed as conventional technologies and this situation is also reflected in the global market with a higher investment cost. So, a future scenario with the half of the present costs is analyzed. Obviously, considering a lower investment cost also the total net present value must be lower, but from the optimization algorithm the new set of components sizes must be examined to understand if there will be some variations respect to the base scenario. Both the base scenario and the CHP-optimized scenario are considered, and the variations are shown in the following figure.

As expected, the NPV is lower for both the scenarios considered. The LCOE and LCOH variation instead are explained in the next table; as an initial assumption, lower values for both the parameters are expected, but mainly for the LCOE because of fuel cell investment that affects only the electricity part.

Different behaviors are observed for the two scenarios under study; initially, for the completely CO_2-free scenario (without CHP) the LCOE decrease but the LCOH increase in the future configuration. For the electricity part, this is mainly due to the reduction in fuel cell

investment cost in concomitance with the reduction of electrolyzer cost, that in part affects the LCOE. But for the mobility part instead, an increase of the LCOH is cannot be explained; part of the reduction in the electrolyzer NPV affects it, but this does not contribute for a LCOH reduction. The only possible reason is that the little sizes variations for electrolyzer and low pressure H_2 storage tank, with an increase for both, affects only the mobility part. The opposite comportment is achieved instead for the CHP-optimized scenarios, with an increase of the LCOE and a reduction in the LCOH. In this case, a little PV size reduction is obtained, so this probably affects mainly the LCOH value, instead the low increase of the hydrogen tank size is mainly due to the electricity part.

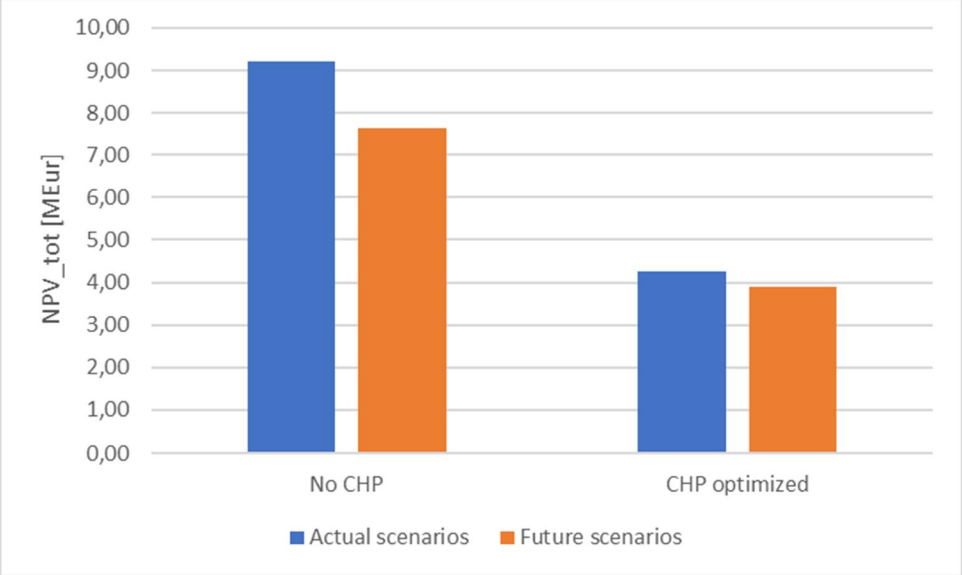

Figure 56 NPV variations with FC and EL investment variations (sensitivity analysis)

Table 51 LCOE and LCOH variations respect to FC and EL investment variations (sensitivity analysis)

	No CHP		**CHP optimized**	
	Actual	**Future**	**Actual**	**Future**
LCOE [€/kWh]	1.28	0.87	0.29	0.34
LCOH [€/kg]	38.29	40.31	33.06	25.41

7 Conclusion

A techno-economic analysis has been performed for demo 3 of Remote project, located in the mountain hamlet Ambornetti; as energy load to be satisfied both the electrical load of the village and the newer mobility load of a Po Valley minibus line are considered. Energy balance simulations over a reference year with 1-hour time step were carried out after defining an energy management strategy for the hybrid P2P and P2H systems. Local RES coupled with a H2 storage system (battery storage system is not taken into account in the annual simulation but only as an auxiliary energy source for start-up or fast change of load) were shown to allow a significantly reduce or even eliminate the usage of fossil-based power generation. In this way, environmental benefits such as reduced CO2 emission due to the lower diesel generator share, avoidance of invasive works because of grid connections and the utilization of CO_2-free automotive solution have to be considered as well.

Different configurations are analyzed for Ambornetti site, with different energy sources; initially, also a wind turbine system is selected but after a more detailed study it has been found that wind production is too low than the other alternatives, and from the optimization algorithm a turbine size of zero is always obtained. This means that only a photovoltaic system and a biomass CHP system are considered. Starting from the base scenario with only PV as energy source, an oversizing of the main system components must be taken into account, because of the issue of intermittence of RES as photovoltaic; during night, the only way to satisfy the loads is the use of electrolyzer and fuel cell. To obtain a completely self-sustainable system in energy terms, the economic investment must be very high respect to the other solutions found in previous Remote report, with a relative too high LCOE and LCOH, mainly due to the electrical load peak during the year; but also for a 1 % of external source configuration the economic parameters are too high. Instead, a completely energy autonomy was found to be possible in Ambornetti thanks to the exploitation of local solar and biomass sources; coupling PV and CHP system together with the adoption of a hybrid P2P system was proved to be more cost effective than traditional options either in the short or longer term. In this way, the component oversizing is avoiding, because of the more continuous and predictable energy production from a CHP system; although an amount of CO_2 is produced, the utilization of local and renewable biomass reduce the total pollutant concentration in the local area. Respect to the initial configuration designed in the Remote project, the adding of a mobility load reduce the LCOE, although an increase in the NPV,

because of the investment partialisation between the two loads; but, considering literature value for the LCOH, it is still too high. This is probably because the remote location, the limited production of RES but also the high investment cost of hydrogen technologies and, mainly, hydrogen refueling station. Reducing the trip distance for the minibus line, a lower investment is achieved but with an increase in the LCOH; this is due to the lower hydrogen produced for the mobility part. An interesting comparison instead has been done between the two technology solutions of electrolyzer; for the alkaline configuration, a lower investment cost must be considered, with a relative decrease in LCOE and LCOH, because of the lower initial and operational cost (due to the higher development state) and, mainly, the higher system lifetime, that means lower replacements. But in the future, a higher development of PEM technologies is expected, with a relative investment reduction; the advantages in using a PEM electrolyzer is the better operation in partial load and at higher pressure, but also the higher energy density. Also a different refueling period of 5-hours, instead of the 12-minutes one, is analyzed, both for the total loads and only mobility load: in the first case a worse economic result is achieved, probably because of a concomitance between the two loads; instead in the second case, an improvement for the economic conditions is obtained, mainly due to the lower size and operational energy requirements of the compressors and intercoolers in the HRS. But between the base scenario and the only mobility one, the investment cost is reduced because of the lower hydrogen load required, but a higher LCOH value is acquired; this is mainly due to the fact that the total investment cost is supported only from the mobility load. The same behavior is obtained considering only the electrical load scenario; in the case of only PV system as energy source, a higher LCOE is studied, for the same reason before. Instead, in the configuration with also the CHP system optimized, a better LCOE is obtained, but it is always higher considering the two-loads configuration with the couple PV-CHP systems as energy sources.

The P2P systems based on hydrogen technologies are expected to be more attractive in the future, mainly due to further development of these technologies and their market diffusion with a reduction in costs. The same reason must be considered for the automotive part of the study; respect to the energy production sector, hydrogen-based vehicles are less developed in favor of the electrical solution, that has a higher development state both in the vehicles and refueling station design. With a continue research and development for hydrogen solution technologies, FCEVs and H_2-technologies in general can become a real solution to the pollution problem also for mobility sector as well as for energy production sector.

References

[1] “Our World In Data.” https://ourworldindata.org/ (accessed Jun. 08, 2020).

[2] “Intergovernmental Panel on Climate Change.” https://www.ipcc.ch/ (accessed Jun. 08, 2020).

[3] UNEP, “COP 21 - Paris France Sustainable Innovation Forum,” 2015. http://www.cop21paris.org/ (accessed Jun. 08, 2020).

[4] G. Buffo, P. Marocco, D. Ferrero, A. Lanzini, and M. Santarelli, *Power-to-X and power-to-power routes*. Elsevier Inc., 2019.

[5] “REMOTE project – Just another WordPress site.” https://www.remote-euproject.eu/ (accessed May 18, 2020).

[6] IEA, “Measuring progress towards energy for all,” *World Energy Outlook 2012*, pp. 529–548, 2012.

[7] H. Farhangi, “The path of the smart grid,” *IEEE Power Energy Mag.*, vol. 8, no. 1, pp. 18–28, 2010, doi: 10.1109/MPE.2009.934876.

[8] P. Dondi, D. Bayoumi, C. Haederli, D. Julian, and M. Suter, “Network integration of distributed power generation,” *J. Power Sources*, vol. 106, no. 1–2, pp. 1–9, 2002, doi: 10.1016/S0378-7753(01)01031-X.

[9] G. Pepermans, J. Driesen, D. Haeseldonckx, R. Belmans, and W. D’haeseleer, “Distributed generation: Definition, benefits and issues,” *Energy Policy*, vol. 33, no. 6, pp. 787–798, 2005, doi: 10.1016/j.enpol.2003.10.004.

[10] W. El-Khattam and M. M. A. Salama, “Distributed generation technologies, definitions and benefits,” *Electr. Power Syst. Res.*, vol. 71, no. 2, pp. 119–128, 2004, doi: 10.1016/j.epsr.2004.01.006.

[11] K. Agbossou *et al.*, “Renewable energy systems based on hydrogen for remote applications,” *J. Power Sources*, vol. 96, no. 1, pp. 168–172, 2001, doi: 10.1016/S0378-7753(01)00495-5.

[12] M. Santarelli, M. Call, and S. Macagno, “Design and analysis of stand-alone hydrogen energy systems with different renewable sources,” *Int. J. Hydrogen Energy*, vol. 29, no. 15, pp. 1571–1586, 2004, doi: 10.1016/j.ijhydene.2004.01.014.

[13] M. Gökcek, “Hydrogen generation from small-scale wind-powered electrolysis system in different power matching modes,” *Int. J. Hydrogen Energy*, vol. 35, no. 19, pp. 10050–10059, 2010, doi: 10.1016/j.ijhydene.2010.07.149.

[14] “HOMER Pro - Microgrid Software for Designing Optimized Hybrid Microgrids.” https://www.homerenergy.com/products/pro/index.html (accessed May 21, 2020).

[15] S. M. Stojković and V. V. Bakić, “Techno-economic analysis of stand-alone photovoltaic/wind/battery/hydrogen systems for very Small-Scale applications,” *Therm. Sci.*, vol. 20, no. January, pp. S261–S273, 2016, doi: 10.2298/TSCI150308195S.

[16] Y. Kalinci, A. Hepbasli, and I. Dincer, “Techno-economic analysis of a stand-alone

hybrid renewable energy system with hydrogen production and storage options," *Int. J. Hydrogen Energy*, vol. 40, no. 24, pp. 7652–7664, 2015, doi: 10.1016/j.ijhydene.2014.10.147.

[17] L. Gracia, P. Casero, C. Bourasseau, and A. Chabert, "Use of hydrogen in off-grid locations, a techno-economic assessment," *Energies*, vol. 11, no. 11, 2018, doi: 10.3390/en11113141.

[18] P. Rullo, L. Braccia, P. Luppi, D. Zumoffen, and D. Feroldi, "Integration of sizing and energy management based on economic predictive control for standalone hybrid renewable energy systems," *Renew. Energy*, vol. 140, pp. 436–451, 2019, doi: 10.1016/j.renene.2019.03.074.

[19] J. P. Torreglosa, P. García-Triviño, L. M. Fernández-Ramirez, and F. Jurado, "Control based on techno-economic optimization of renewable hybrid energy system for stand-alone applications," *Expert Syst. Appl.*, vol. 51, pp. 59–75, 2016, doi: 10.1016/j.eswa.2015.12.038.

[20] E. I. Zoulias and N. Lymberopoulos, "Techno-economic analysis of the integration of hydrogen energy technologies in renewable energy-based stand-alone power systems," *Renew. Energy*, vol. 32, no. 4, pp. 680–696, 2007, doi: 10.1016/j.renene.2006.02.005.

[21] Ø. Ulleberg and R. Hancke, "Techno-economic calculations of small-scale hydrogen supply systems for zero emission transport in Norway," *Int. J. Hydrogen Energy*, vol. 45, no. 2, pp. 1201–1211, 2020, doi: 10.1016/j.ijhydene.2019.05.170.

[22] M. Gökçek and C. Kale, "Techno-economical evaluation of a hydrogen refuelling station powered by Wind-PV hybrid power system: A case study for İzmir-çeşme," *Int. J. Hydrogen Energy*, vol. 43, no. 23, pp. 10615–10625, 2018, doi: 10.1016/j.ijhydene.2018.01.082.

[23] S. Nistor, S. Dave, Z. Fan, and M. Sooriyabandara, "Technical and economic analysis of hydrogen refuelling," *Appl. Energy*, vol. 167, pp. 211–220, 2016, doi: 10.1016/j.apenergy.2015.10.094.

[24] S. H. Siyal, D. Mentis, and M. Howells, "Economic analysis of standalone wind-powered hydrogen refueling stations for road transport at selected sites in Sweden," *Int. J. Hydrogen Energy*, vol. 40, no. 32, pp. 9855–9865, 2015, doi: 10.1016/j.ijhydene.2015.05.021.

[25] D. Apostolou, P. Enevoldsen, and G. Xydis, "Supporting green Urban mobility – The case of a small-scale autonomous hydrogen refuelling station," *Int. J. Hydrogen Energy*, vol. 44, no. 20, pp. 9675–9689, 2019, doi: 10.1016/j.ijhydene.2018.11.197.

[26] M. E. Baran and N. R. Mahajan, "DC distribution for industrial systems: Opportunities and challenges," *IEEE Trans. Ind. Appl.*, vol. 39, no. 6, pp. 1596–1601, 2003, doi: 10.1109/TIA.2003.818969.

[27] A. H. Al-Badi, H. Yousef, O. Alaamri, M. Alabdusalam, Y. Alshidi, and N. Alharthy, "Performance of a stand-alone renewable energy system based on hydrogen energy storage," *ISCCSP 2014 - 2014 6th Int. Symp. Commun. Control Signal Process. Proc.*, vol. 19, no. 3, pp. 356–359, 2014, doi: 10.1109/ISCCSP.2014.6877887.

[28] M. S. P. Marocco, D. Ferrero, M. Gandiglio, "REMOTE deliverable 2.2. Technical specification of the technological demonstrators," no. 2, pp. 1–60, 2019.

[29] J. P. Barton and D. G. Infield, “Energy Storage and Its Use WithIntermittent Renewable Energy,” vol. 19, no. 2, pp. 441–448, 2004.

[30] K. Sundseth, K. Midthun, M. Aarlott, and A. Werner, “Deliverable D2.1 - Analysis of the economic and regulatory framework of the technological demonstrators,” 2018.

[31] P. Marocco *et al.*, “A study of the techno-economic feasibility of H2-based energy storage systems in remote areas,” *[in Manuscript]*, vol. 211, no. March, p. 112768, 2019, doi: 10.1016/j.enconman.2020.112768.

[32] “IRIS s.r.l. – Playground fon new ideas.” https://www.irissrl.eu/ (accessed May 18, 2020).

[33] W. M. Haynes, D. R. Lide, and T. J. Bruno, *Handbook of chemistry and physics - Edition 95*. .

[34] I. Staffell *et al.*, “The role of hydrogen and fuel cells in the global energy system,” *Energy Environ. Sci.*, vol. 12, no. 2, pp. 463–491, 2019, doi: 10.1039/c8ee01157e.

[35] O. Schmidt, A. Gambhir, I. Staffell, A. Hawkes, J. Nelson, and S. Few, “Future cost and performance of water electrolysis: An expert elicitation study,” *Int. J. Hydrogen Energy*, vol. 42, no. 52, pp. 30470–30492, 2017, doi: 10.1016/j.ijhydene.2017.10.045.

[36] M. Lehner, R. Tichler, and M. Koppe, *Power-to-Gas : Technology and Business Models*. 2014.

[37] D. Ferrero, M. Gamba, A. Lanzini, and M. Santarelli, “Power-to-Gas Hydrogen: Techno-economic Assessment of Processes towards a Multi-purpose Energy Carrier,” *Energy Procedia*, vol. 101, no. September, pp. 50–57, 2016, doi: 10.1016/j.egypro.2016.11.007.

[38] B. Li, “Sizing and Operation of Multi-Energy Hydrogen-Based,” Université Bourgogne Franche-Comté, 2018.

[39] A. Forrai, H. Funato, Y. Yanagita, and Y. Kato, “Fuel-cell parameter estimation and diagnostics,” *IEEE Trans. Energy Convers.*, vol. 20, no. 3, pp. 668–675, 2005, doi: 10.1109/TEC.2005.845516.

[40] S. G. Chalk and J. F. Miller, “Key challenges and recent progress in batteries, fuel cells, and hydrogen storage for clean energy systems,” *J. Power Sources*, vol. 159, no. 1 SPEC. ISS., pp. 73–80, 2006, doi: 10.1016/j.jpowsour.2006.04.058.

[41] EG&G Technical Services, *Fuel Cell Handbook (Seventh Edition)*, vol. 7. 2004.

[42] M. Santarelli, “Notes on high pressure electrolysis.” .

[43] Tractebel and Hinicio, “Study on Early Business Cases for H2 in Energy Storage and More Broadly Power To H2 Applications,” *EU Comm.*, no. June, p. 228, 2017, [Online]. Available: http://www.hinicio.com/inc/uploads/2017/07/P2H_Full_Study_FCHJU.pdf%0Ahttp://www.fch.europa.eu/sites/default/files/P2H_Full_Study_FCHJU.pdf%0Ahttp://www.hinicio.com/file/2018/06/P2H_Full_Study_FCHJU.pdf.

[44] M. Santos and I. M. Tecnalia, “Energy analysis of the Raggovidda integrated system.”

[45] Frank de Bruijn, “PEMFC Lifetime and Durability an overview,” 2011, [Online]. Available: http://iet.jrc.ec.europa.eu/fuel-cells/sites/fuel-cells/files/files/documents/events/pemfc_lifetime_and_durability-an_overview_-

_f.debruijn.pdf.

[46] A. El-Kharouf, A. Chandan, M. Hattenberger, and B. G. Pollet, “Proton exchange membrane fuel cell degradation and testing: Review,” *J. Energy Inst.*, vol. 85, no. 4, pp. 188–200, 2012, doi: 10.1179/1743967112Z.00000000036.

[47] A. Ursúa, I. San Martín, E. L. Barrios, and P. Sanchis, “Stand-alone operation of an alkaline water electrolyser fed by wind and photovoltaic systems,” *Int. J. Hydrogen Energy*, vol. 38, no. 35, pp. 14952–14967, 2013, doi: 10.1016/j.ijhydene.2013.09.085.

[48] J. Brauns and T. Turek, “Alkaline water electrolysis powered by renewable energy: A review,” *Processes*, vol. 8, no. 2, 2020, doi: 10.3390/pr8020248.

[49] A. Ursúa, E. L. Barrios, J. Pascual, I. San Martín, and P. Sanchis, “Integration of commercial alkaline water electrolysers with renewable energies: Limitations and improvements,” *Int. J. Hydrogen Energy*, vol. 41, no. 30, pp. 12852–12861, 2016, doi: 10.1016/j.ijhydene.2016.06.071.

[50] Y. Kuroda, T. Nishimoto, and S. Mitsushima, “Self-repairing hybrid nanosheet anode catalysts for alkaline water electrolysis connected with fluctuating renewable energy,” *Electrochim. Acta*, vol. 323, p. 134812, 2019, doi: 10.1016/j.electacta.2019.134812.

[51] D. Stolten and B. Emonts, *Hydrogen Science and Engineering : Materials, Processes, Systems and Technology*, vol. 1–2. Weinheim, Germany: Wiley-VCH Verlag GmbH & Co. KGaA, 2016.

[52] “JRC Photovoltaic Geographical Information System (PVGIS) - European Commission.” https://re.jrc.ec.europa.eu/pvg_tools/en/tools.html (accessed Mar. 25, 2020).

[53] J. J. Hwang, L. K. Lai, W. Wu, and W. R. Chang, “Dynamic modeling of a photovoltaic hydrogen fuel cell hybrid system,” *Int. J. Hydrogen Energy*, vol. 34, no. 23, pp. 9531–9542, 2009, doi: 10.1016/j.ijhydene.2009.09.100.

[54] S. G. Tesfahunegn, *Fuel Cell Assisted PhotoVoltaic Power Systems*, no. May. 2012.

[55] A. Bouakkaz, S. Haddad, J. A. Martín-García, A. J. Gil-Mena, and R. Jiménez-Castañeda, “Optimal scheduling of household appliances in off-grid hybrid energy system using PSO algorithm for energy saving,” *Int. J. Renew. Energy Res.*, vol. 9, no. 1, pp. 427–436, 2019.

[56] Y. Riffonneau, S. Bacha, F. Barruel, and S. Ploix, “Optimal power flow management for grid connected PV systems with batteries,” *IEEE Trans. Sustain. Energy*, vol. 2, no. 3, pp. 309–320, 2011, doi: 10.1109/TSTE.2011.2114901.

[57] C. M. T. Huang, Y. C. Huang, and K. Y. Huang, “A hybrid method for one-day ahead hourly forecasting of PV power output,” *Proc. 2014 9th IEEE Conf. Ind. Electron. Appl. ICIEA 2014*, pp. 526–531, 2014, doi: 10.1109/ICIEA.2014.6931220.

[58] B. Laoun, A. Khellaf, M. W. Naceur, and A. M. Kannan, “Modeling of solar photovoltaic-polymer electrolyte membrane electrolyzer direct coupling for hydrogen generation,” *Int. J. Hydrogen Energy*, vol. 41, no. 24, pp. 10120–10135, 2016, doi: 10.1016/j.ijhydene.2016.05.041.

[59] R. E. Bird and R. L. Hulstrom, “A Simplified Clear Sky Model for Direct and Diffuse Insolation on Horizontal Surfaces,” Golden, Colorado 80401, 1981.

[60] A. Singh, P. Baredar, and B. Gupta, “Techno-economic feasibility analysis of hydrogen fuel cell and solar photovoltaic hybrid renewable energy system for academic research building,” *Energy Convers. Manag.*, vol. 145, pp. 398–414, 2017, doi: 10.1016/j.enconman.2017.05.014.

[61] B. Li, R. Roche, and A. Miraoui, “Microgrid sizing with combined evolutionary algorithm and MILP unit commitment,” *Appl. Energy*, vol. 188, pp. 547–562, 2017, doi: 10.1016/j.apenergy.2016.12.038.

[62] S. Sinha and S. S. Chandel, “Prospects of solar photovoltaic-micro-wind based hybrid power systems in western Himalayan state of Himachal Pradesh in India,” *Energy Convers. Manag.*, vol. 105, pp. 1340–1351, 2015, doi: 10.1016/j.enconman.2015.08.078.

[63] L. Xu, X. Ruan, C. Mao, B. Zhang, and Y. Luo, “An improved optimal sizing method for wind-solar-battery hybrid power system,” *IEEE Trans. Sustain. Energy*, vol. 4, no. 3, pp. 774–785, 2013, doi: 10.1109/TSTE.2012.2228509.

[64] G. Cau, D. Cocco, M. Petrollese, S. Knudsen Kær, and C. Milan, “Energy management strategy based on short-term generation scheduling for a renewable microgrid using a hydrogen storage system,” *Energy Convers. Manag.*, vol. 87, pp. 820–831, 2014, doi: 10.1016/j.enconman.2014.07.078.

[65] Spanner Re^2 GmbH, “Biomass CHP HKA 49.” https://www.holz-kraft.com/it/ (accessed May 18, 2020).

[66] “WES, Wind Energy Solutions | Bringing renewable energy everywhere.” https://windenergysolutions.nl/ (accessed Mar. 25, 2020).

[67] WES Energy Solutions, “WES50 Datasheet,” 2019.

[68] C. G. Justus, W. R. Hargraves, A. Mikhail, and D. Graber, “Methods for estimating wind speed frequency distributions.,” *J. Appl. Meteorol.*, vol. 17, no. 3, Mar. 1978. pp. 350–353, 1978, doi: 10.1175/1520-0450(1978)017<0350:mfewsf>2.0.co;2.

[69] N. Qin and P. Brooker, “EVTC - Hydrogen Fueling Stations Infrastructure,” 2014.

[70] K. K. Müller, F. Schnitzeler, A. Lozanovski, S. Skiker, and M. Ojakovoh, “Deliverable No. 5.3 Final Report,” 2016. [Online]. Available: https://www.fuelcellbuses.eu/sites/default/files/documents/Final Report_CHIC_28022017_Final_Public.pdf.

[71] L. Viktorsson, J. T. Heinonen, J. B. Skulason, and R. Unnthorsson, “A step towards the hydrogen economy - A life cycle cost analysis of a hydrogen refueling station,” *Energies*, vol. 10, no. 6, pp. 1–15, 2017, doi: 10.3390/en10060763.

[72] J. X. Weinert, L. Shaojun, J. M. Ogden, and M. Jianxin, “Hydrogen refueling station costs in Shanghai,” *Int. J. Hydrogen Energy*, vol. 32, no. 16, pp. 4089–4100, 2007, doi: 10.1016/j.ijhydene.2007.05.010.

[73] J. Wong, “Compressed hydrogen infrastructure,” pp. 1–12, 2005, [Online]. Available: http://ieahia.org/pdfs/Case-Studies/Compressed_Hydrogen_Infrastructure.aspx.

[74] B. Gim and W. L. Yoon, “Analysis of the economy of scale and estimation of the future hydrogen production costs at on-site hydrogen refueling stations in Korea,” *Int. J. Hydrogen Energy*, vol. 37, no. 24, pp. 19138–19145, 2012, doi: 10.1016/j.ijhydene.2012.09.163.

[75] M. F. Andrea, R. H. Sara, D. Z. Luca, S. S. Giovanni, and B. Enrico, “Techno-economic analysis of in-situ production by electrolysis, biomass gasification and delivery systems for Hydrogen Refuelling Stations: Rome case study,” *Energy Procedia*, vol. 148, pp. 82–89, 2018, doi: 10.1016/j.egypro.2018.08.033.

[76] L. Zhao, J. Brouwer, and S. Samuelsen, “DYNAMIC ANALYSIS OF A SELF-SUSTAINABLE RENEWABLE HYDROGEN FUELING STATION,” in *ASME 2014 12th International Conference on Fuel Cell Science, Engineering and Technology*, 2016, pp. 1–11.

[77] G. Dispenza *et al.*, “Development of a solar powered hydrogen fueling station in smart cities applications,” *Int. J. Hydrogen Energy*, vol. 42, no. 46, pp. 27884–27893, 2017, doi: 10.1016/j.ijhydene.2017.07.047.

[78] H. Ammerman, Y. Ruf, S. Lange, D. Fundulea, and A. Martin, “Fuel Cell Electric Buses - Potential for Sustainable Public Transport in Eurpoe,” p. 74, 2015, [Online]. Available: http://www.fch.europa.eu/sites/default/files/150909_FINAL_Bus_Study_Report_OUT_0.PDF.

[79] M. Ball and M. Weeda, “The hydrogen economy - Vision or reality?,” *Int. J. Hydrogen Energy*, vol. 40, no. 25, pp. 7903–7919, 2015, doi: 10.1016/j.ijhydene.2015.04.032.

[80] IEA, “Technology Roadmap: Hydrogen and fuel cells,” *SpringerReference*, 2015, doi: 10.1007/springerreference_7300.

[81] D. Viesi, L. Crema, and M. Testi, “The Italian hydrogen mobility scenario implementing the European directive on alternative fuels infrastructure (DAFI 2014/94/EU),” *Int. J. Hydrogen Energy*, vol. 42, no. 44, pp. 27354–27373, 2017, doi: 10.1016/j.ijhydene.2017.08.203.

[82] Hydrogen Mobility Europe, “The most ambitious hydrogen mobility initiatives in Europe have joined forces to support the introduction of hydrogen-fuelled transport,” 2019.

[83] “Stations Map | H2 Station Maps.” https://h2stationmaps.com/ (accessed May 22, 2020).

[84] “Home | California Fuel Cell Partnership.” https://cafcp.org/ (accessed May 22, 2020).

[85] “Hydrogen fueling station - Pure Energy Centre.” https://pureenergycentre.com/hydrogen-fueling-station/ (accessed Apr. 20, 2020).

[86] J. X. Weinert and T. E. Lipman, “An Assessment of the Near-Term Costs of Hydrogen Refueling Stations and Station Components,” *Inst. Transp. Stud.*, vol. Issues in, no. 530, pp. 57–66, 2006, doi: 10.1007/s11116-007-9132-x.

[87] J. X. Weinert, “A Near-Term Economic Analysis of Hydrogen Fueling Stations,” *Res. Rep. UCD-ITS-RR-05-04*, no. 530, 2005.

[88] G. Parks, R. Boyd, J. Cornish, and R. Remick, “NREL - Hydrogen Station Compression, Storage, and Dispensing Technical Status and Costs: Systems Integration,” *U.S. Dep. Energy Hydrog. Fuel Cells Progr.*, no. May, p. Medium: ED; Size: 74 pp., 2014, [Online]. Available: http://www.osti.gov/scitech//servlets/purl/1130621/.

[89] M. Melaina and M. P. Nrel, “Hydrogen Station Cost Estimates - Comparing Hydrogen Station Cost Calculator Results with other Recent Estimates,” *Natl. Renew. Energy*

Lab. NREL, no. September, pp. 1–36, 2013.

[90] Cambridge Econometrics, “En route pour un transport durable,” Covent Garden, Cambridge, 2015.

[91] “J2601A: Fueling Protocols for Light Duty Gaseous Hydrogen Surface Vehicles - SAE International.” https://www.sae.org/standards/content/j2601_201612/ (accessed Mar. 31, 2020).

[92] A. L. Allen, “EFFICIENCY AND PERFORMANCE MEASUREMENTS OF A PDC INC. SINGLE STAGE DIAPHRAGM HYDROGEN COMPRESSOR,” HUMBOLDT STATE UNIVERSITY, 2009.

[93] G. Napoli, S. Micari, G. Dispenza, S. Di Novo, V. Antonucci, and L. Andaloro, “Development of a fuel cell hybrid electric powertrain: A real case study on a Minibus application,” *Int. J. Hydrogen Energy*, vol. 42, no. 46, pp. 28034–28047, 2017, doi: 10.1016/j.ijhydene.2017.07.239.

[94] “Dolomitech.” http://www.dolomitech.com/index.php (accessed Mar. 25, 2020).

[95] J. Cerny and DPMB, “Analysis and possibilities of e-minibus operation and test of e-buses in Brno,” no. March 2016.

[96] F. Töpler, L. Eckstein, G. Geulen, and J. Homann, “econnect Germany - performance and evaluation of an electrically propelled minibus for public transportation,” *World Electr. Veh. J.*, vol. 6, no. 1, pp. 64–70, 2013, doi: 10.3390/wevj6010064.

[97] F. Baronti *et al.*, “Implementation of the fast charging concept for electric local public transport: The case-study of a minibus,” *Proceeding - 2015 IEEE Int. Conf. Ind. Informatics, INDIN 2015*, pp. 1284–1289, 2015, doi: 10.1109/INDIN.2015.7281920.

[98] “Motiv Power Systems - EPIC All-Electric Chassis Manufacturer.” https://www.motivps.com/motivps/ (accessed Mar. 25, 2020).

[99] ISPRA, “Fattori di emissione atmosferica di gas ad effetto serra e altri gas nel settore elettrico,” 2018.

[100] G. J. Offer, D. Howey, M. Contestabile, R. Clague, and N. P. Brandon, “Comparative analysis of battery electric, hydrogen fuel cell and hybrid vehicles in a future sustainable road transport system,” *Energy Policy*, vol. 38, no. 1, pp. 24–29, 2010, doi: 10.1016/j.enpol.2009.08.040.

[101] I. Bartolozzi, F. Rizzi, and M. Frey, “Comparison between hydrogen and electric vehicles by life cycle assessment: A case study in Tuscany, Italy,” *Appl. Energy*, vol. 101, no. January, pp. 103–111, 2013, doi: 10.1016/j.apenergy.2012.03.021.

[102] A. Ajanovic and R. Haas, “Economic and Environmental Prospects for Battery Electric- and Fuel Cell Vehicles: A Review,” *Fuel Cells*, vol. 19, no. 5, pp. 515–529, 2019, doi: 10.1002/fuce.201800171.

[103] M. Granovskii, I. Dincer, and M. A. Rosen, “Economic and environmental comparison of conventional, hybrid, electric and hydrogen fuel cell vehicles,” *J. Power Sources*, vol. 159, no. 2, pp. 1186–1193, 2006, doi: 10.1016/j.jpowsour.2005.11.086.

[104] M. a Kromer and J. B. Heywood, “Electric Powertrains: Opportunities and Challenges in the U.S. Light-Duty Vehicle Fleet,” *Challenges*, no. May, p. 153, 2007, [Online]. Available: http://web.mit.edu/sloan-auto-

lab/research/beforeh2/files/kromer_electric_powertrains.pdf.

[105] Y. Bicer and I. Dincer, “Comparative life cycle assessment of hydrogen, methanol and electric vehicles from well to wheel,” *Int. J. Hydrogen Energy*, vol. 42, no. 6, pp. 3767–3777, 2017, doi: 10.1016/j.ijhydene.2016.07.252.

[106] M. Li, X. Zhang, and G. Li, “A comparative assessment of battery and fuel cell electric vehicles using a well-to-wheel analysis,” *Energy*, vol. 94, no. January, pp. 693–704, 2016, doi: 10.1016/j.energy.2015.11.023.

[107] S. W. Lin, K. C. Ying, S. C. Chen, and Z. J. Lee, “Particle swarm optimization for parameter determination and feature selection of support vector machines,” *Expert Syst. Appl.*, vol. 35, no. 4, pp. 1817–1824, 2008, doi: 10.1016/j.eswa.2007.08.088.

[108] LG, “LG NeON® R solar module.” http://www.lg-solar.com/downloads/spec-sheet/DS_NeONR_60cells.pdf (accessed Apr. 20, 2020).

[109] M. Boussetta, R. El Bachtiri, M. Khanfara, and K. El Hammoumi, “Assessing the potential of hybrid PV–Wind systems to cover public facilities loads under different Moroccan climate conditions,” *Sustain. Energy Technol. Assessments*, vol. 22, no. 2017, pp. 74–82, 2017, doi: 10.1016/j.seta.2017.07.005.

[110] IRENA International Renewable Energy Agency, *Renewable Power Generation Costs in 2018*. 2018.

[111] P. Menanteau, M. M. Quéméré, A. Le Duigou, and S. Le Bastard, “An economic analysis of the production of hydrogen from wind-generated electricity for use in transport applications,” *Energy Policy*, vol. 39, no. 5, pp. 2957–2965, 2011, doi: 10.1016/j.enpol.2011.03.005.

[112] WindEurope, “Wind energy in Europe in 2019 - Trends and statistics,” 2019.

[113] J. Proost, “State-of-the art CAPEX data for water electrolysers, and their impact on renewable hydrogen price settings,” *Int. J. Hydrogen Energy*, vol. 44, no. 9, pp. 4406–4413, 2019, doi: 10.1016/j.ijhydene.2018.07.164.

[114] R. Turton, R. C. Baillie, W. B. Whiting, and J. A. Shaeiwitz, *Analysis, Synthesis, and Design of Chemical Processes*, Third Edit. Boston, Massachusetts, USA, 2009.

[115] D. S. Street, P. Adamson, Y. Yo, and S. Hoy, “P2G Roadmap for Flanders - Final report,” Brussels, 2016.

[116] Battelle Memorial Institute, “Manufacturing Cost Analysis of PEM Fuel Cell Systems for 5- and 10-kW Backup Power Applications,” 2016.

[117] Battelle Memorial Institute, “Manufacturing Cost Analysis: 1, 5, 10 and 25 kW Fuel Cell Systems for Primary Power and Combined Heat and Power Applications,” 2017.

[118] M. F. Shehzad, M. B. Abdelghany, D. Liuzza, V. Mariani, and L. Glielmo, “Mixed logic dynamic models for MPC control of wind farm hydrogen-based storage systems,” *Inventions*, vol. 4, no. 4, pp. 1–17, 2019, doi: 10.3390/inventions4040057.

[119] Scott Jankins, “2019 Chemical Engineering Plant Cost Index Annual Average.” 2020, Accessed: 14-Apr-2020. [Online]. Available: https://www.chemengonline.com/2019-chemical-engineering-plant-cost-index-annual-average/.

[120] E. S. Hecht and J. Pratt, “Comparison of conventional vs. modular hydrogen refueling stations, and on-site production vs. delivery,” 2017. [Online]. Available:

https://www.energy.gov/sites/prod/files/2017/03/f34/fcto-h2first-reference-station-phase2-2017.pdf.

[121] “Aiel - Associazione Italiana Energie Agroforestali.” https://www.aielenergia.it/ (accessed May 20, 2020).

[122] Federal Ministry for Economic Affairs and Energy, *Markets for Battery Storage - Sub-sector analysis on the market potential for battery storage in Tanzania*. Berilin, 2015.

[123] Aguas de Portugal Serviços, “Establishment of cost functions for construction of various types of public water services assets in Portugal,” 2010.

[124] R. E. W. Max S. Peters, Klaus D. Timmerhaus, “Plant Design and Economics for Chemical Engineers - 5th Edition,” 2003. https://www.mheducation.co.uk/plant-design-and-economics-for-chemical-engineers-9780071198721-emea#tab-label-product-description-title (accessed Apr. 20, 2020).

[125] “Net Present Value (NPV).” https://www.investopedia.com/terms/n/npv.asp (accessed Apr. 21, 2020).

[126] “Weighted Average Cost of Capital – WACC Definition.” https://www.investopedia.com/terms/w/wacc.asp (accessed Apr. 21, 2020).

[127] US Department of Energy, “Quality Guidelines for Energy Systems Studies - Cost Estimation Methodology for NETL Assessments of Power Plant Performance,” 2011.

[128] “Rendimento Titoli di Stato europei e Tassi in tempo reale.” https://mercati.ilsole24ore.com/obbligazioni/titoli-di-stato/rendimenti-titoli-stato-europa/1?refresh_ce (accessed Apr. 21, 2020).

[129] “Equity Market Risk Premium 2020 - KPMG Nederland.” https://home.kpmg/nl/nl/home/insights/2020/04/equity-market-risk-premium-2020.html (accessed Apr. 21, 2020).

[130] KPMG, “Equity Market Risk Premium - Research Summary December 2019,” 2019. [Online]. Available: https://assets.kpmg.com/content/dam/kpmg/nl/pdf/2018/advisory/equity-market-risk-premium-research-summary-september-2018.pdf.

[131] “Listino Tassi IRS - Tassi IRS aggiornati su Il Sole 24 Ore.” https://mercati.ilsole24ore.com/tassi-e-valute/tassi/irs?refresh_ce=1 (accessed Apr. 21, 2020).

[132] R. Dufo-López and J. L. Bernal-Agustín, “Multi-objective design of PV-wind-diesel-hydrogen-battery systems,” *Renew. Energy*, vol. 33, no. 12, pp. 2559–2572, 2008, doi: 10.1016/j.renene.2008.02.027.

[133] A. Maleki and A. Askarzadeh, “Optimal sizing of a PV/wind/diesel system with battery storage for electrification to an off-grid remote region: A case study of Rafsanjan, Iran,” *Sustain. Energy Technol. Assessments*, vol. 7, pp. 147–153, 2014, doi: 10.1016/j.seta.2014.04.005.

[134] Ø. Skarstein and K. Uhlen, “Design Considerations with Respect to Long-Term Diesel Saving in Wind/Diesel Plants,” *Wind Eng.*, vol. 13, no. 2, pp. 72–87, Mar. 1989, [Online]. Available: http://www.jstor.org/stable/43749369.

[135] A. Q. Jakhrani, A. R. H. Rigit, A. K. Othman, S. R. Samo, and S. A. Kamboh,

"Estimation of carbon footprints from diesel generator emissions," *Proc. 2012 Int. Conf. Green Ubiquitous Technol. GUT 2012*, pp. 78–81, 2012, doi: 10.1109/GUT.2012.6344193.

[136] E. Alsema, "Environmental life cycle assessment of solar home systems," *Dep. Sci. Technol. Soc. Utr. Univ. Utrecht, Netherlands*, no. December 2000, p. 89, 2000.

[137] B. Fleck and M. Huot, "Comparative life-cycle assessment of a small wind turbine for residential off-grid use," *Renew. Energy*, vol. 34, no. 12, pp. 2688–2696, 2009, doi: 10.1016/j.renene.2009.06.016.

[138] R. J. North, "Assessment of real-world pollutant emissions from a light duty diesel vehicle." Citeseer, 2006.

[139] A. Date, *Analytic Combustion*. Cambridge: Cambridge University Press, 2011.

[140] "Diesel Generator - an overview | ScienceDirect Topics." https://www.sciencedirect.com/topics/engineering/diesel-generator (accessed Mar. 25, 2020).

[141] Partnership for policy integrity, "Carbon emissions from burning biomass for energy," 2011. [Online]. Available: https://www.pfpi.net/wp-content/uploads/2011/04/PFPI-biomass-carbon-accounting-overview_April.pdf.

[142] GTT, "Schede tecniche parco veicoli GTT," 2017. doi: 10.1017/CBO9781107415324.004.

[143] DEFRA, "2008 Guidelines to Defra's GHG Conversion Factors: Methodology Paper for Transport Emission Factors Contents," *Dep. Environ. Food Rural Aff.*, no. July, 2008, [Online]. Available: http://www.opsi.gov.uk/click-use/psi-licence-information/index.htm.

Ringraziamenti

Innanzitutto, devo ringraziare chi mi ha permesso con il proprio sostegno di percorrere questo percorso universitario, agevolandomi il più possibile e cercando di tenere vive le mie passioni nonostante gli impegni scolastici: la mia famiglia. Per famiglia intendo ovviamente i miei genitori, sempre presenti e pronti ad aiutarmi, mia sorella Giulia, un punto fisso e di possibile riferimento a Torino, ed infine anche i miei nonni, preoccupati sempre ai miei risultati e pronti a fornire ogni tipo di appoggio.

In secondo luogo, un ringraziamento va dato ai relatori della tesi, i professori Lanzini Andrea e Santarelli Massimo, per avermi dato la possibilità di interagire con il progetto REMOTE e di avere un'esperienza su un impianto innovativo. In particolare, vorrei ringraziare sentitamente il co-relatore Marocco Paolo per essere stato sempre disponibile ad ogni mio dubbio sull'elaborato e per tutti i consigli e suggerimenti che mi ha dato; è stato un punto di riferimento durante tutto il lavoro svolto.

Un ringraziamento speciale va ai miei amici del gruppo di sempre, con i quali ho condiviso in questi anni molte grigliate e non solo, dove la risata e la spensieratezza sono sempre assicurate. Grazie in particolare ai componenti del gruppo "Il metodo Brendy", per aver condiviso una seconda identità tra una birra e l'altra! E come non dimenticare gli amici del Poli, chi conoscevo già e chi ho conosciuto in questi ultimi 5 anni; ovviamente ringrazio i due Simone per i primi tre anni e non solo, i quali mi hanno sempre dato un tetto sopra la testa durante le pause pranzo per non lasciarmi da solo in università (povera vita da pendolare), poi ci sono anche gli amici della magistrale, troppi da citare tutti, come Daniele con il quale troppe sfide a livello sportivo sono ancora aperte, il Conte che ci ha fatto capire come sia la vita non da plebei e tutti gli altri "meccanici caldi" (Luca, Fede, Jack, Fabio, Silvia e Fabri).

Infine, il più importante ringraziamento va a Chiara, che considero la prima persona a credere in me in ogni mia scelta e decisione, con la quale ho imparato a condividere la maggior parte delle esperienze della mia vita. È stata una colonna portante e sempre presente in tutti e 5 gli anni del percorso universitario, supportandomi durante le pause esami e aiutandomi il più possibile quando poteva; senza di lei sicuramente non mi sarei affezionato tanto alla maggior parte degli sport che pratico finora, soprattutto le gite in montagna e di scialpinismo.

A tutti voi, GRAZIE!